Finanziato dall'Unione europea - NextGenerationEU - DM 351 - CUP: I61I22000070007- CB: 38-411-41 DOT1341429-1137

University of Naples Parthenope
Department of Engineering

Doctoral Thesis
in
"Energy Science and Engineering"
XXXVIII Cycle – 2022/2025

Preparation and characteristics of aggregates by recycling municipal solid waste incineration fly-ash and other industrial waste through single-and double-step pelletization process

TUTOR

Prof. Francesco Colangelo

COTUTOR

Dr. Ilenia Farina

CANDIDATE

Jehangeer Raza

Ph.D. COURSE COORDINATOR
Prof. Laura Vanoli

Naples, Italy, 2025

Preface

The research for the realization of the present PhD thesis, entitled "***Preparation and characteristics of aggregates by recycling municipal solid waste incineration fly-ash and other industrial waste through single-and double-step pelletization process***", was performed at the Department of Engineering at Parthenope University of Naples, under the supervision of Professor Francesco Colangelo and Co-supervision of Dr. Ilenia Farina. The PhD project ran from November 2022 to October 2025.

The papers included in the thesis, referred to in the text are:

I. **Raza, J.**, Farina, I., Colangelo, F., & Singh, N. (2024). 5 - Properties of concrete containing polyethylene terephthalate and artificial lightweight aggregates: a case study. In F. Pacheco-Torgal, J. Khatib, F. Colangelo, & R. Tuladhar (Eds.), Reuse of Plastic Waste in Eco-Efficient Concrete (pp. 85-112): Woodhead Publishing.

II. **Raza, J.**, Singh, N., Colangelo, F., & Farina, I. (2024). Sustainability Assessment of Lightweight Artificial Aggregates Made from Industrial Waste Using a Double-Step Cold Bonding Palletization Process. Advances in Science and Technology, 149, 15-19. doi:10.4028/p-4UL6hC

III. Singh, N., & **Raza, J**. (2024). Life Cycle Analysis of Light Weight Artificial Aggregates for Sustainable Construction. Paper presented at the Proceedings of the International Conference on Civil, Structural and Transportation Engineering. https://doi. org/10.11159/iccste24.

IV. Singh, N., **Raza, J.**, Colangelo, F., & Farina, I. (2024). Advancements in Lightweight Artificial Aggregates: Typologies, Compositions, Applications, and Prospects for the Future. Sustainability, 16(21), 9329. doi:ARTN 932910.3390/su16219329

Acknowledgements

All praise to Allah Almighty who gave me the strength and ability to understand, learn and complete my Ph.D. thesis report.

It is a genuine pleasure to express my deep sense of thanks and heartiest gratitude to my research supervisor Prof. Francesco Colangelo and co-supervisor Dr. Ilenia Farina for letting me be part of the research group at MASERG, Department of Engineering, University of Naples “Parthenope”, Italy. I feel privileged to have worked under his kind supervision. It’s the blend of his patience, persistence, guidance and motivation that made me accomplish my research aims in due time. He has taught me the methodology to carry out the research and to present the research work as clearly as possible.

Additionally, I would like to express my appreciation to Prof. Vilma Ducman for warmly welcoming me and providing guidance during my mobility period at the Slovenian National Building and Civil Engineering Institute in Ljubljana, Slovenia.

I am also indebted to everyone at the MASERG Laboratory at the University of Naples Parthenope for their support and camaraderie, which made every day in the lab enjoyable.

Dedication

To my late father, whose love, wisdom, and blessings continue to guide and inspire me in every step of my life and my mother, for her boundless care.

To my wife, the calm in my chaos and the light behind every achievement.

Abstract

Recently across the globe, the use of recycled materials in the construction and building sector has drawn attention to bring sustainability. For this purpose, eco-friendly lightweight artificial aggregates are suitable alternative for natural aggregates. The municipal solid waste incineration fly-ash (MSWI-FA) (75%, 65%, 55%) along with marble sludge (MS) (15%, 25%, 35%) and ordinary Portland cement (OPC) (10%) as binder were used to prepare various mixtures lightweight artificial aggregates (LWA) through cold bonding pelletization (CBP) process. Before pelletization, the MSWI-FA were pre-treated via two-step washing with water, which significantly reduces the chloride and sulfates content. To enhance the performance of aggregates, they were surface treated with ground 50% granulated blast furnace slag (GGBFS), 20% silica fume (SF) and 30 OPC via CBP and these aggregates were named as double bonded. The double-bonded aggregates (DBAs) have shown improved performance as compared to the single-bonded aggregates (SBAs). The water absorption for SBAs is in the range of 12.87% - 14.21% and in case of the DBAs 16.62% - 17.12% was observed. Overall, the apparent density of aggregates was found to be in the range of 2.04 to 1.71 g/cm^3, and mechanical strength was observed in the range of 2.1 to 1.05 MPa. The compressive strength of aggregates decreases as the content of MS increases from 15% to 35% and MSWI-FA decreases from 75% to 55% which is due to reduction in pozzolanic activity. The bigger MS particle size makes it less reactive and remains unreactive in aggregate's matrix. The XRD analysis showed the formation of hydration products but have poor crystalline or amorphous because their peaks were overlapped by others, like calcite overlapped C-S-H while FTIR and TGA confirm their presences. The SEM analysis showed unreacted MSWI-FA and MS in SBAs samples along with the C-S-H gels in the form of continuous cluster with irregular shapes. The leaching analysis shows that the hazardous content was successfully solidified/stabilized in the aggregates matrix and surface treatment further reduces its leaching as it provides physical barrier.

Keywords: MSWI-FA pre-treatment; Single bonded aggregates (SBAs); Double bonded aggregates (DBAs); Cold bonding pelletization (CBP); Lightweight artificial aggregates (LWAs)

Table of content

List of Figures

Chapter 1: INTRODUCTION

Chapater 2: LITERATURE REVIEW

Chapter 3: METHODOLOGY

Chapter 3: RESULTS AND DISCUSSION

List of Tables

List of Abbreviations

Abbreviation:	Description
CBP	Cold bonding pelletization
SBAs	Single bonded aggregates
DBAs	Double bonded aggregates
LWAs	Lightweight artificial aggregates
MSWI-FA	Municipal solid waste incineration fly ash
MSW	Municipal solid waste
MS	Marble sludge
OPC	Ordinary Portland cement
GGBFS	Ground granulated blast furnace slag
SF	Silica fume
S/S	Solidification/stabilization
MIP	Mercury intrusion porosimetery
XRD	X-ray diffraction
TGA	Thermo-gravimetric analysis
FTIR	Fourier Transform Infrared Spectroscopy
SEM	Scan electron microscopy
CO_2	Carbon dioxide

Chapter 1: INTRODUCTION

1.1 Background

Globalization, urbanization, population increase, expanding economies and changing lifestyle leading towards the higher consumption of natural resources and environmental concerns. With the population increase and industrialization, competent infrastructure is required which stimulates the construction activities. Such higher construction activities result in shortage of the raw materials for concrete production and cause excessive greenhouse gas emissions, especially due to use of cement. For the construction, the natural aggregates are already excessively explored, and, in such scenarios, long term sustainability is required [1, 2]. For environmental preservation some countries like Sweden [3], Germany [4], Netherland [5] and Norway [6] have already banned or restricted exploration of natural resources for construction purposes. To reduce ecological damage and encourage circular construction techniques, the European Commission's 2021 report seeks to restrict the consumption of natural aggregates, particularly from marine and coastal areas. Concrete is the second most common material used by humankind after water [7]. The concrete significantly consists of the aggregates which is about 60-70% of the total concrete volume. In 2018, about 51.7 billion tons of the demand for concrete were reported and which increase by 5.8% per year [8]. This alarming situation draws the attention of researchers across the globe to work for sustainability in the construction industry.

Global development produces huge sums of waste in the form of industrial, agricultural, and domestic waste. The waste is mostly disposed of in landfills, which leads to environmental concerns in the form of leachate. These wastes may contain hazardous contents such as volatile and toxic organic compounds and heavy metals which can leach out into ecological system [9]. To reduce environmental concerns and attain sustainability it is necessary to recycle and reuse these waste materials. The construction industry has the higher potential to use these types of waste materials. However, some of these materials cannot be used directly, for which pre-treatment procedures are required [10].

Recently, the attention has been focused on the recycling and reuse of the construction and industrial waste as secondary resources [11]. Such as the use of the recycled concrete aggregates as an alternative aggregate in construction sector has gain success [12] along with other industrial wastes like coal fly ash used as filler or supplementary cementitious material [13]. It should be noted that industrial waste has its own intrinsic properties which sometimes enhance the application characteristics while in other cases it negatively impacts its performance. For instance, the presence of metallic aluminum in MSWI-FA cause to produce hydrogen gas which negatively affect concrete strength [14] but the same feature is useful in aerated concrete as it act as aerating agent [15]. Such interesting features of wastes, attract the researchers to identify its specific application in order to transfer its negative impacts into positives [16].

1.1 Problem statement

Among the wastes, the domestic or municipal solid waste (MSW) production was recorded about 2 billion tons in 2016 and with this growth rate it is expected that it hit the mark of 3.5 billion tons in 2025 [17]. Incineration is one of the most effective treatment processes for MSW. This process reduces the MSW volume by 85-90% and the mass by 60-90% and generates power [18]. After the incineration process, some residue remain in the form of fly ash (10-20%) and bottom ash (80-90%) [19]. The fly ash can contain various heavy metals, sulphates and chlorides [20, 21],which can be harmful to the environment and human health [22]. Therefore in many countries, municipal solid waste incineration fly ash (MSWI-FA) is categorized as hazardous materials due to the presence of high quantity of potentially toxic elements like Pb, Cd, Ni, Hg, Se and Mo as well as other contaminants such as sulphates, chlorides, dioxins, furans and acids etc [23]. The pre-treatment is necessary for MSWI-FA before its disposal in accordance with the regulations to control pollution from its collection to disposal [24, 25]. Otherwise, these contaminants might leach out and contaminate underground water reservoirs and affect negatively the exposed organisms and environment [26-28]. In USA the MSWI ash is disposed in landfills because its recycling is not legislated [29]. While in Europe, the Waste Framework Directive 2008/98/EC established that a waste must be classified as “hazardous waste” if it has at least one of the hazardous properties like explosive, oxidizing, flammable, irritant,

toxic, ecotoxic, infectious, mutagenic, sensitizing and corrosive etc [30]. The MSWI-FA was classified as "Ecotoxic" and listed as hazardous waste, reinforcing the importance of their recovery in Europe [31]. Initially, following the classification of the MSWI-FA as hazardous waste, it has to be pre-treated to stabilize the harmful components and minimize leaching before to disposal in a landfill [32, 33]. However, landfilling is an expensive procedure, rendering the recycling and recovery of MSWI-FA an appealing alternative in Europe [30]. Such a situation leads the researchers towards the treatment and recycling technologies for MSWI-FA.

1.2 Research hypothesis

Cold bonding, sintering, and autoclaving are three commonly used processes for producing synthetic lightweight aggregates. Cold bonded pelletization (CBP) technology has recently been regarded as the most viable solidification/stabilization method since it uses less energy and emits less pollutants, making it economical and environmentally friendly [34]. In this process, the fine particles in the presence of suitable binder like cement and fluid agglomerate into granules. The gravitational and centrifugal forces are responsible for the formation of the aggregates from fine powder [34]. These consolidated, large, aggregated particles are referred to as artificial aggregates. These aggregates typically exhibit low bulk density and sufficient structural integrity, representing a significant advantage of the CBP technique [2]. The aggregates produced by CBP efficiently can encapsulate the hazardous components in a aggregate matrix to reduce leaching and environmental impact [35]. CBP is so flexible that it is suitable for a wide range of industrial wastes, including ash, sludge, slags and other fine particles, making it suitable for many waste sources [36]. These LWAAs are further utilized in the construction industries to produce concrete which is named lightweight concrete.

1.3 Objectives of study

In this study, a novel integrated approach was used for valorization of MSWI-FA through CBP along with two-step water washing pre-treatment. The key theme was to solidify/stabilize hazardous content in MSWI-FA and to prepare alternative construction materials to bring sustainability in construction sector. The

experimental work carried out in this thesis is in line with the literature. The main objectives of this research work are:

- Two-step water washing of MSWI-FA to reduce chloride and sulfate content.
- Preparation of SBA via CBP by using washed MSWI-FA and MS as precursor materials and OPC as binder.
- Developing an outer layer over the SBA samples via CBP by using GGBFS, SF and OPC.
- The physical, chemical, mechanical, morphological and leaching analysis of LWAs were studied.

The MSWI-FA were first pre-treated via two-step washing then solidified and stabilized by converting into aggregates with the help of cement and marble sludge. The aggregates further went through second pelletization step to develop an outer layer (composed of GGBFS, silica fume (SF) and ordinary Portland cement (OPC)) around it, which enhanced the performance of aggregates environmentally, physically and mechanically. Unlike other studies which either solely focus on the pre-treatment methods or type of binder or composition of the aggregate matrix, but this work strategically reduces the use of cement (10%) and only proportion of MSWI-FA and marble sludge were varied to reduce the environmental impact and cost. The pre-treatment of MSWI-FA significantly reduces the chlorides and sulfates contents to mitigate leaching and minimize their negative effect on cementitious matrix like cracking. The outer layer developed due to surface treatment of aggregates, markedly improved the mechanical and leaching behavior. This optimized combination of waste in aggregates matrix, environmentally economical MSWI-FA pre-treatment and surface treatment for performance enhancement offers a pathway to produce artificial aggregates with enhanced quality to meet both the civil applications and environmental safety standards.

1.4 Scope of study

The MSWI-FA were first pre-treated via two-step washing then solidified and stabilized by converting into aggregates with the help of cement and marble sludge. The aggregates further went through second pelletization step to develop an outer layer (composed of GGBFS, silica fume (SF) and ordinary Portland cement (OPC)) around it, which enhanced the performance of aggregates

environmentally, physically and mechanically. Unlike other studies which either solely focus on the pre-treatment methods or type of binder or composition of the aggregate matrix, but this work strategically reduces the use of cement (10%) and only proportion of MSWI-FA and marble sludge were varied to reduce the environmental impact and cost. The pre-treatment of MSWI-FA significantly reduces the chlorides and sulfates contents to mitigate leaching and minimize their negative effect on cementitious matrix like cracking. The outer layer developed due to surface treatment of aggregates, markedly improved the mechanical and leaching behavior. This optimized combination of waste in aggregates matrix, environmentally economical MSWI-FA pre-treatment and surface treatment for performance enhancement offers a pathway to produce artificial aggregates with enhanced quality to meet both the civil applications and environmental safety standards. The scope of the research is shown in Figure 1.1

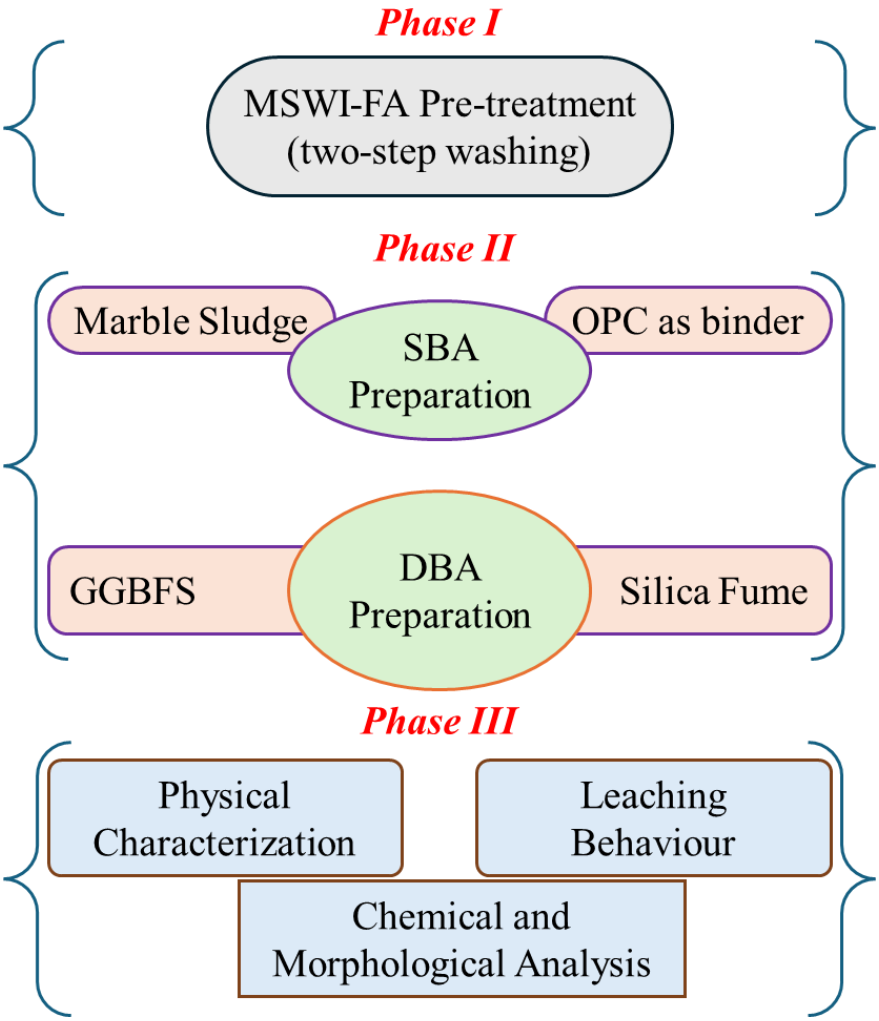

Figure 1.1 Steps involved in research scope.

1.5 Flow chart of thesis

The literature was initially carried out to find sustainable management for MSWI-FA, instead of disposing it in landfill sites. After choosing MSWI-FA recycling approach, MSWI-FA was pre-treated via two-step water washing. Then SBAs were prepared via CBP from MSWI-FA, MS and OPC and cured for 28 days. After curing an outer layer were applied to aggregates through CBP by using GGBFS, SF and OPC.

The aggregates were characterized in terms of physical properties (water absorption, density, porosity via MIP analysis), mechanical properties, chemical composition (XRD, FTIR, TGA), morphologically (SEM) and leaching behavior. Thesis flow diagram is shown in Figure 1.2

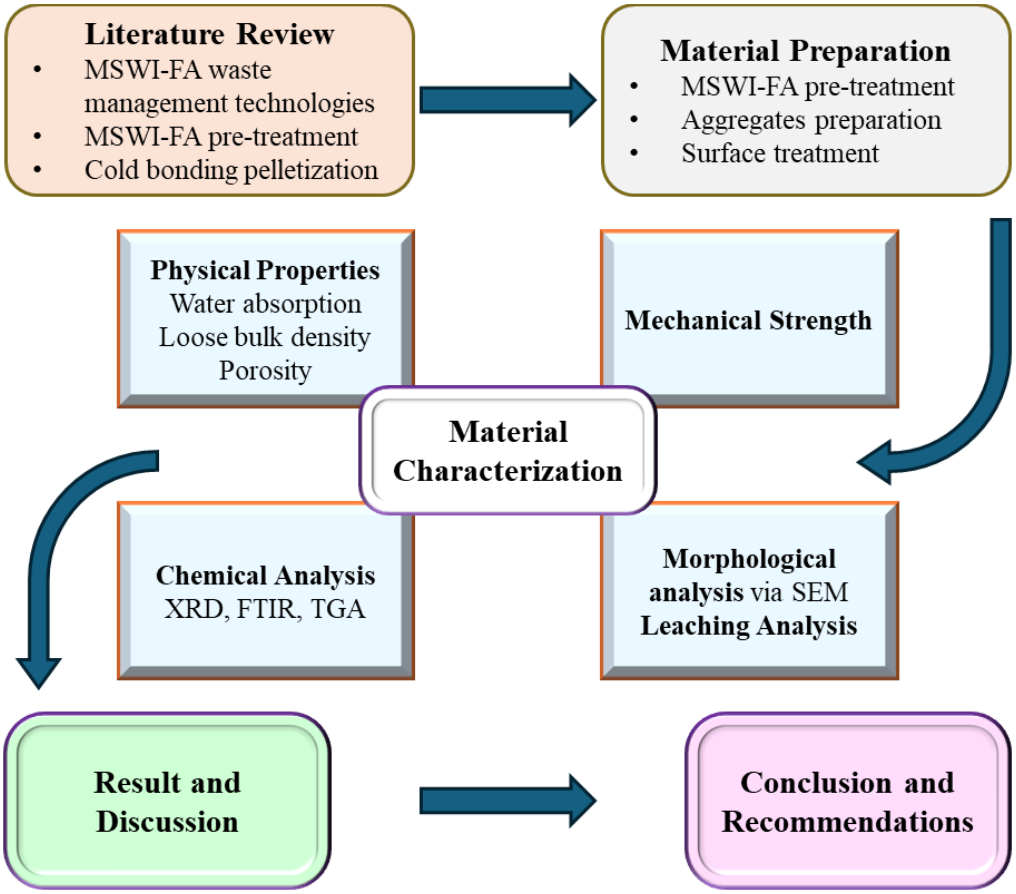

Figure 1.2 Thesis flow diagram.

Chapter 2: LITERATURE REVIEW

2.1 Graphical representation of literature review

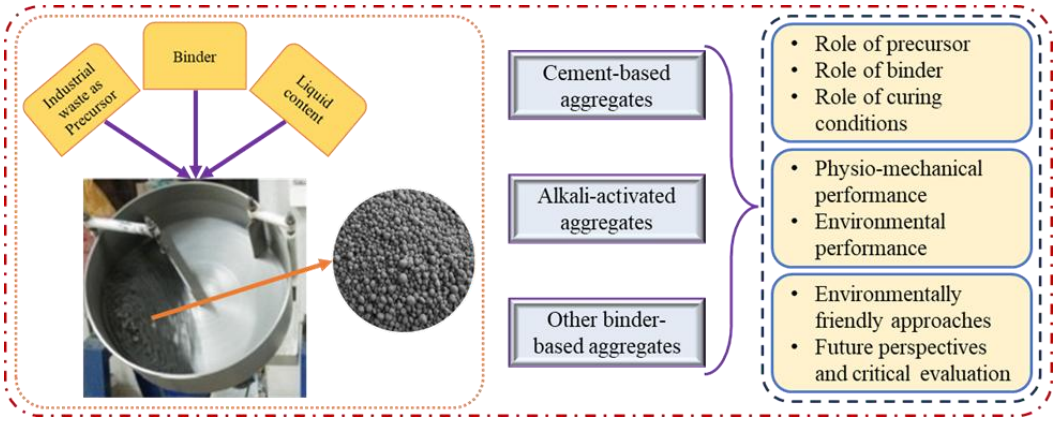

Figure 2. 1 Graphical representation of literature review chapter.

2.2 Sustainable construction sector

A sustainable construction industry requires alternative aggregates to produce concrete because the extraction of natural resources is already restricted to protect nature in some countries or regions [37, 38]. The direct use of solid waste as an aggregate substitute in concrete is the most desirable option and materials like recycled aggregates fulfill this condition [39]. Recycled aggregates are waste from the construction industry (CDW – construction and demolition waste is defined as waste material by United States Environmental Protection Agency 2019 [40]) that is reused in the same industry wastes into artificial aggregates is one way of reducing their negative impact on the environment and provides suitable substitute materials for construction. The aggregates for concrete manufacturing are categorized into three types, as seen in Figure 2.2.

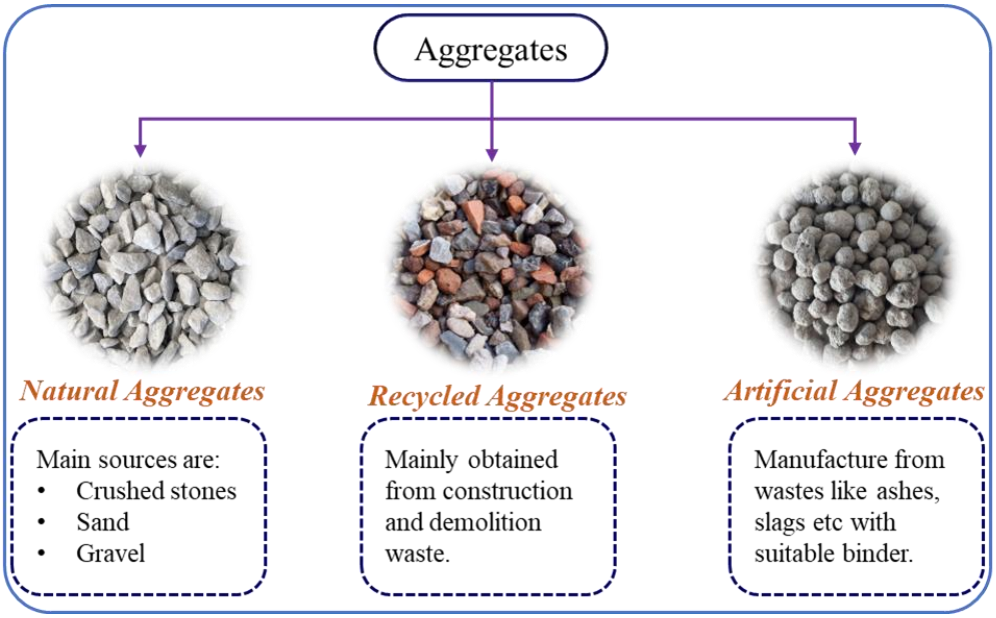

Figure 2.2 Aggregate types used for concrete production.

Artificial aggregates are usually produced by the process of granulation or pelletization, also known as agglomeration. Other methods like pressure compaction or crushing are also used to prepare artificial aggregates. In the process of pelletization the fine solid waste is placed in a granulator together with a suitable binder and provided with a sufficient amount of liquid, and due to the cohesive and tumbling force, the particles bind together and form somewhat rounded pellets/granules [41]. Initially, the strength of artificial aggregates is very low, but curing them in certain environments makes them strong and the curing environment parameters have a significant impact on their final performance. The final properties of artificial aggregates depend on several factors like the type and content of the precursor materials and binder, physical and chemical properties of the precursor materials and the parameters of the granulator. Based on the curing temperature, artificial aggregates are divided into two groups; high temperature artificial aggregates cured at around 1000 ℃ and cold bonded artificial aggregates cured at ambient temperature [42]. High temperature treatment is the most common method used for the preparation of artificial aggregates and was introduced in 1950 in the United Kingdom (UK) [37]. At the higher temperature, the particles of the granulate fuse together at their points of mutual contact [43] and complex physical and chemical reactions occur [37], where gases are released, some of which are trapped in the structure, reducing the density and providing better sound and thermal insulation characteristics to aggregates [44, 45]. The final strength of high

temperature artificial aggregates depends on the characteristics of precursor materials and the curing temperature [37], as these conditions define aggregate's performance [46]. The environmentally friendly characteristics and promising properties, like strength, porosity and air permeability make the CBAAs a suitable choice for concrete production [47]. The advantage of high temperature artificial aggregates is also a high production rate because the aggregates are treated at high temperature for shorter duration after granulation and are then ready for use. However, the disadvantages of these aggregates are their high energy consumption and the release of hazardous gases during curing.

CBAAs are considered effective and sustainable as they are cured at room temperature, making them more environmentally friendly in comparison to high temperature processes. Additionally, CBAAs which contain Ca-based carbonate-able compounds react with CO_2, which is advantageous because it not only sequesters CO_2 but also improves the aggregate's performance. Using alternative binders such as alkali activators can further improve environmental performance [48]. However, there are some economic implications, as the production of artificial aggregates is more expensive than that of natural aggregates, due to the need for machinery and skilled labour [49]. However, incentives from governments and supportive polices could help to stimulate the market and encourage investors and consumers towards its use.

In literature review, cold bonded artificial aggregates (CBAAs) which are divided into three groups based on their binder: cement-based, alkali-activated and other binder-based artificial aggregates are discussed in detail. The factors affecting the microstructure of cold bonded artificial aggregates and their relationship with physio-mechanical and environmental properties are analyzed. The performance enhancement and environmentally friendly approach named carbonation are also discussed in detail and its effect on the overall performance of artificial aggregates is elaborated. Finally, arguments are developed for the critical evaluation of future challenges, barriers and perspectives that artificial aggregates will face while upscaling to a commercial scale. Recommendations for future research and the upscaling of production to a commercial scale are given.

2.3 Literature review methodology

For literature review, the research articles published in last two decades were selected with focus on the latest advancement in the field of cold-bonded artificial aggregates. Research articles are selected from web of science, science direct and google scholar using the key word “lightweight artificial aggregates” and 350 articles were selected using the filter 2006-2025. By analyzing the title and abstract of these articles, the high temperature aggregate (sintered aggregates)-based articles were excluded and 180 articles were selected which only focused on cold-bonded-based aggregate articles. The major chunk of these articles is published in the last 6 years (2019-2025 (January)) which indicates the recent advancement in the field of CBAAs and geographically China is the major contributor followed by South Korea, India as shown in Figure 2.3. Those countries which have published 20 or more articles in the most recent time.

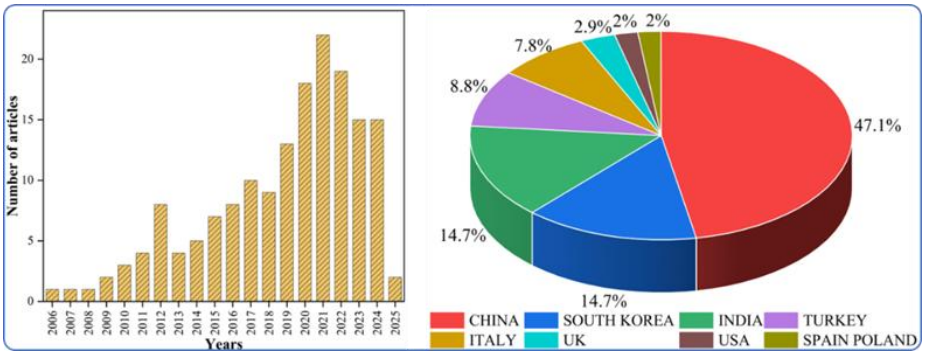

Figure 2.3 Distribution of paper over the years and location.

For this article, the research articles published in last two decades were selected with focus on the latest advancement in the field of cold-bonded artificial aggregates. Research articles are selected from web of science, science direct and google scholar using the key word “lightweight artificial aggregates” and 350 articles were selected using the filter 2006-2025. By analyzing the title and abstract of these articles, the high temperature aggregate (sintered aggregates)-based articles were excluded and 180 articles were selected which only focused on cold-bonded-based aggregate articles. The major chunk of these articles is published in the last 6 years (2019-2025 (January)) which indicates the recent advancement in the field of CBAAs and geographically China is the major contributor followed by South Korea, India as shown in Figure 2.2. Those countries which have published 20 or more articles in the most recent time.

2.4 Artificial aggregates

The aggregates prepared from the wastes like ashes, slags and sludges etc. with the help of a suitable binder and fluid are known as artificial aggregates. Artificial aggregates are broadly classified into two types based on curing temperature, as depicted in Figure 2.4.

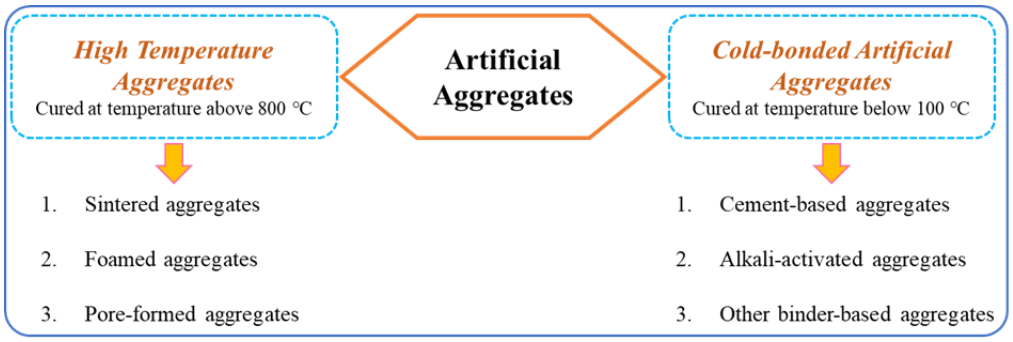

Figure 2.4 Categories and sub-categories of artificial aggregates.

Synthesized fresh granules or pellets (artificial aggregates) cured at temperatures above 800 °C have short curing time are called as high temperature artificial aggregates [50]. The properties of high temperature aggregates are primarily influenced by the precursor's characteristics, curing temperature and duration, and heating and cooling rate [51, 52].

2.5 Cold bonded aggregates

2.5.1 Cement-based aggregates

Cement-based aggregates are those in which cement is used as the binder. The aggregates gain strength from cement hydration products and the pozzolanic activity of precursor materials such as fly ash and slags. Both reactions enhance strength, durability, and resistance to chemical attack due to the formation of C-S-H gel. [53, 54], wherein the pozzolanic reaction is slower than the hydration reaction [55].

Physio-mechanical performance

The important properties to consider when selecting aggregates for construction applications are mechanical strength, water absorption, and density. The properties of cement-based cold-bonded artificial aggregates (CB-CBAAs) are related to their porosity and microstructure, which depend on the physical

properties and chemical composition of the precursor materials [56], binder (type and content), curing conditions [57] and surface treatment [58]. The curing conditions significantly affect aggregate performance; high temperature and humidity curing favour the development of hydration products and enhance the physical performance of aggregates [57, 59, 60]. In addition to the curing conditions, surface treatment of cement-based aggregates significantly enhances their physio-mechanical properties [56, 58, 61].

The following are some of the main factors which affect the physio-mechanical performance of cement-based artificial aggregates:

Precursor materials

The properties of cement-based artificial aggregates depend on the bonding forces developed through cement hydration and pozzolanic reactions. Therefore, selecting suitable raw materials and their appropriate proportions for aggregate preparation is a crucial step. The chemical composition influences the formation of hydrated products and subsequently affects the properties of CB-CBAAs. Various industrial waste materials, such as ashes (fly and bottom), GGBFS, and silica fume, are commonly used as precursor materials for the preparation of CB-CBAAs. Among these, fly ash is the most commonly used raw material for the preparation of cement-based aggregates due to its physical and mechanical properties [62]. According to ASTM C 618, fly ashes are divided into two classes: Class F fly ash, which contains less than 10% CaO, and Class C fly ash, which contains more than 10% CaO. The CaO content affects the formation of hydration products [63] which in turn affects the performance of the aggregates. Figure 2.5 shows that aggregate made from fly ash with lower CaO content has a denser microstructure and improved physical and mechanical performance compared to that with high CaO content. Higher CaO content imparts some cementitious properties of the precursor; in such cases, the addition of activators such as gypsum, NaOH, Na_2SO_4, or water glass is required to enhance binding [56]. SiO_2 is also important because it plays a critical role in the formation of C-S-H, and precursors with a high percentage of SiO_2 have shown better performance. The CaO to SiO_2 ratio is crucial for the formation of the hydration product (C-S-H); if this ratio is unbalanced, it negatively affects the formation of the hydration product, which in turn impacts the

microstructure and ultimately the strength of the aggregates. Excess CaO leads to the formation of weak $Ca(OH)_2$ phases, resulting in a more porous structure and aggregates with inferior performance. Higher SiO_2 content favors later-stage pozzolanic activity and develops a more refined pore structure, but due to lower CaO, it limits the formation of C-S-H and disrupts the reaction kinetics, ultimately affecting early-stage strength. Therefore, it is important to select the binder and precursor with a balanced chemical composition, rather than choosing a precursor with either higher CaO or SiO_2 content [56, 64].

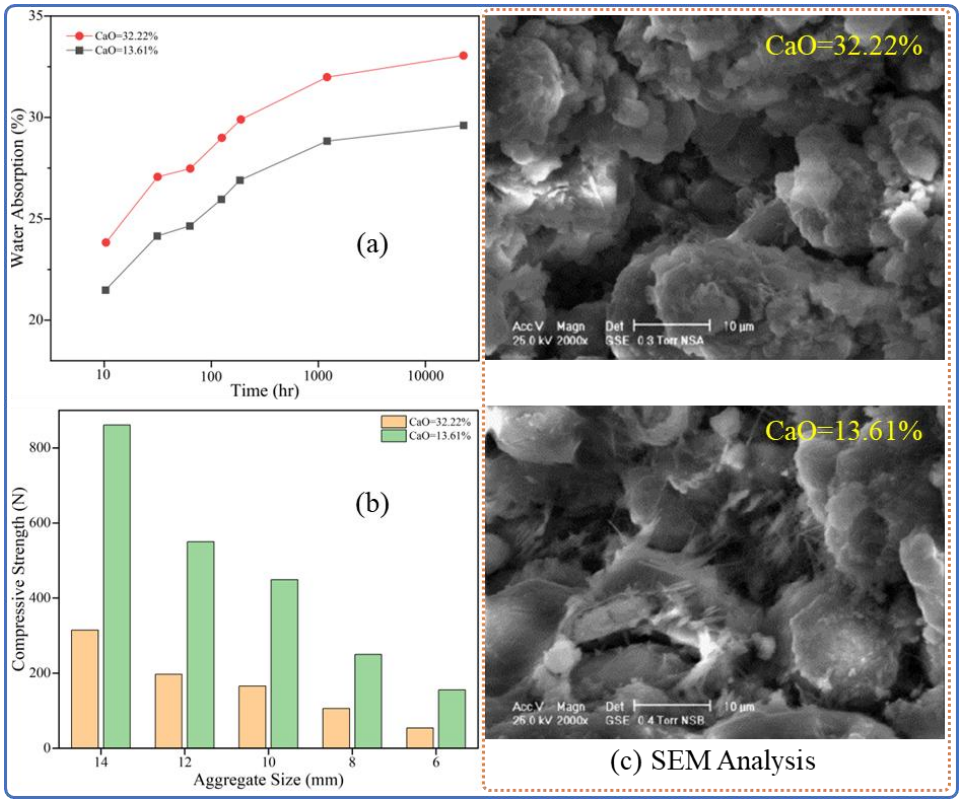

Figure 2.5 Effect of CaO content on (a) water absorption, (b) Compressive strength and (c) morphology of aggregate, reproduce. Adapted with permission from Ref. [56].

The physical characteristics of precursor materials also influence the properties of aggregates. Aggregates produced from fly ash with a lower specific weight (2.4) and higher specific surface area (3928 cm^2/g) have approximately 14% lower water absorption, 3.3% lower specific gravity, and 30% higher mechanical strength compared to those made from fly ash with a specific weight of 2.56 and a specific surface area of 3206 cm^2/g. [56, 64]. Due to the lower specific surface area, some ash particles remain unreacted and do not participate in the hydration reaction, resulting in a porous structure and poorer aggregate performance.

Generally, it was observed that mechanical strength improves by adding of cement, and it increases as the cement addition to fly ash increases [65].

Mechanical activation is a pre-treatment technique used to increase the fineness of precursors to achieve higher pelletization efficiency and improved properties [66] as it increases ash reactivity to form more reaction products [67]. Impact and shearing effects were used for size reduction in a centrifugal mill. Aggregates produced with activated fly ash have 22.73% lower water absorption and 33.61% higher mechanical strength compared to those made with non-activated fly ash [68]. In another ash pre-treatment, the municipal solid waste incineration fly ash was washed twice as a pre-treatment step, and through this process, some of the chlorides and sulfides leached out of the incineration fly ash [69, 70]. The washed fly ash aggregates have a smooth surface, while others have cracks due to the presence of chlorides and sulphates in the fly ash, as shown in Figure 2.6.

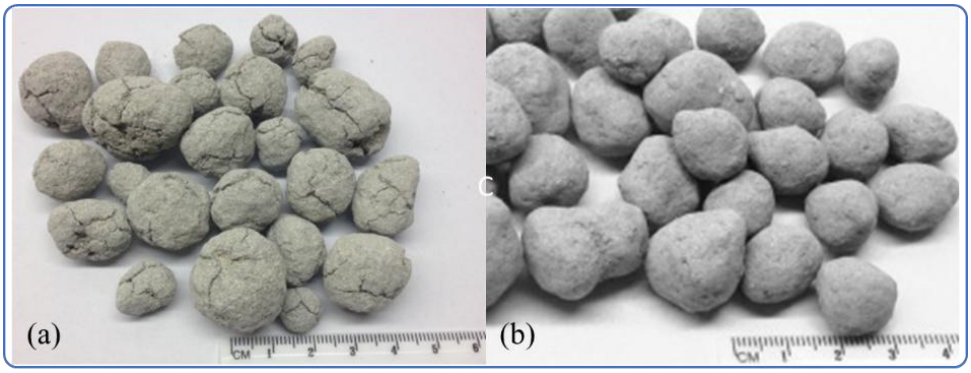

Figure 2.6 (a) Unwashed fly ash and (b) washed fly ash-based artificial aggregates. Adapted with permission from Ref. [69].

Aggregates matrix's

The composition of the precursors and binder impacts the physio-mechanical properties of aggregates. For example, in the literature, engineering muck-based aggregates were prepared by adding fly ash and slag as supplementary materials. The results, presented in Table No. 2.1 clearly demonstrate that physio-mechanical performance improves with an increase in cement content [71]. The aggregate's performance was found to be closely related to hydration activity. Replacing a portion of cement with fly ash reduces aggregate performance due to a decrease in hydration products, as fly ash has lower hydration activity compared to cement. [72]. When cement is replaced with slag, the physio-mechanical

performance also declines; however, it remains superior to that of aggregates containing fly ash, due to the high CaO content of slag [71]. Slag hydration is generally enhanced in the presence of calcium hydroxide (alkaline environment), but Ca and Mg in the pore solutions of the pastes may inhibit the consumption of Al, while the high Al content in turn inhibits the consumption of Ca, resulting in the slow formation of hydrates [73].

Generally, binder content (percentage) plays a decisive role in the microstructure and performance of aggregates. However, higher binder content increases density, cost, and environmental impacts without providing proportional improvements in aggregate strength. Therefore, optimal binder content should be used to balance the reactivity of precursors, microstructure, sustainability, and technological performance of aggregates.

Table 2.2 Composition and physico-mechanical performance of aggregates [71]

Samples No.	**Aggregates composition by wt. %**				**Mechanical Strength (MPa)**	**Loose Bulk density (gm/cm^3)**	**Water absorption (%)**
	Cement	Fly ash	Slag	EM			
C8	8	/	/	92	6.06	1.16	13.66
C16	16	/	/	84	8.76	1.13	12.98
C24	24	/	/	76	11.77	1.12	12.57
F8C16	16	8	/	76	10.41	1.09	16.67
F16C8	8	16	/	76	6.52	1.05	20
F24C0	0	24	/	76	1.22	0.91	23.31
S8C16	16	/	8	76	10.61	1.13	14.17
S16C8	8	/	16	76	7.86	1.125	15.15
S24C0	0	/	24	76	1.71	1.12	17.6

Note: “C” denotes cement, “F” represent fly ash and “S” stands for slag, “EM” represent Engineering muck (Heavy silty clay)

In the case of cement-based aggregates, it was observed that the size of the

aggregates also affects the physio-mechanical performance, as larger aggregates are more likely to have a porous structure, which is considered responsible for poor aggregate performance, as shown in Figure 2.7 [61, 74]. The better performance of the small-sized aggregates is due to the release of water during the final compaction phase of granulation, while, due to the high porosity of larger aggregates, water becomes trapped in these pores [69]. The relationship between aggregate size is not necessarily proportional, as another study found that the strength of aggregates increases with size. This is because the aggregate matrix contains more material and more hydration products, which develop a better microstructure (not compacted) with more closed pores that resist the applied mechanical load. [56]. An example of the performance of such aggregate, as discussed above, is shown in Fig. 4, where it is clearly observed that the mechanical strength increases with the size of the aggregate. Another study observed mixed trends regarding the size, porosity, and performance of aggregates. [61], while yet another study found that size has no significant influence on the strength of aggregates. [42].

From the above discussion, it can be inferred that the pozzolanic reaction or the hydration products determines the mechanical and physical properties of the cement-based cold-bonded artificial aggregates. It is critical to choose the appropriate material and percentage because an excess of one material can result in unreacted materials and impair the performance of the aggregate. There are three important parameters to consider for LWAs: strength, reduced density, and microstructure. The microstructure determines the other two characteristics, as it defines the type of porosity – either closed (structural) porosity or open (interconnected) porosity. In both cases, the density of the aggregates decreases. However, closed porosity enhances aggregate performance, while open porosity negatively affects performance by causing high water absorption, lower strength, and poor solidification or stabilisation of hazardous content. Generally, as the size of the LWAs increases, their open porosity also increases, which decreases aggregate performance. However, if a high binder content and reactive precursors are used in a controlled pelletization process, the size will not affect aggregate performance. Conversely, with lower binder content, poorly reactive precursors, and uncontrolled pelletization, an increase in LWA size leads to increased open

porosity, resulting in poor aggregate performance.

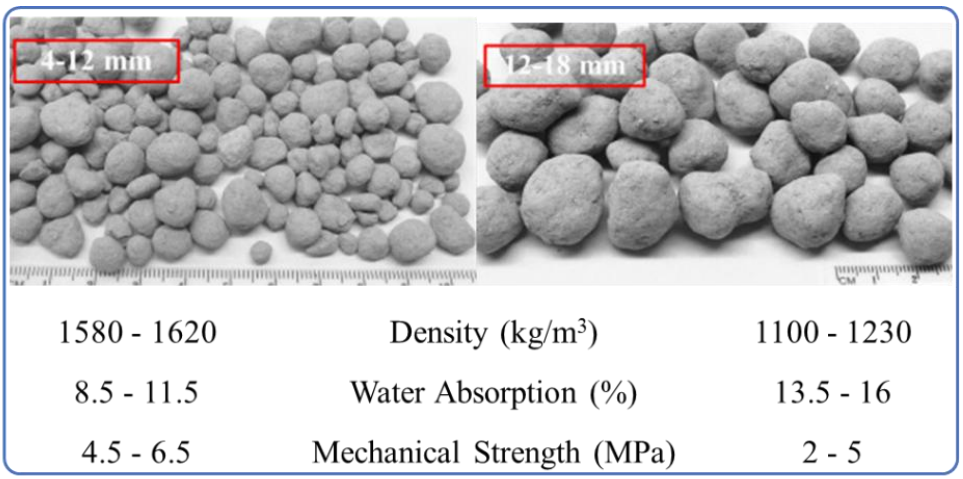

1580 - 1620	Density (kg/m^3)	1100 - 1230
8.5 - 11.5	Water Absorption (%)	13.5 - 16
4.5 - 6.5	Mechanical Strength (MPa)	2 - 5

Figure 2.7 Effect of aggregates size on its performance. Adapted with permission from Ref. [69].

From the above discussion, it can be inferred that the pozzolanic reaction or the hydration products determines the mechanical and physical properties of the cement-based cold-bonded artificial aggregates. It is critical to choose the appropriate material and percentage because an excess of one material can result in unreacted materials and impair the performance of the aggregate.

Curing condition

The usual curing conditions in the cold bonding method are ambient conditions, which require a longer time for the aggregates to gain sufficient strength and reduce production rates. To increase production capacity and improve the properties of the aggregates, various accelerated curing conditions have been applied. The curing condition has three important parameters that affect the performance of the aggregates: (1) temperature, (2) humidity, and (3) time. Curing methods such as ambient conditions, immersion in water at ambient or specific temperatures (below 100°C), steam curing, autoclave curing, or sealing the aggregate in a plastic bag are used in the literature for aggregate curing [60]. The high temperatures accelerate the formation of hydration products, which embed the particles in the aggregate matrix. Figure 2.8 shows the cross-sectional image displaying the various contents in the aggregate prepared from MSWI-BA, GGBFS, and cement, and cured under different conditions, along with physio-

mechanical properties.

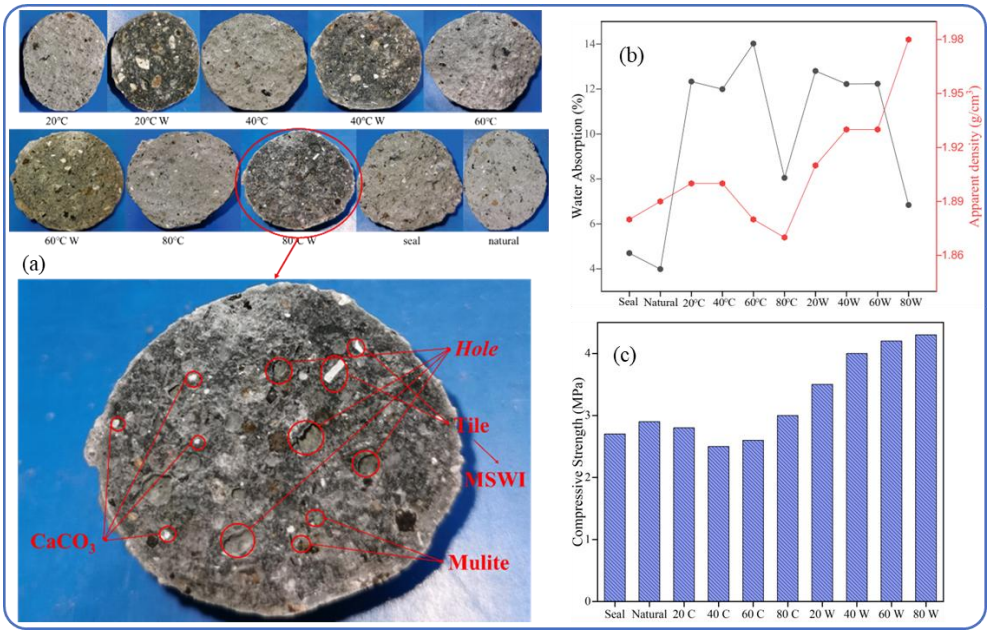

Figure 2.8 (a) Cross sectional image, (b) water absorption and density and (c) mechanical strength of aggregates cured at various temperatures. Adapted with permission from Ref. [57].

The morphology of the hot water-cured aggregate confirms the presence of various hydration products, such as binding gels and ettringite (needle-shaped). These products are responsible for a denser structure and improved performance [75] as shown in Figure 2.9.

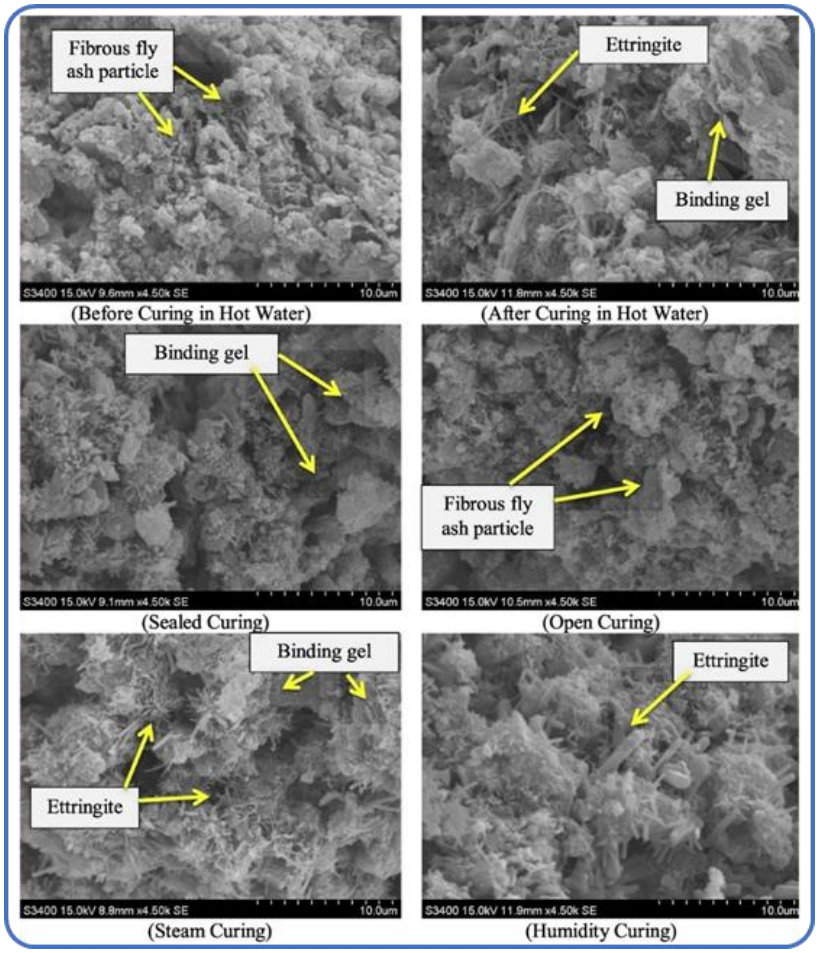

Figure 2.9 SEM analysis of aggregates cured at various regimes. Adapted with permission from Ref. [60].

At ambient conditions, more time is required to form sufficient hydration products [76]. As the curing period increases, more hydration products are formed, developing a dense microstructure that provides strength to the aggregates. [65].

Surface treatment

Surface treatment of cold-bonded artificial aggregates can be performed to enhance their physio-mechanical and leaching characteristics [69], and to increase the utilization of the waste materials [58]. Various surface treatment techniques, such as immersing the aggregates in slurry for a specific period [56], spraying particular materials [59], and double step cold bonding [58] have been used to improve aggregate performance. For example, fly ash-based artificial aggregates with OPC as the binder were surface treated by placing them for 30 minutes in water glass (Na_2SiO_3) which significantly enhanced the aggregates' physio-mechanical performance, as shown in Figure 2.10 along with SEM micrographs

[56]. along with SEM micrographs [56]. From the mechanical strength results, it can be observed that increasing the size of the aggregate improves the mechanical strength and enhances the effect of the surface treatment. This is because larger aggregates have more pores, allowing more alkaline solutions to penetrate the aggregate matrix and form geopolymer gel, which accumulates in these pores. SEM analysis confirms that the surface of the treated aggregate is smoother compared to the untreated aggregate, as the water glass fills the open porosity and results in the formation of a glassy surface with higher Si content, as confirmed by the EDS study [56].

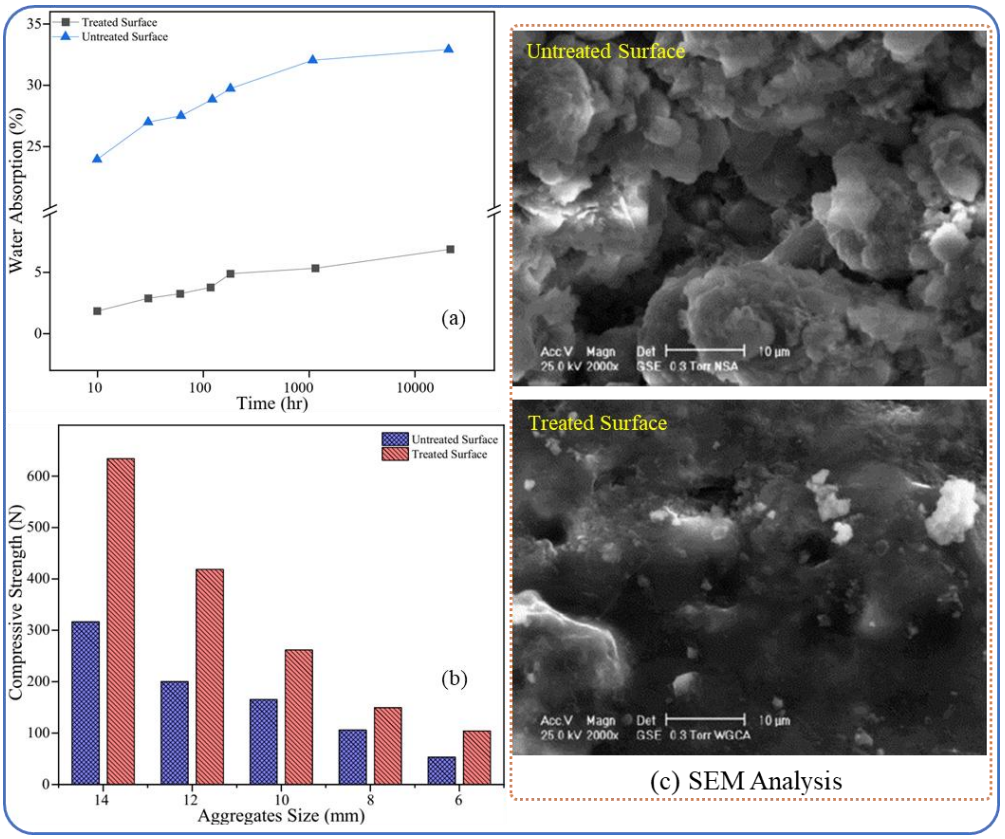

Figure 2. 10 SEM analysis of (a) untreated and (b) treated aggregate surface, EDS study of (c) treated and (d) untreated aggregate surface. Adapted with permission from Ref. [56].

If an extra material is used for surface treatment, an additional outer layer is developed over the surface of the aggregate through various techniques, such as soaking in slurry [77], spraying slurry on aggregates [59] and multiple pelletization [58]. An illustrative and optical image is shown in Figure 2.11 for such treat aggregates.

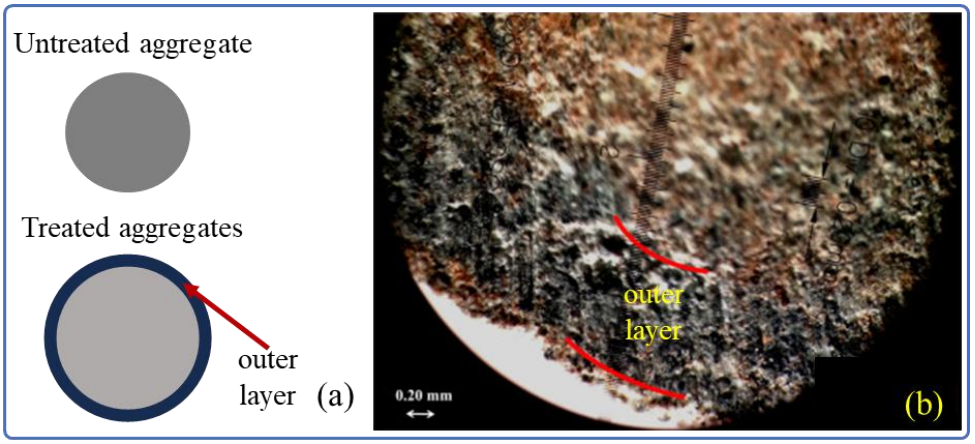

Figure 2.11 (a) Illustrative diagram of single and double step cold bonded granules and (b) optical image of double layered aggregate. Adapted with permission from Ref. [69].

In the case of multiple pelletization, the aggregates were first cured for a certain period to gain strength, as the fresh pellets do not have sufficient strength. In the literature, two types of multiple pelletization were performed on aggregates in two different studies. In the first method, the aggregates were cured for 28 days. After curing, the aggregates were placed again in the granulator operating at 45 rpm and set at 45°, sprayed with water to moisten them, and then the mixture prepared for the outer layer was slowly added along with continued water spraying. [61]. In another study, aggregates were cured in sealed plastic bags for 24 hours and then surface treated using a multiple pelletization method. In this method, aggregates were soaked in water for 5 minutes, then placed in a pelletizer rotating at 15 rpm, and a slurry mixture was slowly sprayed onto the aggregates. [59].

In the literature, these two surface treatments were compared, and it was observed that immersion in slurry is an ineffective surface treatment, as it sometimes negatively affects the physio-mechanical properties of the aggregates by forming protrusions on the surface, resulting in lower filling capacity or having very little effect [59]. The slurry immersion method is low cost and requires less time, but it does not cover the entire surface of the aggregate and produces an irregular shape [77]. The effects of these surface treatments on physical and mechanical properties are listed in Table No. 2.2, along with a comparison of these methods. The thickness of the outer layer and the size of aggregates selected for treatment also affect performance. For example, in literature, CBAAs were produced with 80% phosphogypsum, 15% GGBFS, and 5% OPC (aggregate matrix) and surface-treated with 45% phosphogypsum, 50% GGBFS, and 5% OPC (outer layer) by

multiple pelletization. The 6 mm aggregates were coated with a 1 mm outer layer (P80-6); 5 mm aggregates had a 1.5 mm outer layer (P80-5), while a 2 mm outer layer was developed on 4 mm aggregates (P80-4). The author observed that P80-5 had a mechanical strength of 6.20 MPa, followed by P80-4 with 6.02 MPa, and P80-6 with 5.06 MPa, which was the lowest among the surface-treated aggregates. It was observed that inconsistent shrinkage between the aggregate and the outer layer affects the performance of the aggregates [77]. Summarizing Table No. 2.2, it seems that among the surface treatment methods, multiple pelletization was found to be the most effective, as it produces a uniform outer layer and a consistently densified aggregate surface. Slurry immersion is economical, simple, and timesaving, but it does not provide complete surface coverage, resulting in irregularly shaped aggregates and surface protrusions that negatively affect aggregate performance. However, it was observed that the thickness of the outer layer, aggregate size, material selection (shrinkage compatibility), and pelletization parameters influence the performance of surface-treated aggregates.

Table 2. 3 Physio-mechanical properties of untreated and treated aggregates

Aggregates composition	Outer layer composition	Surface treatment	UMS (MPa)	TMS (MPa)	UWA (%)	TWA (%)	Ref
5% OPC + 15% GGBFS + 80% MSWI-FA	70% Marble Sludge + 30% OPC	Multiple pelletization	1.33	1.95	16.81	11.50	[58]
10% OPC + 10% GGBFS + 80% MSWI-FA			1.45	5.36	15.48	6.96	
15% OPC + 5% GGBFS + 80% MSWI-FA			1.86	10.92	12.18	15.51	
18% OPC + 49% FA + 33% Expanded perlite particles	10% Silica Fume + 90% OPC	Multiple pelletization	3.11	3.55	44	32	[59]
		Slurry immersion	3.11	2.77	44	42	
80% Phosphogypsum + 15% GGBFS + 5% OPC	GGBFS + FA (1:1) with water glass solution at liquid-solid ratio of 0.7	Multiple pelletization	8.3	9.4	7.5	5.8	[77]
		Slurry immersion	8.3	8.6	7.5	6.15	

UMS: Untreated aggregates mechanical strength, TMS: Treated aggregates mechanical strength, UWA: Untreated aggregates water absorption, TWA: Treated aggregates water absorption.

2.5.2 Alkali-activated aggregates

The alkali-activated aggregates gain strength through the dissolution of reactive aluminum and silicate oxides in the presence of the alkaline solution and the formation of silicate-aluminate gel [46, 78, 79]. The gel hardens and binds the unreacted particles of the precursor materials to enhance the strength of the aggregates [46]. Raw materials (waste) containing aluminosilicate minerals are considered suitable for the preparation of alkali-activated aggregates. [80]. Such AA aggregates are also successfully prepared with alkali solutions derived from waste, which brings sustainability and economic benefits [81].

Physio-mechanical performance

The physio-mechanical properties of alkali-activated materials largely depend on the chemical composition of the precursor material, curing conditions, and the concentration of the activator solution. The SiO_2/Al_2O_3 ratio in the precursor material [82, 83] and alkalis concentration contributes to the development of the polymerization gel, which affects the structure of the aggregate and determines its physio-mechanical performance [84]. High temperature (≥ 80 °C) and 100% humidity curing are favorable conditions for achieving greater and earlier strength, along with improved physical characteristics [81, 85]. It should be noted that (prolonged) curing at high temperatures may contribute to the contraction in polymerization gel, as cracks appear in the aggregate matrix which affect its performance [86].

The factors which affect the physical and mechanical performance of alkali-activated aggregates are presented below.

Precursor materials

Waste materials containing chemically active aluminosilicate minerals are considered suitable precursor materials for the preparation of alkali-activated aggregates [80]. The most common raw materials are various industrial wastes (including ash of brickyard), agricultural wastes, municipal wastes [87]. The reactivity of the raw materials in the alkali medium is crucial and depends on the

mineralogical and morphological properties, particle size distribution, and elemental composition. The mechanical performance of the alkali-activated aggregates was found to depend on the solubility of SiO_2 and Al_2O_3 [88, 89], and their relationship is shown in Figure 2.12.

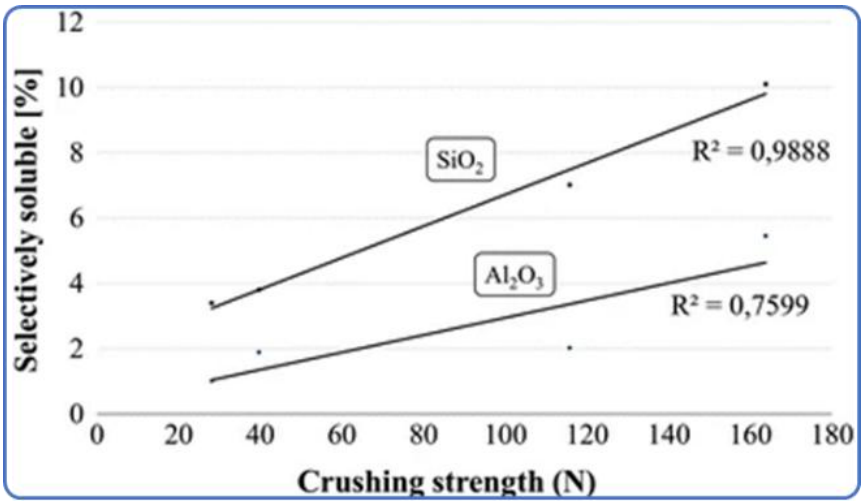

Figure 2.12 Correlation between the selectively soluble SiO_2 and Al_2O_3 and crushing strength of aggregates. Reprinted with permission from Ref. [89].

The amorphous phase of the reactive aluminosilicate dissolves in the presence of a high concentration of OH− ions (basic pH) and releasing Si^{4+} and Al^{3+} ions in the form of monomeric groups in the solution [90]. The chemical composition of the precursor material determines the rate of aluminosilicate dissolution [91]. Water is necessary for gel formation, as it facilitates the dissolution of solid aluminosilicates via alkaline hydrolysis, and the resulting aluminate and silicate species in the aqueous phase lead to the precipitation of N-A-S-H gel [92]. The water consumed in the dissolution process is released during condensation, and some time is required for the supersaturated aluminosilicate solution to form a continuous gel [92]. The addition of GGBFS enhances mechanical strength [82, 93], as most studies observed that adding a certain amount of GGBFS (main components are CaO and SiO_2) to fly ash-based alkali-activated aggregates significantly improves physio-mechanical performance [46, 82, 93-95]. The high CaO content in the GGBFS enhances the binding ability of the precursor materials by contributing to the formation of C-S-H gel [93]. This leads towards more dense and compact structure with refined pore size of aggregate [96, 97].

The effect of GGBFS on MWBA (municipal woody biomass ash)-based alkali-activated aggregates is shown in Figure 2.13 which demonstrates that mechanical strength increases with higher GGBFS content due to reduced porosity and fewer interconnected pores (as seen in cross-sectional and SEM images) [82]. Recently, lithium slag-based alkali-activated aggregates were prepared, and it was again observed that increasing the percentage of GGBFS enhanced their performance [98]. Similarly, in another study, the characterization of mine tailing-based alkali-activated aggregates showed that increasing the slag content from 10% to 30% had a pronounced impact on their physical (23% reduction in water absorption) and mechanical (enhanced by 22.38%) properties [99]. At lower slag content (≤ 15%), the geopolymerization process did not progress optimally, as unreacted mica sheets remained in the geopolymer structure, while a higher percentage of slag resulted in a well-geopolymerized gel [99, 100]. The same research group in another study analyzed the effect of different percentages of FA on mine tailing -based AAAs. It was found that increasing FA from 10% to 30% reduced water absorption by 20% while increasing mechanical strength by 111% [100]. Comparing both studies, it was concluded that the Si/Al ratios play a significant role in determining the performance of AAAs, which is closely related to the chemical composition of the precursor. For instance, in the same study [99], it was observed that increasing slag content up to 20% significantly increased the Si/Al ratio, but further increases in slag content decreased the ratio, which negatively impacted aggregate performance. However, increasing FA content beyond 20% improved the Si/Al ratio, thereby enhancing performance. In AAAs, various compositions of phosphorus tailings (PT), fly ash (FA), soda residue (SR), and granulated blast furnace slag (GGBS) were studied [101]. It was observed that a mixture of 40% PT, 20% FA, 30% SR, and 10% GGBS exhibited superior performance compared to other compositions, as this combination provides the most suitable aluminosilicate content. Alkaline compounds play a dual role by breaking down the active Si-Al networks (silicon oxides and silicates) and enhancing the dissolution of ions [101]. This process supports the hydration reaction and promotes the development of gel-like structures, such as C-S-H, which in turn improves the stability, strength, and durability of the material [102].

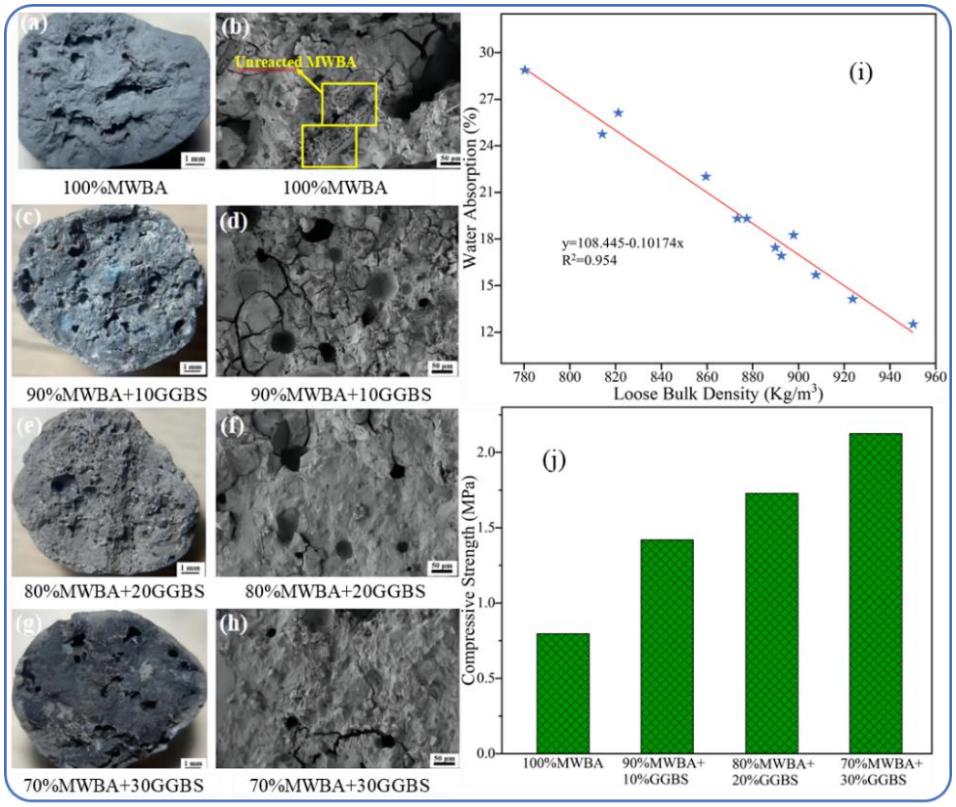

Figure 2.13 (a, c, e, g) Cross Sectional, (b, d, f, h) SEM images, (i) loose bulk density relation with water absorption and (j) crushing strength of MWBA-based aggregates with different GGBS content. Adapted with permission from Ref. [82].

Similarly, the addition of cement to alkali-activated aggregates enhances the performance of the aggregates because cement develops a C-S-H phase alongside the gel phase formed by alkali activation [95]. The presence of this additional phase results in a dense microstructure and enhances the bonding between particles in the aggregate matrix, leading to aggregates with improved performance. For example, the addition of cement increases the density by 15.24%, while mechanical strength almost triples and water absorption is reduced by 35.06% in sewage sludge ash and GGBFS-based aggregates. [95]. Figure 2.14 shows SEM micrographs with and without the addition of 15% cement. However, this contradicts the main aim of using alkali-activated aggregates, which is to reduce cement usage and protect the environment.

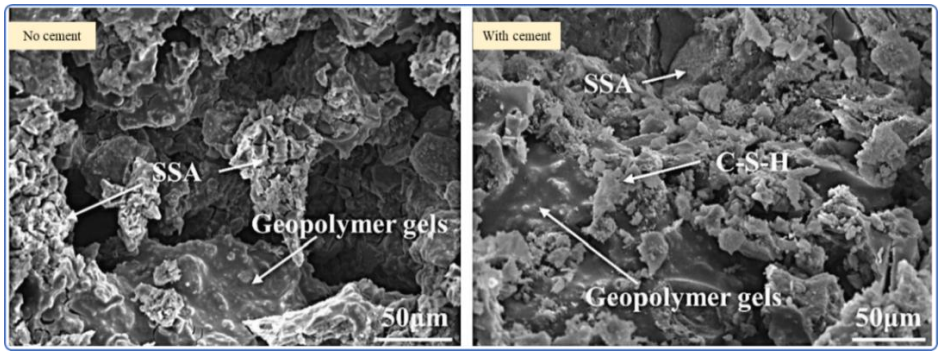

Figure 2.14 SEM analysis of sewage sludge ash and GGBFS-based aggregates with and without cement and their respective physical and mechanical properties Adapted with permission from Ref [95].

Activator solution

The alkaline solution is used as a binder and provides the moisture content required for granule formation. The most used alkaline solution contains sodium hydroxide (NaOH) and sodium silicate (Na2SiO3). The molarity of NaOH significantly affects the properties of the aggregates. [103-105]. he activator solution in the aggregate matrix physically binds and encapsulates unreacted precursor particles in an equilibrium combination of C-(A)-S-H and N-A-S-H gels [106] as well as a spongy microstructure, which are aluminosilicate and alkali-activated slag – the primary stabilizing reaction products [107]. In the literature, the effect of different concentrations (0, 4, 6, 8, 10, 12) of NaOH was analyzed [105] and it was found that as the concentration increased from 4 to 8, the performance of the aggregates improved. The SEM micrographs, along with the apparent density, water absorption, and mechanical strength, are shown in Figure 2.15. In the absence of NaOH in the aggregate matrix, geopolymer gel is absent and some unreacted precursor particles are present, which affect aggregate performance. Such reactions increase porosity and cause cracks to develop in the aggregates, which negatively affect aggregate performance [105]. The high content of NaOH delays the development of polymerization strength due to the hydrolysis and precipitation of Al^{3+} and Si^{4+} in solid aluminosilicate [108]. Rapid dissolution and reprecipitation rates are observed at higher NaOH concentrations, restricting the development of the polymerization gel and disrupting the suitable microstructure required for improved aggregate performance [84]. Such reactions cause increased porosity and even cracks in the aggregates [105]. Higher NaOH content favors the formation of

N-A-S-H gel and magadiite [109] and retards the formation of high-strength gels such as C-S-H and C-A-S-H [110, 111]. It should be noted that, irrespective of the raw material content, the alkaline solution affects the properties of the aggregates, and it was observed that these properties improved with increasing alkaline solution content within limits [82]. Recently, the effect of NaOH molarity (6 M –14 M) on lithium-slag-based AAAs was analyzed [98]. Water absorption decreased from 15.87% to 5.88%, while mechanical strength increased from 2.33 MPa to 10.87 MPa as the molarity increased from 6 M to 12 M. Further increases in molarity had only a slight effect on performance.

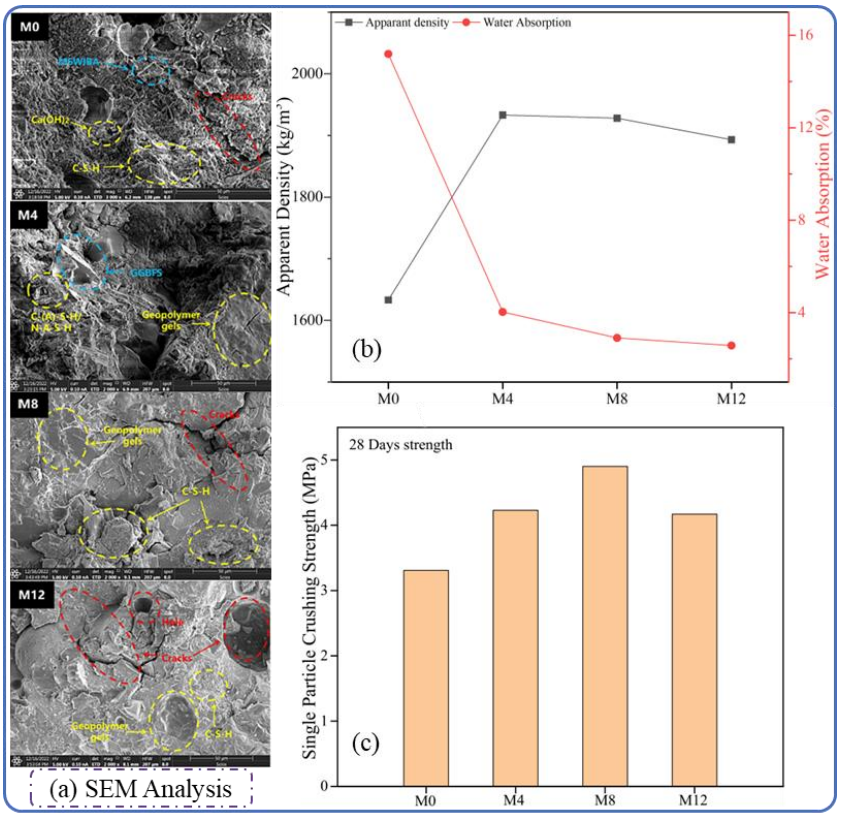

Figure 2.15 (a) SEM micrographs, (b) apparent density, water absorption and (c) crushing strength of aggregates with various concentration and without NaOH Adapted with permission from Ref. [105].

The other activator like $NaAlO_2$ and NaOH as well as K-silicate and KOH combination were also used in the preparation of aggregates [46]. The aggregates with high concertation of solutions will remain unreacted and contribute to disturbance of the micro-structure which affects the performance of aggregates.

Curing conditions

The reaction mechanism under various curing conditions for alkali activated aggregates [85] is depicted in Figure 2.16. It was observed that as temperature and humidity increase, the formation of large polymerization gels improves compared to dry and room temperature curing [85]. The polymerized gel provides a dense and compact microstructure to the aggregate, resulting in better performance. However, it should be noted that prolonged curing at higher temperatures can cause defects or shrinkage in the polymer gel and cracks in the aggregate matrix, which adversely affect performance [86, 90].

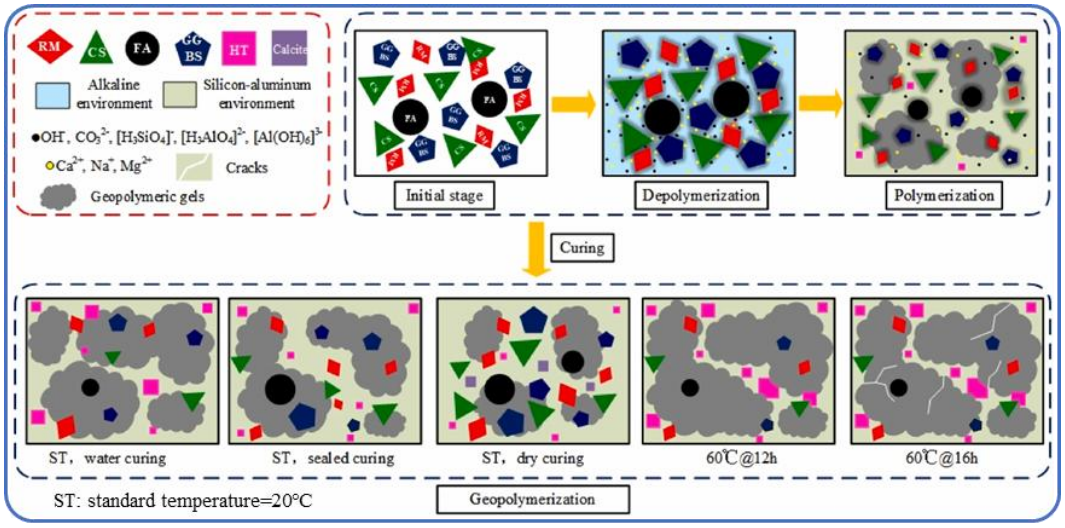

Figure 2.16 Schematic diagram of reaction mechanism of alkali activated aggregates cured at various temperatures. Reprinted with permission from Ref. [85].

The SEM micrograph, bulk density, water absorption and cylinder compressive strength of the aggregates cured under various curing conditions [81] are presented in Figure 2.17. The steam-cured aggregate, treated at 60°C for 12 hours, enhances condensation and depolymerization of precursor materials, which improves the crystallinity of hydration products and produces dense, compact structures [81].

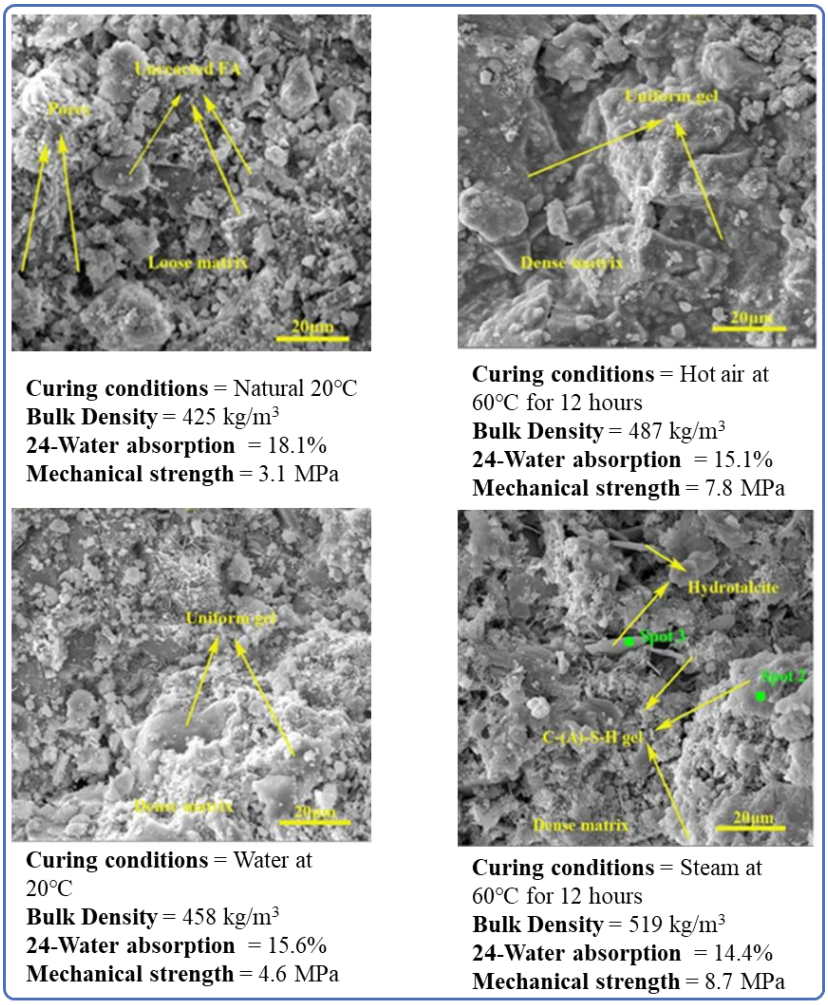

Figure 2.17 Alkali-activated aggregates cured at different conditions with their respective SEM analysis, water absorption, bulk density and cylinder crush strength. Adapted with permission from Ref. [81].

Under ambient conditions, curing duration will be prolonged [112], while at higher temperatures it may be shorter. In addition to curing time, temperature, and humidity, pressure also affects the performance of alkali-activated aggregate [88]. High curing temperature (≥ 80°C) and humidity (100%) are favorable conditions for achieving greater and earlier strength, along with improved physical characteristics. [81, 85]. It should be noted that prolonged curing at high temperatures disturbs the polymerization gel, as cracks appear in the aggregate matrix and affect its performance [86].

In summary, for alkali activated aggregates the SiO_2/Al_2O_3 ratio and activator concentration are crucial factors, as these define the development of the

microstructure and polymerization gel, which determine the physio-mechanical characteristics. For accelerated curing, high temperature and humidity are recommended in the literature, but prolonged exposure impairs aggregate performance.

2.1.3 Other Binder-based aggregates

For cold bonded aggregates the most commonly used binders are cement and lime [37]. Cement-based aggregates and alkali-activated aggregates were discussed in detail in the previous sections. This section will summarize other binder-based cold bonded aggregates. The commonly used alternative binders, such as lime and bentonite, have shown poorer performance compared to cement or alkali activated cold bonded aggregates [69, 113-116]. In one of the study, lime- and cement-based aggregates were compared, and it was observed that lime-based aggregates exhibited poor physio-mechanical performance and leaching behavior [69]. However, in the same aggregates, when 25% coal fly ash was added and lime was reduced to 15% with 60% MSWI-FA, the performance of the aggregates improved as shown in Figure 2.18.

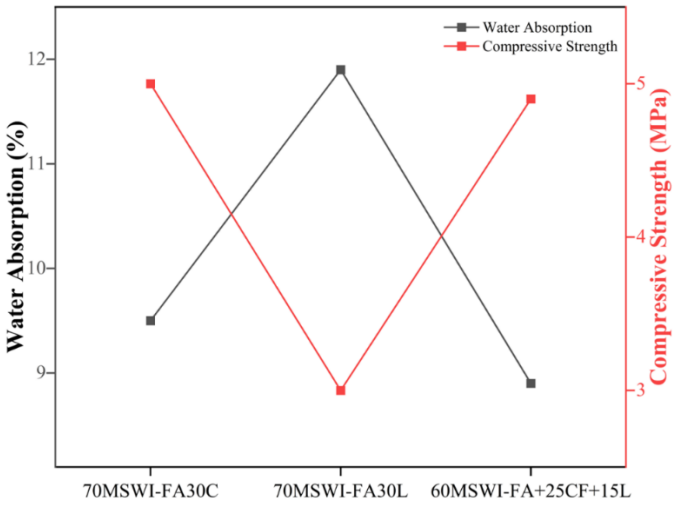

Figure 2.18 Water absorption and mechanical strength of cement and lime-based aggregates. Adapted with permission from Ref. [69].

However, sometimes higher "Ca" content hinders the formation of hydration products (i.e C-S-H, C-A-S-H) or a lack of other suitable components such as Si and Al, which are required for the hydration reaction to react with "Ca" to form

hydration products [56]. In the case of FA the crushing strength of aggregates increased, and the water absorption decreased with increasing amounts of either PC or Ca(OH)2 up to 10% and 5%, respectively. [117]. The hydration products are primarily responsible for the strength of the cementitious materials while other Ca-based compounds assist in improving their characteristics. Figure 2.19 presents physio-mechanical performance and the SEM micrographs, from which it can be observed that cement-based aggregates have a dense structure with C-S-H phases that contribute to better aggregate performance, while calcium hydroxide-based aggregates exhibit porosity and some unreacted binder, which is responsible for poor physio-mechanical characteristics.

Sample ID	Composition			Performance		
	OPC (%)	$Ca(OH)_2$ (%)	FA	Density (kg/m^3)	Water absorption (%)	Crushing strength (N)
90FA10PC	10		90	1765	13.34	557.4
90FA10CH		10	90	1609	18.46	285.8

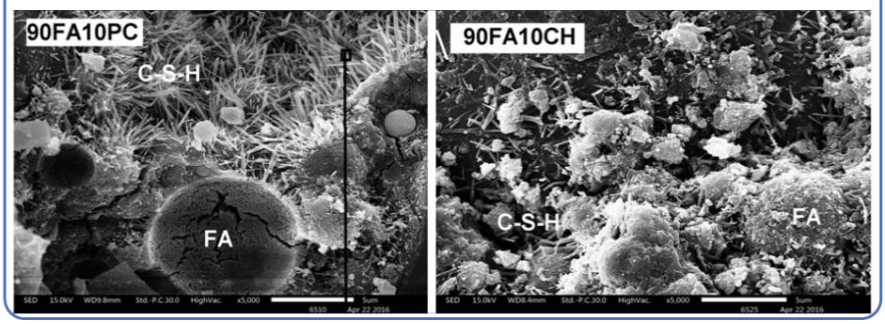

Figure 2.19 (a) Water absorption, density and (b) crushing strength along with SEM analysis of aggregates with OPC and CH. Adapted with permission from Ref. [117].

Lime has been shown to be a poor binder compared to cement when used alone as a binder in municipal solid waste incinerator (MWSI) applications, as only cement and coal fly ash/lime systems provided sufficiently high mechanical strength [69]. In another study, physio-mechanical properties showed the binder effect as follows: cement > cement + lime > lime [118]. However, it has been observed in the literature that adding GGBFS to a matrix of ash-based aggregates with lime as a binder result in better properties compared to cement, because lime activates and reacts with the higher CaO content in GGBFS. GGBFS is hydraulic in nature, hardens in the presence of water, and contributes to the overall strength of the aggregate [114].

Apart from the known binders, industrial waste was effectively utilized in the preparation of aggregates [119-121]. All these investigated materials belong to SCMs, meaning they contain all the essential chemical compounds required to carry out the pozzolanic reaction and form hydration products. The red mud (RM)-based aggregates were prepared using SCMs quarry dust I (limestone), quarry dust II (diabase), aluminum ash, FGD gypsum) as binders and successfully recycled 80% of RM [122] . It was observed that increasing the content of SCMs from 15% to 30% enhances the physio-mechanical performance of aggregates, with similar trends found for pelletization efficiency. Similarly, cold-bonded aggregates were successfully prepared from steel slag (SS) and miscanthus powder (MP). Aggregates prepared with 90% SS and 10% MP showed better water absorption and mechanical performance than those prepared with 100% SS; however, according to the EN 13055 standard, these aggregates are not classified as lightweight [121].

2.6 Environmental Performance

Artificial aggregates environmental assessment is equally significant as the mechanical and physical properties. To study the environmental impacts of artificial aggregates, leaching analysis of the heavy metals from aggregate's matrix is a parameter to be considered.

Leaching is a process in which a liquid (water or another chemical solution) passes through the solid matrix, dissolving and carrying away hazardous heavy metal ions into the surrounding environment. Figure 2.20 schematically shows how the leaching analysis of artificial aggregates is performed in the laboratory. Leaching analysis is one of the tools used to determine the environmental impact of aggregates by analyzing the release of hazardous contents (heavy metals and salts) into the environment.

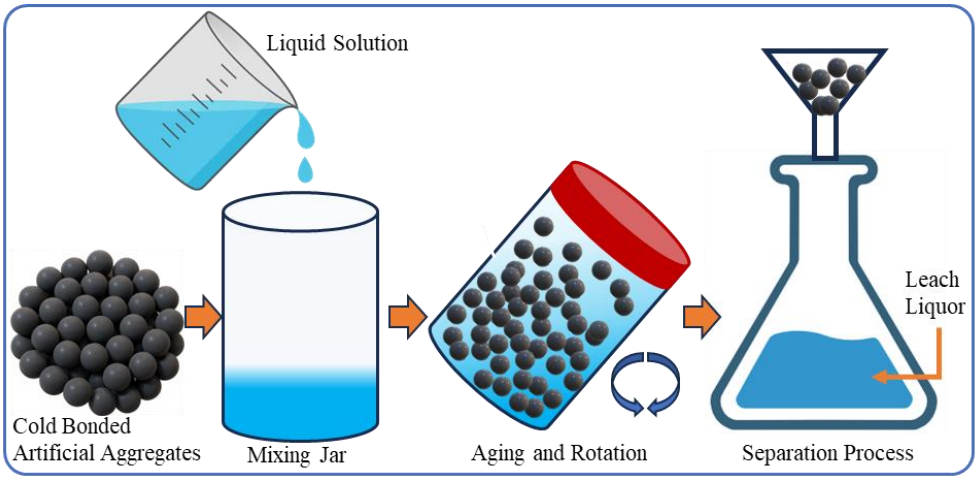

Figure 2.20 Schematic diagram for leaching process of artificial aggregates. Adapted with permission from Ref. [123].

Many waste materials are used in the preparation of artificial aggregates, and these materials contain various hazardous heavy metals. The formation of the C-S-H phase in cement-based artificial aggregates may encapsulate these heavy metals and prevent their escape [124], as C-S-H has lower water permeability [125]. The highly alkaline environment in cement-based aggregates favors the formation of less soluble heavy metal compounds, thereby decreasing leaching [126]. Additionally, heavy metals may also be captured in the hydrate lattice and are strongly bound in the cement matrix [124]. For example, the leaching results for powdered MSWI-BA and MSWI-BA-based aggregates, shown in Figure 2.21 22 indicate that converting waste materials into aggregates significantly reduces leaching behavior [127]. The aggregates solidify and stabilize the heavy metal content within the aggregate matrix and decrease its leaching into the environment [122]. The physicochemical encapsulation by hydration products (Aft, C(N)-A-S-H gel, and U-phase) is the primary reason for heavy metal solidification [128, 129]. Phosphogypsum, a hazardous waste material, releases 128.99 mg/L in its raw form, but this amount is reduced to 0.35 mg/L when converted into cement-based aggregates [130]. The formation of ettringite and C-S-H gel in cementitious materials effectively absorbs and solidifies phosphorus impurities [131].

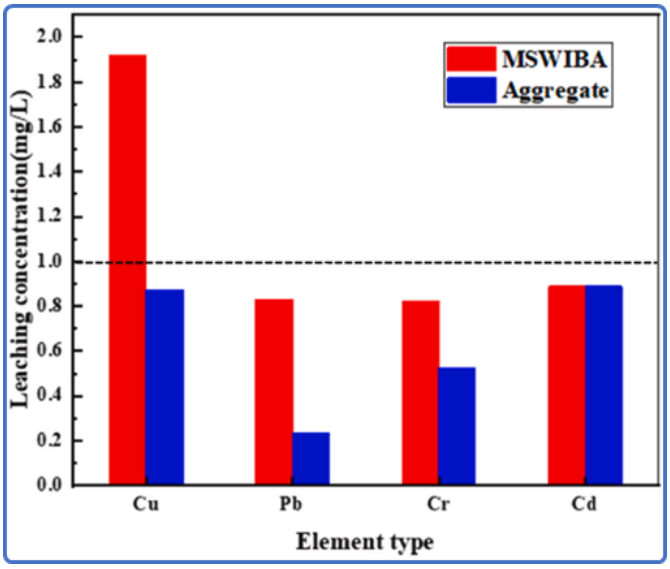

Figure 2.21 Leaching behavior of (a) powder MSWIBA and MSWIBA-based aggregate. Reprinted with permission from Ref. [127].

The leaching performance of two cement types, CEM III/B and CEM I/B, was compared, revealing that CEM III/B demonstrates superior performance due to its chemical composition, which includes a higher percentage of CaO and SiO_2. This facilitates the development of increased hydration products (C-S-H)[132], as also supported by [133]. Figure 2.22 summarizes the effect of the type of precursor used for aggregate preparation – fly ash-based aggregates (F group) compared with GGBFS-based aggregates (K group)—and various curing methods on the leaching behavior of the aggregates [57]. The formation of secondary hydration products in fly ash-based aggregates contributes to improved leaching behavior compared to GGBFS-based aggregates. The ettringite (AFm), which are double-layer hydroxides of calcium aluminum/iron hydrate, react with hazardous heavy metal ions and form interlayer hydroxyl groups [134]. This is also confirmed by XRD results, where dioptase ($CuSiO_3H_2O$) and dolerophanite (Cu_2O (SO_4)) were observed [57]. An increase in curing temperature favors the formation of hydration products and other compounds with heavy metals [57] which leads to decrease in Cu leaching. Greater formation of hydration products (Aft and Al gels) and enhanced pozzolanic activity result in a denser microstructure, which effectively reduces heavy metal migration [135].

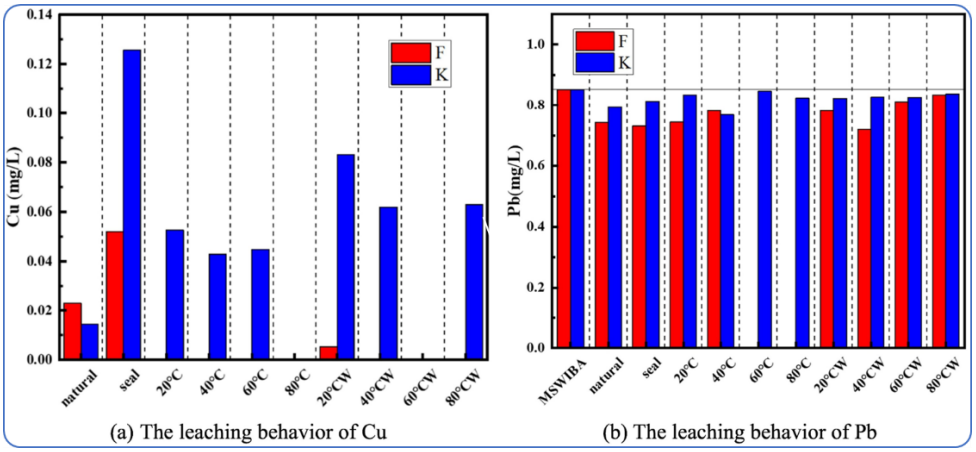

Figure 2.22 Leaching behavior of (a) Cu and (b) Pb elements from F and K group aggregates. Reprinted with permission from Ref. [57].

Usually, as the age of cement-based artificial aggregate increases, the leaching of heavy metal ions decreases. However, for some heavy metals such as Cr, Ni, Zn, As, and P, leaching first decreases during the initial 14 days and then increases [136]. It has been suggested that with longer curing times, the water content in the aggregate matrix is either consumed in further reactions (hydration or pozzolanic) or evaporates, leading to the development of more interconnected pores [136]. This situation allows the aggregate matrix to absorb CO_2 from the surroundings, which reacts with C-S-H, breaking the gel structure and releasing previously stabilized heavy metal ions from the aggregate matrix [137].

Besides the curing conditions and chemical composition of the precursor materials, pH also has a significant effect on the solidification and stabilization of heavy metals. A lower pH provides a favorable environment to reduce leaching, and vice versa. The literature suggests that high $CaCO_3$ and lower $Ca(OH)_2$ content in the aggregate matrix contribute to lowering the pH, which facilitates the solidification of heavy metal ions such as copper [57, 138]. Additives such as nano-silica also lower the pH of the CB-CBAAs matrix, which improves leaching, particularly of sulphates and molybdenum [16]. The origin (location, source, process, etc.) of the precursor materials also affects the leaching behavior of artificial aggregates [18, 69]. Physical properties such as the fineness of the precursor materials also influence the formation of hydration products; a larger surface area results in more hydration, leading to higher initial strength and improved stabilization of hazardous contents [124]. Aggregate physio-mechanical performance is closely related to

leaching behavior, as both depend on the porosity and microstructure of aggregates [69]. Surface treatment, such as double-step pelletization, reduces the leaching of heavy metals compared to untreated aggregates; the treatment material fills the pores and develops a dense structure, which reduces leaching [58, 61, 69, 139]. Surface treatments like double bonding via multiple pelletization provide physical barriers around the aggregate surface to prevent the leaching of heavy metal ions [50]. For example, the leaching behavior of CB-CBAAs prepared from phosphogypsum (80%) and slag (15%) improved by 43% when surface treated with an outer layer (50% slag, 45% phosphogypsum, 5% OPC) developed by dual-step granulation [140]. In another study by the same research group, double-step pelletization surface treatment was compared with slurry soaking for the same aggregates, but in this case, the material used for surface treatment was alkali-activated fly ash-slag. It was observed that slurry soaking reduced sulphate leaching by 86%, while multiple pelletization reduced it by 90% [77].

Alkali-activated aggregates more effectively solidify and stabilize contaminants in waste materials used as precursors, compared to the same waste in powder form [89, 105]. Alkali-activated cement effectively solidify/stabilize hazardous content in its matrix as compared to the Portland cement [141]. The type of precursor material (chemical composition) affects the leaching behavior of alkali-activated materials; for example, leaching of oxyanionic species (As, Cr, Mo, and V) in geopolymer with higher sodium content as compared to calcium because such composition favors oxyanions dissolution [142]. Also, the high pH of alkali-activation increases leaching of oxyanionic species which however, contradict the statement that some precursor like fly ashes have high pH prior to alkali activation [89]. But on the other side the leaching of elements like Pb, Cd and Ni decrease with increasing the pH and also the BFS presence showed better solidification/stabilization as compared to the fly ash [143]. The NaOH concentration affects the leaching behaviors of alkali-activated aggregates, as shown in Figure 2.23 [105]. Aggregates with higher NaOH concentration demonstrate better environmental stability. The higher alkaline environment help in curing heavy metals and promotes formation of various hydroxides, carbonates, silicates, and aluminates [144]. In alkali-activated aggregates, the presence of the

alkali activator results in the formation of polymer gels that encapsulate heavy metals and create a robust polymer molecular chain backbone [145].

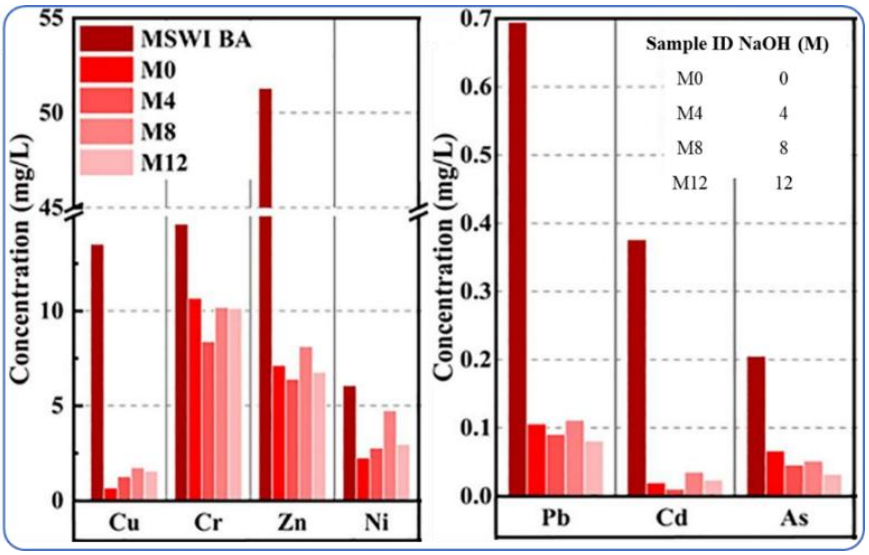

Figure 2.23 Effect of NaOH concentrations on MSWIBA+GBBFS-based alkali activated aggregates leaching behavior along with raw MSWIBA. Adapted with permission from Ref. [105].

The type of precursor affects leaching behavior; for example, blast furnace slag (BFS)-based geopolymers have been found to be better than fly ash-based geopolymers [143]. The main reason is the superior buffering capacity of BFS-geopolymers, due to the formation of C-A-S-H gel instead of N-A-S-H gel in FA-based geopolymers [143]. The type of heavy metal (i.e. Cr, Pb, Ni) and ion charge (anion or cation) affect the leaching process and its interaction with the precursor materials in the aggregate matrix [146]. Curing conditions influences the leaching mechanism of the heavy metal ion, as they affect the rate of chemical reactions and the formation of crystal growth [147]. The type of heavy metal in the precursor materials also shows dependence on the curing conditions [148, 149]; for example, in steam curing at 80 °C, copper forms a stable compound [148] but arsenic leaching increases because high temperature and humidity increase its diffusion and migration to the surface [150]. However, curing conditions that encourage the formation of a dense structure affect the physical retention of the heavy metal in the aggregate matrix [151].

The inclusion of cement in alkali-activated aggregate enhances leaching performance by forming additional hydration products alongside geopolymer gels [152]. In

literature, studies have been conducted on the leaching analysis of various alkali-activated waste materials, such as ashes and slags, for civil applications [153, 154] but studies on alkali-activated aggregates are very limited. Further research should be conducted on the leaching behavior of alkali-activated aggregates to identify specific influencing factors. In the field of alkali-activated materials, most existing research has focused on bulk materials, while relatively few studies have systematically addressed the behavior of aggregates. Although insights from the broader field of alkali-activated materials can be partially applied to aggregates, such knowledge transfer is not always directly appropriate. Aggregates represent a specific branch of alkali-activated materials, characterized by properties such as porosity, which might significantly influence leaching behavior.

2.7 Environmentally friendly and performance-boosting approach

An environmentally friendly and performance-enhancing approach, known as carbonation or accelerated carbonation, is applied to cold-bonded artificial aggregates. In this process, CO_2 reacts with the aggregate materials, where it is sequestered and forms compounds that improve the performance of the aggregates. The carbonation treatment of artificial aggregates is valuable as it reduces the curing period, increases strength, and stores carbon dioxide [155]. This approach contributes positively to addressing climate change [156, 157], as global warming remains an ever-growing concern. Wastes such as steel slag, incinerated ashes, and paper ashes are suitable materials for the preparation of carbonated aggregates [158, 159]. The carbonation methods applied to artificial aggregates are broadly divided into two types: the first is “post-granulation carbonation”, where fresh aggregates are treated in a CO_2 environment; the second is the “during and post-granulation carbonation” approach, in which CO_2 is supplied both during the granulation process and after granulation to the fresh granules. Both methods are explained in the following sections.

2.7.1 Post granulation-carbonation

The post-granulation carbonation approach, also known as “accelerated carbonation”, has been found useful in the literature and applied to aggregates to

increase strength and absorb CO_2. The main purposes are to enhance the properties of the aggregates and to sequester CO_2. The carbonate-able phase in the artificial aggregates absorbs CO_2 to form stable compounds that improve performance. [160]. The oxides present in the waste-based aggregates act as a medium to capture CO_2 [161, 162]. The calcium silicate phase and CH react with CO_2. An illustrative diagram of post carbonation is presented in Figure 2.24.

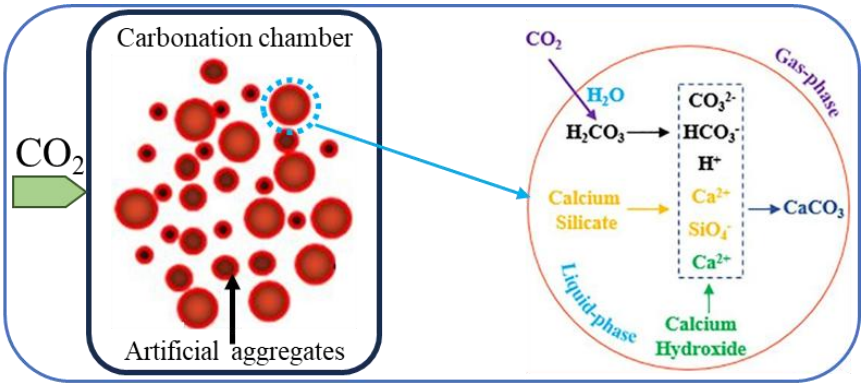

Figure 2.24 Carbonation process of artificial aggregates. Adapted with permission from Ref. [81].

The post-carbonation process occurs in four steps [81]:

Step 1: The gaseous CO_2 reacts with H_2O and forms H_2CO_3 solution, a process facilitated by the pores in the artificial aggregates.

Step 2: H_2CO_3 immediately decomposes into H^+, HCO^{3-}, and CO^{3-} ions, which lowers the pH value.

Step 3: The CH phase releases Ca^{2+} and SiO^{4-} as calcium silicate dissolves.

Step 4: The dissolution of the CH phase and carbonation of calcium silicate results in the formation of $CaCO_3$, which accumulates on the surface of the aggregates.

The following are the possible reactions that occur when aggregates are placed in a CO_2 environment, depending on the precursor materials. [81, 163].

$$Ca(OH)_2 + CO_2 \leftrightarrow CaCO_3 + H_2O \quad \text{Eq. 1}$$

$$CO_2 + H_2O \leftrightarrow H_2CO_3 \quad \text{Eq. 2}$$

$$Ca(OH)_{2_{H_2CO_3}} \leftrightarrow CaCO_3 + 2H_2O \quad \text{Eq. 3}$$

$$3CaO \cdot 2SiO_2 \cdot 3H_2O + H_2CO_3 \leftrightarrow CaCO_3 + 2SiO_2 + 6H_2O \quad \text{Eq. 4}$$

CO_2 sequestration reduces the environmental impact of CBAAs and improves the

performance of aggregates [81]. For example, Table No. 2.3 lists the properties of carbonated and uncarbonated aggregates prepared from wastepaper fly ash (WPFA), clearly indicating that their physical and mechanical properties are enhanced [164].

Table 2.4 Physical and mechanical properties of artificial aggregates before and after carbonation [164].

Specifications	Units	Non-carbonated LWA	Carbonated LWA
Aggregate form	–	Round	Round
Granular class	mm	2–16	2–16
Absolute density	(kg/m3) (±15%)	2105	2370
Bulk density	(kg/m3) (±15%)	897	902
Compressive strength	MPa (±10%)	3.15	7.6
Porosity	%	29	21
Water absorption (24 h)	% (±10%)	27.9	19.8

Figure 2.25(a) shows the optical images of the aggregates, clearly indicating that the aggregates have numerous pores (black spots) and a less densified surface before carbonation, while after carbonation, the aggregates exhibit a denser surface [164]. This densification occurs due to the formation of $CaCO_3$, which blocks these pores and forms a layer on the outer surface of the aggregate [136], as illustrated in the schematic diagram of pre- and post-carbonation aggregates in Figure 2.25(c). The internal structure of artificial aggregates is porous due to the entrapment of air bubbles during granulation [164] or due to physical and chemical characteristics of the precursor. The microstructure, with interconnected pores, has detrimental effects on performance; therefore, several treatment techniques are applied to aggregates to mitigate the effects of porosity and improve aggregate performance, such as treatment with CO_2, which reacts with calcium to form $CaCO_3$ and fills these pores to develop a dense microstructure [136]. Exposure of cementitious materials to a CO_2 environment enhance the performance [163], but prolonged carbonation has adverse effects [165]. The SEM micrographs of internal structures of aggregates, along with illustrations, are shown in Figure 2.25(b, d), which had pores and cracks before carbonation, but $CaCO_3$ formation fills these pores and cracks after carbonation.

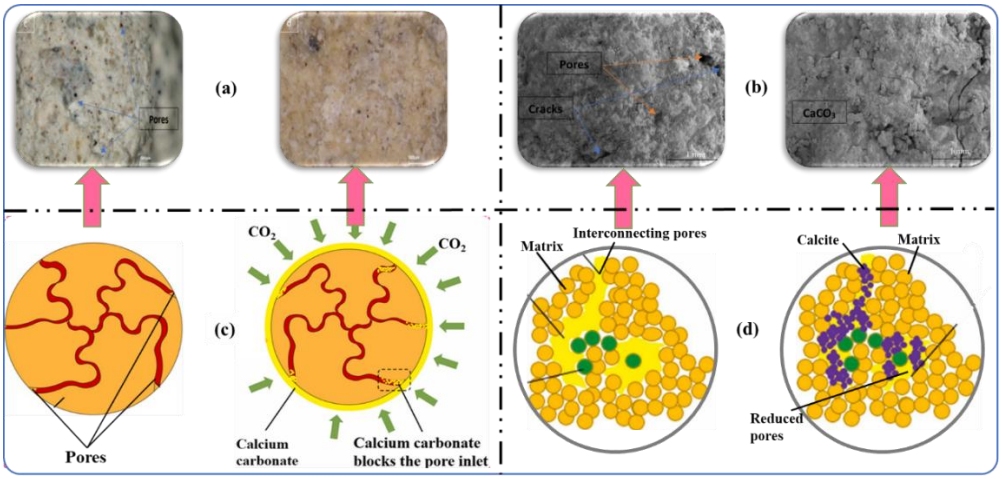

Figure 2.25 (a) Optical images, (b) SEM micrographs. Adapted with permission from Ref. [164] and (c,d) illustrative diagram of outer surface and internal structure of aggregates pre- and post-carbonation. Adapted with permission from Ref. [136].

Precursor materials with a higher content of calcium-based compounds were found to be more effective for carbonation because they react with CO_2 to form $CaCO_3$ [166]. Along with the hydration products in aggregate matrix, calcite precipitation [164, 167] acts as binding medium. In general, for CB-CBAAs, as the cement content increases, the strength of the aggregates increases. However, when subjected to carbonation, the strength decreases because higher cement content leads to greater CO_2 absorption, forming a strong and dense layer on the surface of the aggregates which hinders further CO_2 absorption and impairs additional carbonation [168]. In addition, the carbonation reaction is initially very intense due to the higher cement content. It is exothermic in nature increases the temperature of the curing chamber, creating thermal stresses in the aggregate matrix that lead to expansion, affecting the internal structure and causing cracks on the surface of the aggregates, thereby reducing mechanical strength [168]. For example, the mechanical strength of CBAAs prepared from MSWI-FA with 10% cement was 2.24 MPa, increasing to 3.14 MPa after carbonation. However, when the cement percentage increased to 50%, the strength dropped from 5.25 MPa to 4.09 MPa after carbonation [168]. Precursors with a higher Ca/Si ratio will form more C-(A)-S-H gel in the aggregate matrix, making it more vulnerable to decalcification during carbonation and resulting in more carbonaceous holes and cracks, which affect the original aggregate structure and negatively impact its strength [105]. Hence, for

carbonation, precursors with higher calcium-based compounds are desirable but should be added in an optimum amount to the aggregate matrix to maximize the carbonation effect.

The addition of organic precursors such as miscanthus powder increases CO_2 uptake by the aggregate matrix but decreases its strength if added above the optimum amount [121]. These materials have high intra particle porosity which allows to absorb more water and act as intermedia for CO_2 activation which accelerate carbonation and lead higher CO_2 sequestration [121, 169]. However, the amount should be optimised because higher levels of miscanthus powder-like materials themselves have poor mechanical characteristics. The SEM micrographs, together with the schematic microstructure and physio-mechanical characteristics of steel slag (SS) and miscanthus powder (MP)-based aggregate, are presented in Figure 2.26. The microstructure shows that the addition of MP increases porosity and allows more CO_2, but also decreases the bonding between slag particles, which reduces aggregate performance [121].

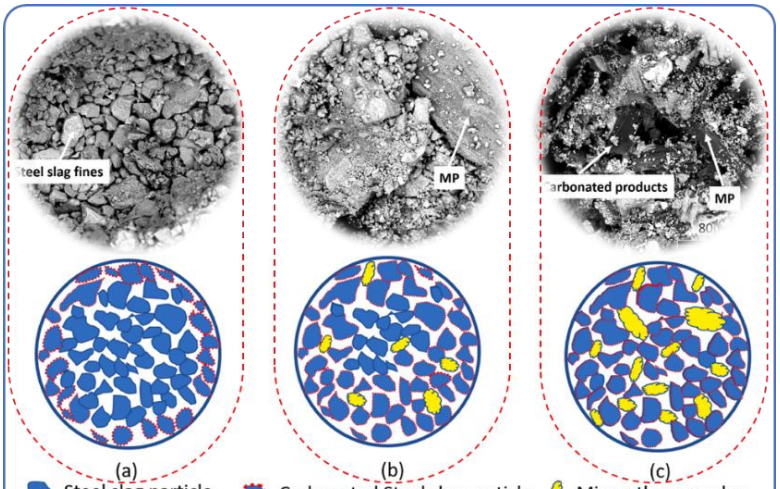

Water absorption (%)	5.86	5.09	18.83
Loose bulk density (kg/m^3)	1630	1300	760
Bulk crushing resistance (MPa)	4.0	4.8	0.99
CO_2 uptake (wt%/g pellets)	4.17	4.37	14.13

Figure 2.26 SEM morphology with schematic inner structure of (a) 100%SS, (b) 90%SS10%MP and (c) 65%SS35%MP aggregates along with physical mechanical and CO_2 uptake characteristic. Adapted with permission from Ref. [121].

The precursors with porous morphology generally enhance CO_2 sequestration but

do not necessarily improve aggregate performance. When porous material such as biochar (at 5%, 10%, 15%, and 20%) was added to CB-CBAAs prepared from red mud, the carbonation effectively decrease water absorption from the range of 17.96%–20.46% to 16.71%–17.04%, and increase bulk density from the range of 1.85 g/cm³–1.98 g/cm³ to the range of 2.02 g/cm³–1.83 g/cm³. However, mechanical strength decreased from 2–1.3 MPa to 1.6–1.3 MPa [170]. The mechanical strength decreases with the addition of biochar because the surface of the aggregates becomes denser after carbonation due to the formation of carbonation products such as calcite. This gives the aggregates a core-shell-like structure, as the calcite forms a dense layer on the surface of the aggregates, causing the densities inside and outside the aggregates to vary and resulting in non-uniform behavior under compressive load [170].

Carbonation was found to be most favorable for enhancing the performance of cement-based aggregates because of the presence of calcium-based components in the aggregate matrix, which react with CO_2 to form $CaCO_3$, while in alkali-activated aggregates, the polymerization gel is responsible for their performance, and the accumulation of carbonation products causes it to shrink and become more vulnerable to defects [105]. Before and after carbonation, SEM and EDS analysis of alkali-activated aggregates is shown in Figure 2.27 which clearly indicates that with the formation of carbonation products, cracks appear in the gel [105]. Secondly, the change in the polymer structure occurs due to the formation of sodium carbonate by extracting Na+ from the alkaline aluminosilicate geopolymer matrix, which disturbs the original structure of the aggregate and adversely affects its performance [171].

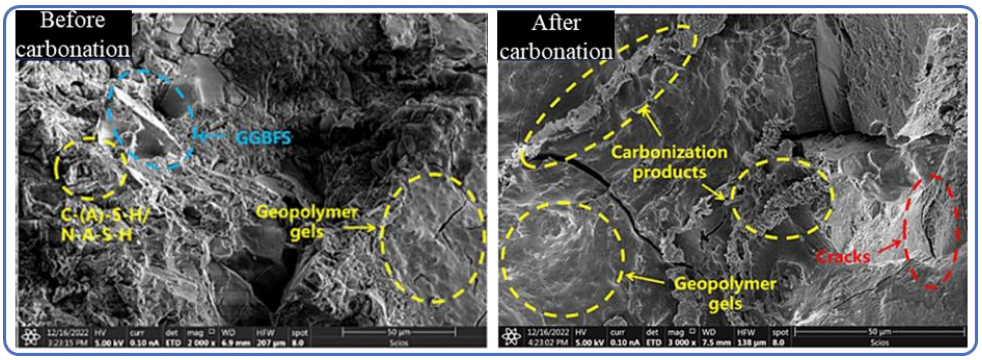

Figure 2.27 SEM/EDS analysis (a) before and (b) after carbonation. Adapted with

permission from Ref. [105].

Papers on the effect of carbonation on leaching behavior are scarce; however, it is argued that the accumulation of carbonation products physically retards the migration of heavy metal ions [172]. This is the area that should be further explored.

2.7.2 Factors affecting carbonation

The CO_2 concentration, temperature, humidity, time, and pressure within the carbonation chamber are considered carbonation parameters. These parameters influence the carbonation process and ultimately affect the aggregate's performance. In literature it was observed that faster carbon absorption were observed initially but as the time increase the rate of carbon absorption drops [136]. The slow carbonation in the later stage is due to the slower diffusion of CO_2 into the internal parts of the aggregate matrix [112]. In accelerated carbonation, CO_2 first encounters the aggregate's outer surface and then diffuse slowly along the internal pore network [173]. The development of reaction products densifies the structure, forming more tortuous pore network and slows down the rate at which CO_2 diffuses through the aggregate matrix [112, 174]. Increasing carbonation time will increase carbonation depth, as shown in the phenolphthalein images in Figure 2.28(a) for concrete slurry waste(CSW)-based aggregates [136]. However, the carbonation efficiency (rate) drops significantly. It is evident from Figure 2.28(b) that a high amount of CO_2 is absorbed in the first 7 days, but this decreases to 12–37% after 56 days for various CSW-based aggregates [136].

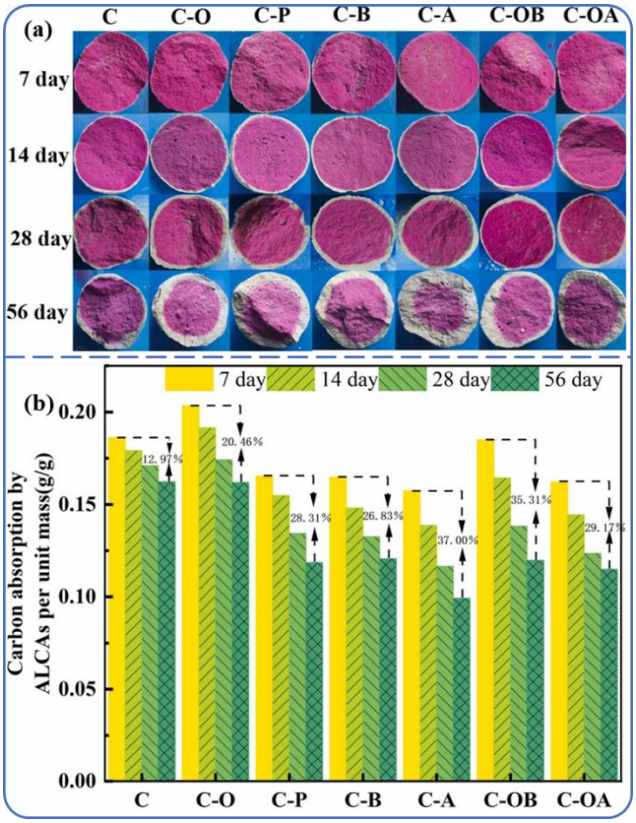

Figure 2.28 Phenolphthalein pictures and absorbing content of CO_2 for CSW-based aggregates cured for 7, 14, 28 and 56 days. Adapted with permission from Ref. [136].

Lengthy carbonation is ideal for sequestering CO_2, but when assessing the performance of aggregates, it can occasionally have a detrimental impact on the aggregate's properties. In the literature, it was observed for red mud-based aggregates that as the carbonation duration increases, the density increases and water absorption decreases, but mechanical performance declines after a certain carbonation period [81].The increase in density and drop in water absorption are due to formation of $CaCO_3$ [175], which accumulates in the pores present in the aggregate matrix. For example, for red mud and fly ash-based aggregates, after 6 hours of carbonation, a bulk density of 975 kg/m³ was recorded, which increased to 1019 kg/m³ after 24 hours of carbonation, while 24-hour water absorption decreased from 10.9% to 7.8%. Mechanical performance improves as carbonation time increases from 6 hours (7.6 MPa) to 12 hours (8.1 MPa) but then decreases to 7.8 MPa as carbonation time increases to 24 hours. The decrease in strength with increased carbonation time was attributed to the shrinkage of gel-like products, which causes micro-cracks and reduces strength [81].

The curing temperature in the carbonation chamber also affects the formation of carbon-based products. The temperature during carbonation influences the dissolution rate of precursor constituents, CO_2 solubility, nucleation, growth, morphology, and mineralogy of the carbon-based products. [176]. At higher temperatures (but still ≤ 100 °C), the dissolution rate of Ca-based compounds from precursor materials such as slag increases [177, 178]. It should be noted that the solubility of CO_2 in water decreases at higher temperatures, which might negatively affect carbonation [179]. An increase in temperature therefore leads to opposing effects on two main steps of the carbonation reaction: (1) the leaching of Ca^{2+} and Mg^{2+} from the precursor, and (2) CO_2 dissolution in water. For stainless steel slag-based aggregates, carbonation at high temperatures (60°C) showed that initially, calcium dissolution from the slag was higher compared to CO_2 dissolution, resulting in the dissolved CO_2 precipitating as $CaCO_3$ due to the higher concentration of Ca^{2+} ions [176]. Such a situation in the aggregate matrix disrupts $CaCO_3$ formation and results in a less dense microstructure with many small pores, which negatively impacts the physio-mechanical performance of the aggregates. At lower temperatures, CO_2 dissolution is higher compared to Ca-silicate, resulting in a higher CO_2 concentration in the aggregate matrix than Ca^{2+} ions. In this scenario, $CaCO_3$ precipitation occurs on slag Ca-rich particles. Such slow and controlled diffusion results in a dense microstructure with a small number of large pores, which imparts better physio-mechanical properties to the aggregates [176]. Figure 2.29 schematically shows in detail the leaching of Ca^{2+} and CO_2 details the leaching of Ca^{2+} and CO_2 dissolution, alongside the development of microstructure, with BSE-SEM images of aggregates cured in CO_2 at two different temperatures.

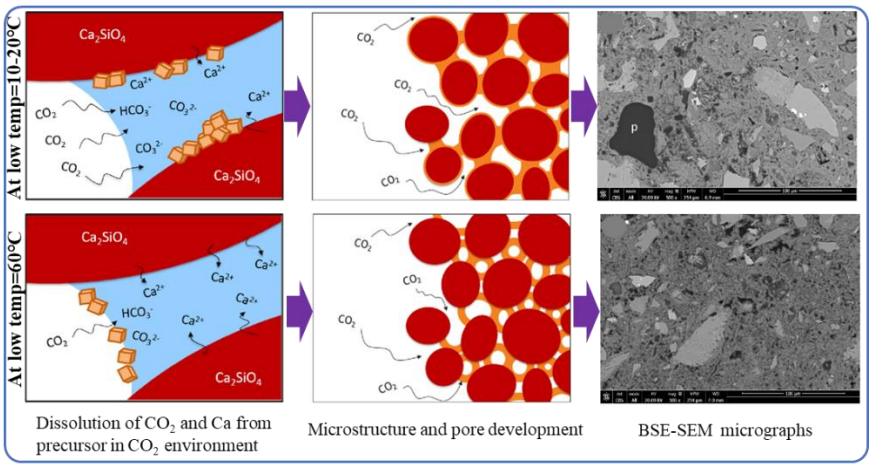

Figure 2.29 Schematic diagram of Ca^{2+} leaching and CO_2 dissolution to develop microstructure along with BSE-SEM images. Adapted with permission from Ref. [176].

Similarly, CO_2 concentration affects carbon uptake, the formation of carbonation products, and the development of the microstructure, but it has been argued that its effect is not as significant as that of temperature. A high rate of carbonation reaction has been observed at higher CO_2 concentrations, and When CO_2 concentration is lower, the rate of carbonation is not as high, but over time, a high conversion rate is achieved, producing more carbonation products [176].

The humidity during post-carbonation curing affects the solubility of CO_2 and thus determines the formation of $CaCO_3$. Carbonation is an exothermic process which rises temperature and cause to evaporation of water from aggregates and also the some water content used during hydration reaction or absorbed by amorphous silica which cause to reduces the intensity of carbonation [176]. In one study, the wet carbonation method involved placing aggregates in a porous basket and immersing them in water at a 10:1 liquid-to-solid ratio. CO_2 was injected into the water at a flow rate of 0.2 L/min. The aggregates were then placed in a drying chamber for 24 hours at 50°C and 50% relative humidity [167]. The author observed that bulk density increased by 4%, water absorption decreased by 14%, and mechanical performance improved by 8% in biomass ash and slurry waste-based aggregates. The wet carbonation process was found to be efficient, as water-dissolved CO_2 penetrated the porous aggregate structure, where small $CaCO_3$ particles formed, filling the pores and creating a denser structure [167]. However, the duration of such carbonation is short, so some pores remain partially unfilled, which may slightly

affect the aggregate's performance [167]. By comparing dry carbonation with wet carbonation, the latter was found to be more effective. For example, natural curing, dry carbonation, and wet carbonation were compared for CBAAs prepared from recycled concrete powder (RCP) and GGBFS. It was observed that mechanical strength increased by 25–40% with dry carbonation and by 70–90% with wet carbonation, compared to natural curing, while the effect on physical properties was not as significant as on mechanical properties. The authors observed that wet carbonation produced dense microstructures because water helps CO_2 penetrate the internal pores of the aggregates and react with Ca to form $CaCO_3$[166].

The application of pressure for a short duration during CO_2 curing has minimal effect on the physio-mechanical properties of aggregates, but this effect is more pronounced compared to wet carbonation. Biomass ash and slurry waste-based aggregates are placed in a sealed container, vacuumed to 0.5 bar pressure, and then CO_2 gas is injected at 0.1 bar while maintaining 50% relative humidity in the chamber. [175]. The author observed that bulk density and mechanical strength increased by 8% and 9% respectively, while water absorption decreased by 23%. However, if high pressure is maintained for a longer period, it forces CO_2 to penetrate the innermost parts of the aggregates, ensuring the formation of more calcite to fill the pores and develop a denser microstructure with improved physio-mechanical properties [167].

2.7.3 During and post granulation-carbonation

As the name suggests, carbonation occurs during the granulation process, and after granulation, the aggregates are treated in a carbon environment. An illustrative diagram is presented in Figure 2.30. The primary function of carbonation during granulation is to increase the reactivity of precursor materials and binders, decrease pores, and promote the growth of connective pores, thereby enhancing post-granulation carbonation and ultimately improving aggregate performance [180]. However, carbonation is an exothermic reaction that releases heat and requires additional water for granulation. The CO_2 concentration should be optimal to prevent the formation of aggregates with defective microstructure, which would affect the aggregate's performance [159, 180]. Very few studies were found on such

carbonation treatment, therefore, in this article two such studies were presented.

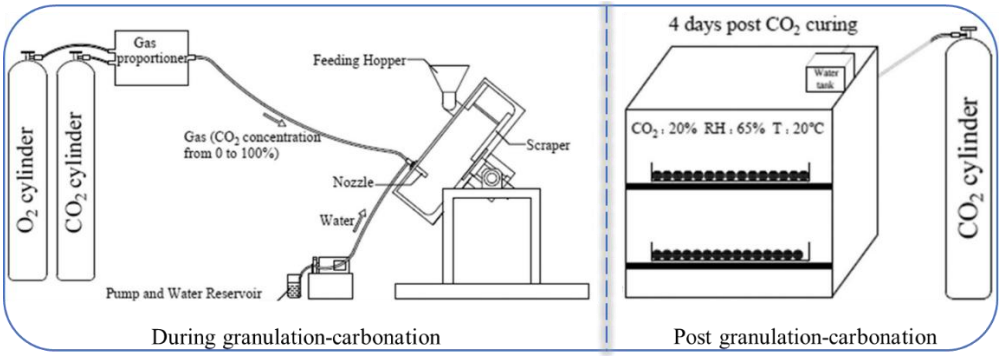

Figure 2.30 Illustrative diagram of during and post granulation-carbonation. Adapted with permission from Ref. [180].

Case Study 1 [180]: Different concentrations of CO_2 (x = 0, 10, 20, 34, 60, 80, 100%) were applied during granulation of BOFS-based aggregates and are divided into two groups, CxC and CxA, where "x" represents the CO_2 concentration during granulation. The CxC group aggregates are cured in a carbonation chamber for 4 days at 20 °C, 65% relative humidity, and 20% CO2 concentration. After 4 days, the aggregates are further cured in air under ambient conditions. The second group, CxA aggregates, are cured under ambient conditions. The influence of granulation carbonation on the mechanical performance (at 4, 14, and 28 days) of aggregates cured in a carbon environment and under ambient conditions is depicted in Figure 2.31(a) and water absorption after 4 days is shown in Figure 2.31(b). Considering the effect of CO_2 concentration during granulation, the results show that aggregates prepared with 40% CO_2 concentration during granulation perform better due to the early development of $CaCO_3$ [181, 182]. The higher concentration of CO_2 during granulation disrupts the microstructural development of aggregates, as the exothermic nature of the carbonation reaction leads to water evaporation, accelerating the drying of the aggregates and hindering the formation of hydration products, ultimately resulting in inferior aggregate performance [159]. Also, higher CO_2 concentration during granulation causes rapid precipitation of $CaCO_3$, forming a passive layer that prevents further carbonation [176, 183].

If the effect of the post-granulation curing regime is considered, aggregates cured in a carbonated environment have shown better performance compared to those

cured under ambient conditions. In post-granulation carbonation, the continuous availability of CO_2 allows complete reaction of CO_2 with $Ca(OH)_2$, C_3S, and C_2S present in BOFS, forming $CaCO_3$ and C-S-H. This results in a denser structure, enhancing mechanical strength and reducing water absorption [184, 185]. Compared to room temperature-cured aggregates, post-granulation carbonated aggregates contain a higher proportion of these products, resulting in a denser microstructure. The X-ray computed tomography images shown in Figure 2.31(c) (0 day and 4 days CO_2 curing) clearly indicate that aggregates prepared with 40% CO_2 concentration (C40C) during granulation have more pores (1.15% connected and 3.03% total porosity) when measured directly after granulation. The interconnected pores facilitate the diffusion of CO_2 into the aggregate matrix during post-granulation carbonation and ensure its reaction with the precursor materials, which reduces the pores and increases the carbon sequestration capacity. In contrast, for aggregates prepared with 100% CO_2 concentration (C100C) during granulation, the XCT image shows that their structure consists of granules of various sizes with a carbonated layer inside the aggregate matrix. At higher CO_2 concentrations, CO_2 reacts with BOFS particles and hinders their reaction with the binder and the formation of hydration products. Aggregates with such a structure, regardless of the curing regime post-granulation, negatively affect the physio-mechanical performance of the aggregate.

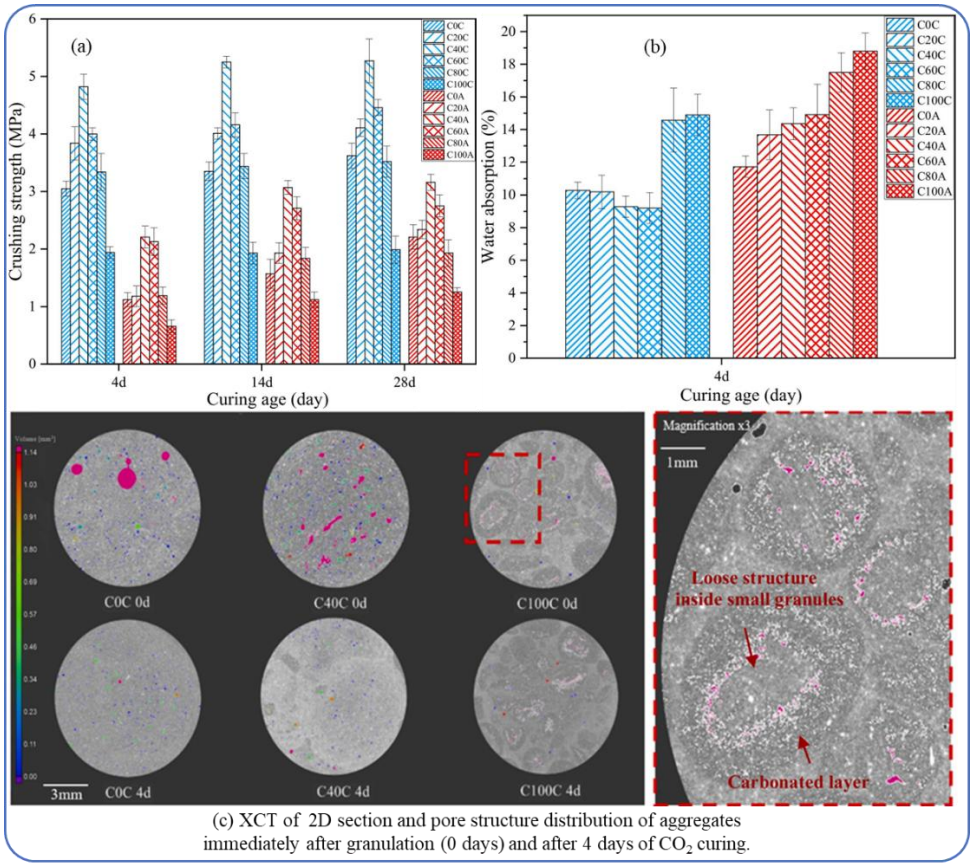

(c) XCT of 2D section and pore structure distribution of aggregates immediately after granulation (0 days) and after 4 days of CO_2 curing.

Figure 2. 31 (a) Crushing strength at 4, 14 and 28 days, (b) water absorption after 4 days and XCT-images of aggregates. Adapted with permission from Ref. [180].

Case Study 2 [159]: Another study prepared basic oxygen furnace slag (BOFS)-based aggregates and treated them under three different curing regimes; the performances are presented in Figure 2.32. The author compared the effects of the three curing regimes on the aggregates:

1. During and post granulation-carbonation (CC): 99.9% CO_2 concentration during granulation, followed by curing for 4 days in a controlled environment with 20% CO_2 concentration, 65% relative humidity, and a temperature of 20°C.

2. Post carbonation (AC): aggregates prepared in an ambient environment, then cured for 4 days in a controlled environment with 20% CO_2 concentration, 65% relative humidity, and a temperature of 20°C.

3. Ambient conditions (AA).

After curing for 4 days in the CO_2 environment, the aggregates were cured at 50% relative humidity and 20°C in air. Their physio-mechanical performance was studied after 7, 14, and 28 days, as shown in Figure 2.32. It was observed that no significant improvement was observed after 14 days.

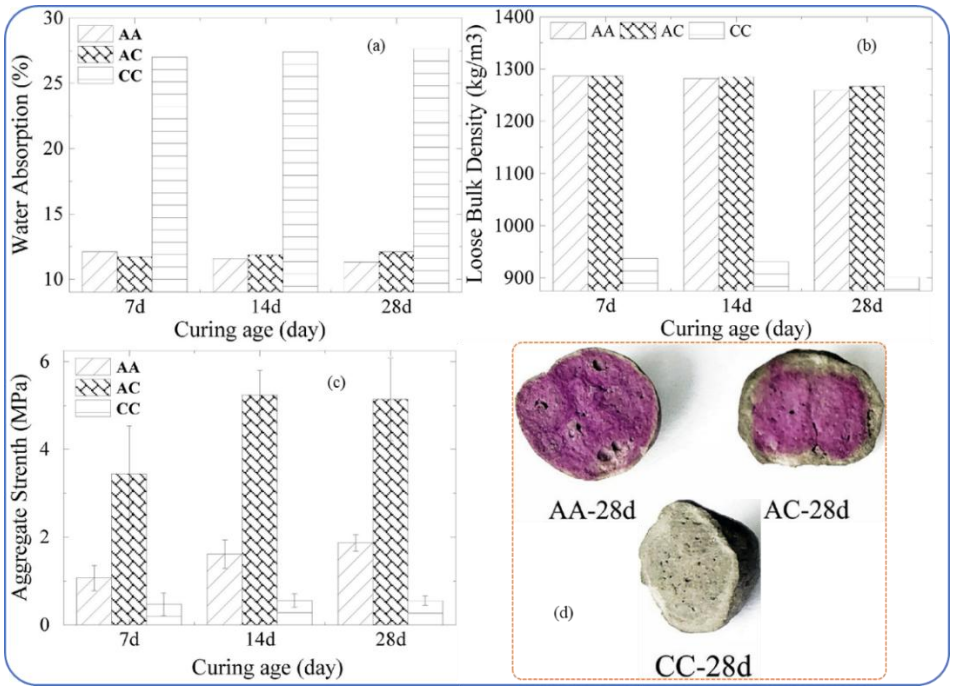

Figure 2. 32 (a) water absorption, (b) loose bulk density, (c) Mechanical strength and (d) Cross sectional image of artificial aggregates cured at various conditions. Adapted with permission from Ref. [159].

Among the aggregates, post-granulation carbonated (AC) aggregates have shown better overall performance compared to the other two types. This performance difference is attributed to the microstructure, as AC-treated aggregates have a denser and more compact structure than AA- and CC-treated aggregates, resulting in lower porosity. Additional carbon-based compounds, along with hydration products, were found in the AC aggregates, contributing to their dense structure. Synchronous carbonation during and after granulation results in aggregates with poorer performance because carbonation is an exothermic process that causes water to evaporate during granulation [159]. Lower water content causes some particles to remain unreacted, voids form in the aggregate matrix, and an increase in pores in the structure, all of which contribute to poor performance. The addition of CO_2 during granulation was found to enhance CO_2 sequestration and rapidly initiate the

formation of $CaCO_3$ and C-S-H products, which produce a dense microstructure and improved mechanical properties. However, a high CO_2 concentration is not favorable because it causes water evaporation and a rapid reaction with precursor materials, leading to the development of small granules with a carbonated layer within the aggregate matrix and reduced aggregate performance. Researchers need to further explore synchronized post- and during-granulation carbonation in terms of the optimum ratio between water addition and CO_2 concentration to improve aggregate properties and optimize CO_2 sequestration. Application of this procedure to different precursor- and binder-based aggregates is recommended, with subsequent performance and microstructure analysis.

2.8 Summary

In this chapter, various types of cold-bonded aggregates are discussed, and the main findings are as follows:

1) Cold-bonded aggregates are suitable as they are cured at ambient conditions or at slightly elevated temperatures (≤80°C). Based on the type of binder used, they are categorized into two main groups: cement-based and alkali-activated aggregates. In cement-based aggregates, hydration products define aggregate performance. The microstructure of cement-based aggregates is highly porous, but increasing the cement content can reduce this porosity, although this has negative cost and environmental impacts. Surface treatment is an effective method that significantly reduces porosity and improves physio-mechanical properties. Alkali-activated aggregates are shown as promise alternative, but the optimal combination of precursors and alkali solution concentration must be determined for each case.

2) These aggregates are made from industrial waste which might contain significant impurities in the form of heavy metals. The vitrified outer layer of high-temperature aggregates locks impurities within the aggregate matrix, while hydration products may encapsulate them in cement-based aggregates. In alkali-activated aggregates, the polymerization gel solidifies and stabilizes these impurities, but this area requires further detailed investigation to make

them suitable for construction applications.

3) Carbonation is an effective method to improve the performance of cold-bonded aggregates and to sequester CO_2. In alkali-activated aggregates, carbonation products can shrink the polymerization gel, which is responsible for aggregate strength. However, further research is needed to determine effective carbonation parameters such as temperature, moisture, and CO_2 concentration, and to provide economically viable solutions.

4) Artificial aggregates have significant potential to reduce pollution, reduce economic burdens and promote sustainability in the construction sector. However, their future still faces considerable challenges and obstacles in social, economic, environmental, technological, and regulatory aspects.

Despite many challenges, artificial aggregates have strong potential to move from laboratory to commercial scale, as they successfully convert waste into value-added materials. The growing demand for sustainable building materials, green building certification, and carbon footprint credits are driving artificial aggregate technology forward. With advances in technology and integration with renewable resources, more environmentally friendly aggregates can be produced. Ongoing research in the field of artificial aggregates is helping to develop and produce aggregates with improved technological properties.

Chapter 3: METHODOLOGY

3.1 Raw materials

The raw materials used to produce LWAAs are the MSWI-FA, marble sludge (MS), silica fume (SF), ground granulated blast furnace slag (GGBFS), and ordinary Portland cement (OPC). All the raw materials used to produce LWAAs are the industrial by-product and are used as secondary materials in the circular economy except OPC. The OPC complies with ASTM Type-I cement and is used as a binder.

Pre-treatment of MSWI-FA

The MSWI-FA collected from incineration plant located in Naples, Italy. According to the European Waste Catalogue (2000/532/EC), MSWI-FA is classified as the hazardous material due to the presence of chlorides, sulphates and other heavy metals [186] and not recommended to be used or disposed without pre-treatment. The presence of sulfates and chlorides in MSWI-FA raises concerns about its utilization in construction products [187]. Chlorides affect the cement's setting and hardening time and cause steel in the concrete to corrode [188], whereas sulfates promote delayed ettringite development, which deteriorates and expands concrete [189]. Therefore, to increase its performance in the cement matrix, the MSWI-FA must be pre-treated before being used in artificial aggregates. Pre-treatment of the MSWI-FA improve its inertization capacity in the cement matrix in order to guarantee the qualitative characteristics of LWAAs [58]. A two-step water washing pre-treatment process employed to MSWI-FA with a liquid-solid ratio of 2.5:1 and 90 minutes of retention time with continuous stirring for each step [190]. MSWI-FA washed with distilled water in two different ratios 2.5 and 10 liter/kg to select the optimum liquid to solid ratio. The change in pH (ΔpH) value of 10 liter/kg and 2.5 liter/kg was observed 3.52 and 3.20, respectively after the first wash. This observation supports that the higher liquid-to-solid do not have major effect, therefore, use of lower liquid-to-solid ratio, which is also supported by the literature [190]. The two-step water washing was justified as it significantly reduces chloride and sulfates concentration after second wash, while change in pH (ΔpH) value also increased. The chloride and sulfate ions concentration were carried out as per European standard (UNI EN 12457/2: 2004) for leaching test of wastes. The

resulting solutions after MSWI-FA washing were analyzed by ICP atomic emission and UV-VIS spectrometry. The H_3BO_3 were added to the solution to develop fluoride complexation and then analyzed to attain fluoride complexation and then ICP atomic emission spectrophotometry were performed. The values for change in pH (**ΔpH**), chlorides and sulphates concentration are listed in Table 3.1.

Table 3.1 The change in pH and chlorides and sulphates concentration after first and second washing cycles.

	First Wash	**Second Wash**
C[Cl^-] (mg/kg)	53852.2	8208.8
C[SO_4^{2-}] (mg/kg)	258392.1	59121.8
ΔpH	3.20	4.14

To observe the effect of pre-treatment washing on mineralogical composition of aggregates, XRD analysis was performed on unwashed and washed MSWI-FA. Figure 3.1 shows that unwashed MSWI-FA have major peaks for sodium chloride, sodium sulfate, calcium sulfate and iron oxide. Chloride and sulfate-based compounds are soluble in water and release Cl^- and SO_4^{2-} as was observed in leaching studies [191]. In XRD pattern (Fig.1) of washed MSWI-FA, the peaks for the chlorides and sulfates are absent compared to unwashed, and new compounds were formed due to dissolution of salts [192]. As MSWI-FA is supplementary cementitious material therefore it can be observed that due washing with water and then drying at 45 °C, some hydration products (hydrate and silicate) were formed.

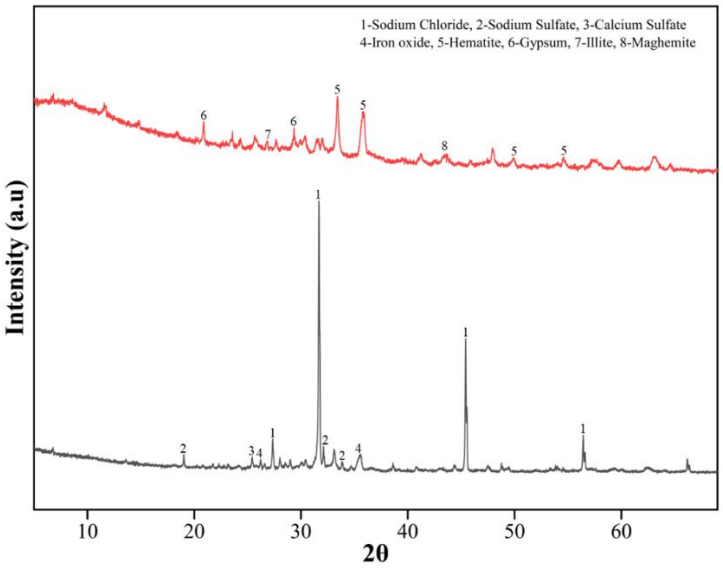

Figure 3.1 XRD patterns of unwashed and washed MSWI-FA.

The illustrative diagram in Figure 3.2 represents the washing method which is applied twice to ensure maximum removal of some hazardous contents. After each washing step, MSWI-FA were dried in the furnace for 24 hours at 45 ℃ which are adopted from the literature [193]. This type of ash treatment process is economically and environmentally viable as it consume less water [190] and also reduce the heavy metal concentration [29].The two-step washing process gives higher retention time to allow the soluble salt to dissolve in the water even at a lower solid-liquid ratio.

Figure 3.2 Illustrative diagram for MSWI-FA washing.

3.2 Aggregates preparation

Artificial lightweight aggregates were prepared through the CBP process. In the single-bonded CBP process, precursor materials such as washed MSWI-FA (75%,

65%, 55%), MS (15%, 25%, 35%) and OPC (10%) were introduced to the pelletizer, according to mix design presented in Table 3. A polit scale disc pelletizer with a diameter of 80 cm and inclination angle of 45º was used to form aggregates. According to previous work [190] the uniform speed of 45 rpm was used to ensure sufficient pelletization parameters. For the first 2-3 minutes the powdered materials were allowed to mix to homogenize and then the granulation fluid (water) was sprayed in intervals to ensure even wetting coverage.

The schematic diagram of aggregate production is shown in Figure 3.3.

Figure 3.3 Production of single and double-bonded artificial aggregates.

For single bonded aggregates (SBA), three different mixtures were produced with a fixed quantity of cement (10%) and variable content of MSWI-FA and MS (Table 3.2). The average amount of water added to the pelletization process is about 26% of the weight of the total dry mass. The fresh pellets were collected and cured at temperature of 18 ℃ and 95% relative humidity for 28 days to attain strength.

Table 3.2 Aggregates mix composition.

Single bonded aggregates				
Sample ID	**MSWI-FA**	**MS**	**OPC**	**Water-Solid Ratio**
S1	75%	15%	10%	0.26
S2	65%	25%	10%	0.26
S3	55%	35%	10%	0.26

After curing, a part of SBA was exposed to double pelletization by applying another

surface layer of GGBFS (50%), SF (20%) and OPC (30%) mixture to enhance mechanical performance. Surface treatment (outer layer) applied to the manufactured or artificial aggregates encapsulates it and improves their physio-mechanical performance [69, 194]. The same mixture was used for all double bonded aggregates (DBA) with 0.26 w/s ratio, using same operational parameters of disc pelletizer (angle 45⁰ and speed 45rpm). DBA was than exposed to temperature of 18 ℃ and 95% relative humidity for 28 days.

Figure 3.4 shows the cross-section of the SBA and DBA along with the outer layer developed over SBA.

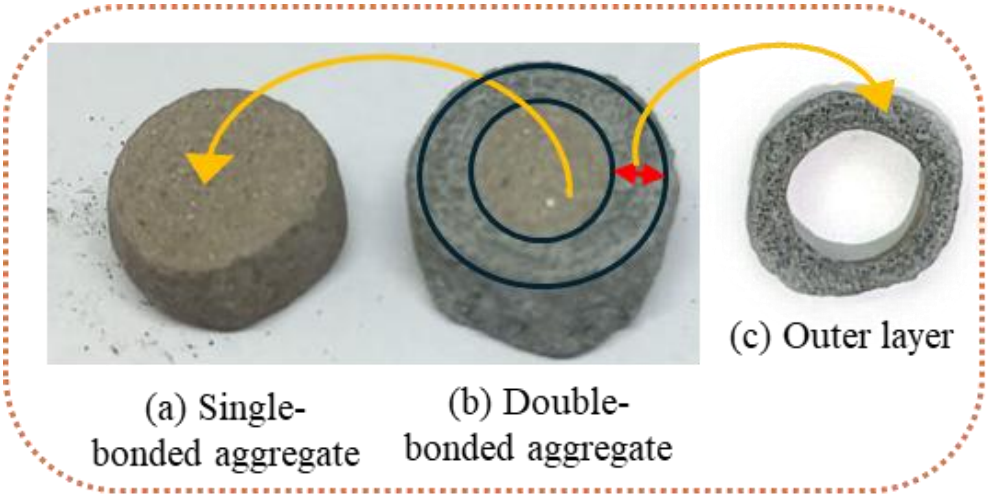

Figure 3.4 Cross-section of (a) single and (b) double bonded aggregate with (c) outer layer.

3.3 Performance evaluation of artificial aggregates

Compressive strength

The compressive strength test on SBAs and DBAs was conducted by using Toni NORM, Berlin, Germany, mechanical testing equipment. Approximately 30 aggregates samples with spherical geometry within the diameter range from 8 mm to 18 mm were tested and statistically examined. The following equation (Eq. 3.1) was used to calculate the compressive strength of single aggregates [68]:

$$\sigma = \frac{P * 2.8}{\pi d^2} \qquad \text{Eq. 3.1}$$

where “σ” stand for compressive strength (MPa), “P” load applied until failure (N), and “d” represent the diameter of aggregates (mm).

Water absorption

The water absorption of SBAs and DBAs was measured by drying aggregates in oven for 24 h at 110 ℃ until constant mass. The dry mass (m_{dry}) was measured and then aggregates were immersed in water for 24 h to measure saturated-surface-dry mass (m_{wet}). The absorption of water was calculated according to Eq. 3.2.

$$Water\ absorption = \frac{m_{wet} - m_{dry}}{m_{dry}} \times 100 \qquad \text{Eq. 3.2}$$

MIP

The mercury intrusion porosimetry (MIP) analysis was performed to study the total porosity, pore size distribution and bulk density of SBAs and DBAs, using MIP Autopore IV 9500 equipment. Aggregates in the size range of 8 mm – 18 mm were selected and dried in oven at 110 ℃ for 24 h.

XRF

To determine the loss of ignition (LOI) of precursors, the samples in powder form were heated at 550 ℃ for 2 h in furnace (Nabertherm B150) to burn out organic content and then further heated at 950 ℃ for 2 h to remove carbonates. The decrease in the mass of the mass of sample relative to the initial mass were presented as mass loss in the results.

For the elemental composition, X-ray fluorescence spectroscopy analysis (XRF) was performed using Thermo Scientific ARL PERFORM’X WD XRF spectrometer. The Fluxana(s) (FX-X50-2, Li-tetraborate and Li-metaborate mixture, mass ratio 1:1) were mixed with ignited precursor samples from the LOI analysis at the ratio of 1:10 to decrease melting temperature during the formation of the molten discs. LiBr solutions were added as the non-sticking agent which help to avoid melt glueing to the Pt crucible. The XRF measurement were analyzed using UniQuant 5 software.

XRD

The mineralogical composition of precursor materials and artificial aggregates were measured with X-ray diffraction (XRD) using Phillips PANalytical X'Pert PRO equipment (Empyrean X-ray diffractometer) with Cu Kα radiation (The Netherlands). The XRD equipment was operated with beam energy of 40kV and intensity being set at 30μA and measurement were made in the angle range of 5 – 80º on the 2θ scale by using Cu K alpha 1 radiations. The X 'Pert HighScore plus 3.0 Plus software developed by PANalytical were used for qualitative analysis of phase composition of each sample. The reference database ICDD PDF-2 was used for analysis of various phases.

FTIR

For observation of chemical bonds and functional groups, Fourier-transform infrared spectroscopy (FTIR; PerkinElmer Spectrum Two) was performed on powdered precursors in the range of 400 – 4000 cm^{-1} wavenumbers.

SEM

For micro-structural evaluation, the aggregate samples were cut into cross-sections and embedded in epoxy resin and polished. The samples were polished and coated with 10nm Au conductive layer. Samples were examined using Jeol JSM-IT500, under high vacuum mode. All the samples were analyzed using accelerated voltage of 20 kV to capture micrographs of 500x magnification and spot size of 50 μm to collect back-scattered electron microscope (BSEM).

TGA

Thermogravimetric analysis (TGA) was performed on crushed and sieved aggregate samples (<63 μm) using a STA 409 PC Luxx Simultaneous Thermal Analyzer (Netzsch-Gerätebau GmbH). The samples were heated from 25 °C to 1000°C at a rate of 10 K min^{-1} under a continuous nitrogen flow of 20 mL min^{-1} to prevent oxidation to assess the thermal stability and mass loss associated with dehydration, dehydroxylation, and decomposition of thermally unstable phases.

Leaching

The leaching test was performed on SBAs and DBAs according to EN 12457-2 standard. Aggregates were crushed bellow 4 mm and mixed with deionized water at a solid/liquid ratio of 1:10. The suspension was mixed at 10 rpm for 24 h at room temperature and then filtered to sperate liquid solution. The liquid leachate was measured using inductively coupled plasma mass spectrometry (ICP-MS, Agilent 7900).

Chapter 4: RESULTS AND DISCUSSION

4.1 Physiochemical properties of the Raw materials

The SEM micrographs for all the precursor materials are shown in Figure 4.1(a). The morphological structure of the silica fume shows polygon-like irregular geometry of sizes which ranges from 10 µm to several thousand microns [195]. The microstructure of GGBFS consist of rounded and irregular shapes morphology of different sizes which agglomerated together due to the shock cooling process [196]. The particle size of GGBFS usually range from 10 – 20 µm [197, 198]. The SEM micrographs of MS showed irregular particles with angular shape which is probably due to the aggressive process like cutting and sawing carried out to on marble [199]. The marble sludge was sieved below 250 µm to select and use very fine particles. The SEM analysis of MSWI-FA shows that its morphology consists of irregular and spheroidal particles [134]. The two-step washing of MSWI-FA significantly decrease the chloride salts which were not detected in the SEM micrographs [192]. The particle size of MSWI-FA are usually below 100 µm [200]. The mineralogical composition of the precursor materials is presented in Figure 4.1(b). XRD examination of SF showed a broad hump indicating an amorphous silica phase [201, 202] while GGBFS peaks for mullite, quartz, gehlenite, and calcite [203, 204] and marble sludge (MS) shows peaks for calcite and dolomite [205, 206]. The mineralogical compounds observed in MSWI-FA are hematite, gypsum, illite and maghemite. The different mineralogical compositions for MSWI-FA were observed in literature because of the composition of feedstock for incinerator changes in different regions. The FTIR spectra for precursors materials are depicted in Figure 4.1(c), in which SF shows strong band around 1050 cm^{-1}, corresponding to the asymmetric stretching of Si-O-Si. This band normally appears in the range 1200-1000 cm^{-1}[207]. Symmetric stretching for Si-O-Si was observed at 799 cm^{-1} band [201]. FTIR spectrum of GGBFS reveals the band vibration at 875 cm^{-1} for Si-O and Al-O were analyzed at 820 cm^{-1}. The aluminosilicate functional group appears in the range of 800-1100 cm^{-1} wavenumber [203]. FTIR spectrum of MS have obvious band at 1410 cm^{-1} which represent asymmetric vibrations and 710 cm^{-1} for symmetric stretching vibration for

carbonate ions [208]. The FTIR spectrum of MSWI-FA have band vibration for Si-O-X (X=Al, Si) at wavenumber equal to 1100 cm^{-1}[209, 210] and band vibration at 990 cm^{-1} represent Al-O-Si group [211]. The XRD and FTIR analysis are in accordance with the XRF observation which are listed in Table. 4.1, which confirm that CaO is more than 10% and classified as class C fly ash according to ASTM C618 standard [212].

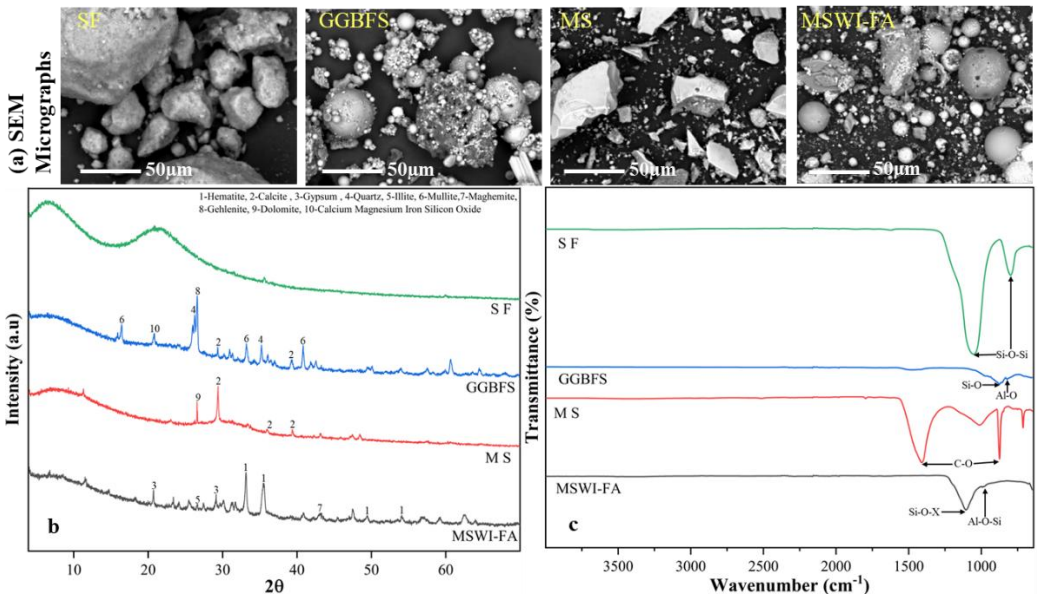

Figure 4.1(a) SEM micrographs, (b) XRD patterns and (c) FTIR spectra of all the precursor materials.

Table 4.1 Chemical composition of precursor materials (SF, GGBFS, MS and MSWI-FA).

	SF	GGBFS	MS	MSWI-FA
Na_2O, wt%	0.32	0.22	0.64	2.39
K_2O, wt%	0.55	0.07	0.97	0.59
CaO, wt%	0.08	9.83	24.27	19.18
MgO, wt%	0.66	4.21	2.24	3.38
Fe_2O_3, wt%	0.16	12.03	1.07	21.61
MnO, wt%	0.01	2.13	0.02	0.46
TiO_2, wt%	0.00	0.52	0.13	8.22
BaO, wt%	0.00	0.18	0.00	1.04
Al_2O_3, wt%	1.19	5.98	5.18	8.83
SiO_2, wt%	58.02	11.49	14.40	16.24
LOI	3.24	0.00	32.22	6.73

4.2 Properties of artificial lightweight aggregates

Mechanical Performance

The cross-sectional image of SBAs is shown in Figure 4.2(a) which are brownish colors as they are composed of blended mixture of MSWI-FA, MS, and OPC. The DBAs cross-sections are depicted in Figure 4.2(b) which is composed of the inner core of SBAs and the outer dark layer, which is composed of GGBFS, SF, and OPC. The SBA has visible white lumps, which indicate MS. The higher the proportion of MS in the aggregate matrix, the larger and more visible the lumps become which due to the reason that some MS particles remain unreacted.

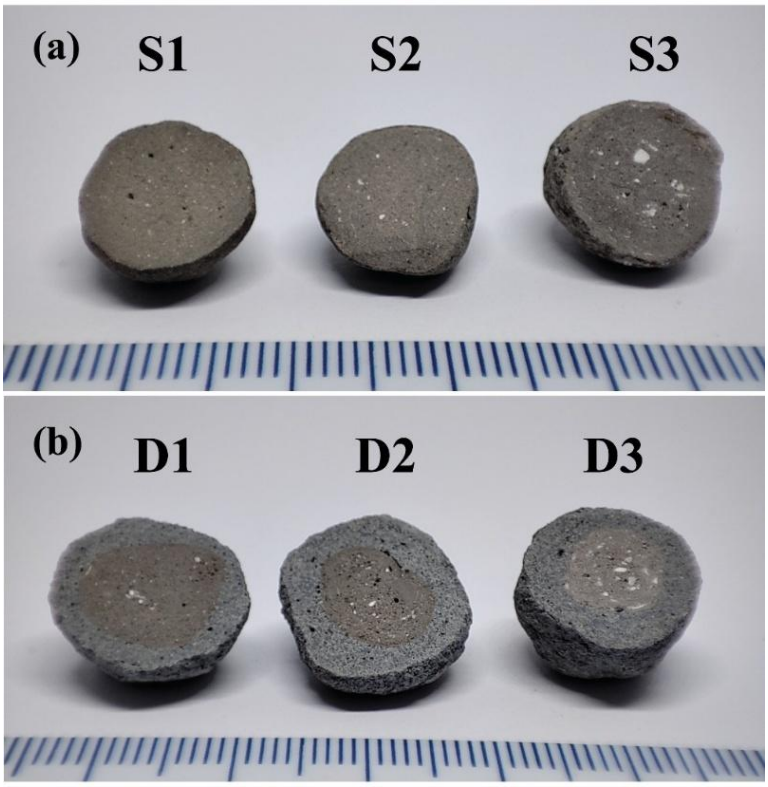

Figure 4.2 Cross-sectional image of SBAs (S1, S2, S3) and DBAs (D1, D2, D3).

The 28-day compressive strength of the SBAs and DBAs are shown in Figure 4.3. The compressive strength of aggregates decreases as the content of MS increases from 15% to 35% and MSWI-FA decreases from 75% to 55% which is due to reduction in pozzolanic activity. The addition of the MS affects the compressive strength of aggregates due to two possible phenomena. First, fill

the pores in an aggregate matrix which reduce porosity and improve material packing but for this purpose inert filling materials can also work [213]. Secondly, MS fine particles act as nucleation sites for the development of products like CH and C-S-H due to the presence of carbonate minerals and high surface area [213, 214]. Lower percentage of MS in cementitious materials will help to enhance the compressive strength of cementitious materials as it will act as filler material, but further increase will have negative impact [214, 215]. Because due to bigger MS particle size which makes it less reactive and remains unreactive in aggregate's matrix as shown in Fig. 7. The literature suggests that the supplementary cementitious materials (SCMs) with higher particle size will negatively impact the mechanical strength of cementitious materials [216]. Also, higher MS content in the cementitious matrix will require more water due to the large surface area of the sludge [217], but in this study fixe water-to-solid of 0.26 were used irrespective of MS content. Higher water content increases the water-cement ratio which leads to a dilution of the main clinker phases such as belite (C_2S) and alite (C_3S), which are responsible for strength development [213, 218]. On average the compressive strength of DBAs is 33.5% higher than the SBAs which is due to addition of outer layer composed of GGBFS (50%), SF (20%) and OPC (30%). The enhancement in the compressive strength of DBAs compared to SBAs are in line with the literature [219, 220]. The presences of OPC along with pozzolanic materials like GGBFS and SF form a strong and dense outer layer which enhance resistance to compressive load. The compressive strength of DBAs decreases from D1 to D3 which is due to the higher content of MS in S3 inner core. In DBAs, high standard deviation was observed which is due to heterogeneous outer layer thickness and observed cracks at interaction face of inner core and outer shell which might appear due to the suboptimal bonding, as confirmed by SEM micrographs.

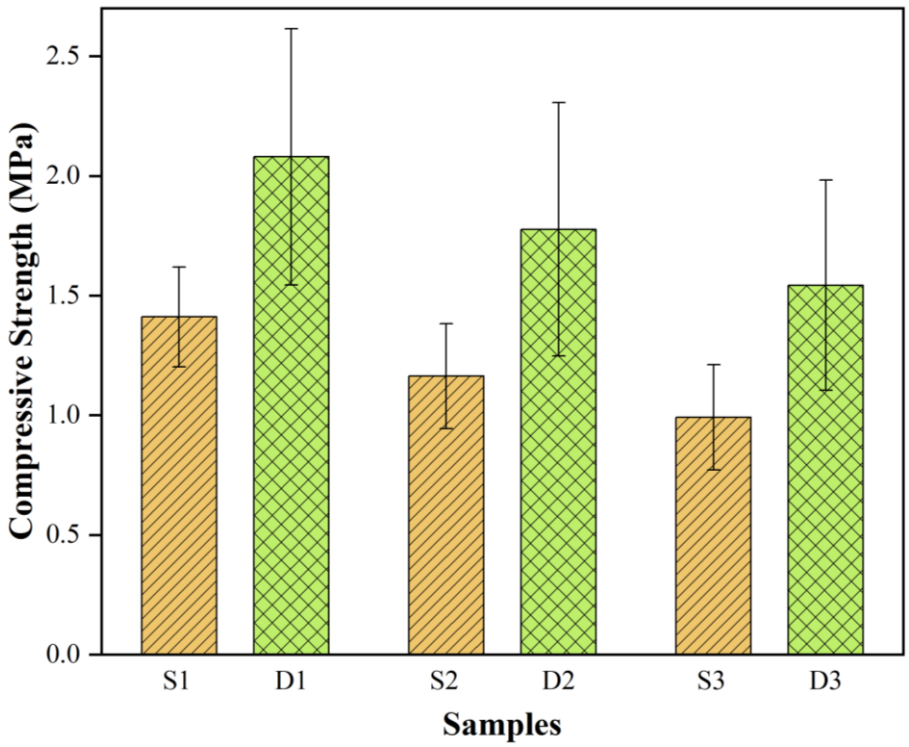

Figure 4.3 Compressive strength of single bonded and double bonded lightweight artificial aggregates.

Water absorption and bulk density

The water absorption and bulk density of the SBAs, DBAs and outer layer are reported in Table 4.2 considering aggregates size in the range of 8-16 mm. The water absorption for SBAs is in the range of 12.87% - 14.21% and in case of the DBAs 16.62% - 17.12% was observed. The values for water absorption are in the range of 10% - 18% which corresponds to the range for commercial artificial aggregates [69]. The aggregates with similar range of water absorption values are of great interest as it can mitigate shrinkage in concrete and allow internal curing [69, 221, 222]. In the case of SBAs, the water absorption and total porosity of the aggregates increase with the increasing MS content while the bulk density decreases, which is due to lower reactive nature of MS which is explained in detail in the section above. The decrease in the bulk density of SBAs with increase in the MS content may be due to the lower specific gravity of the MS (2.67) as compared to other components [218]. The artificial aggregates prepared in this work are classified as lightweight aggregates, as the bulk density values are in the range of 1.4 – 2.4 g/cm^3 outlined in the standard UNI EN 12620 [223].

The outer layer in DBAs slightly increase its water absorption as compared to the SBAs and decreases bulk density while having mixed effect on the total porosity. The physical properties of both lightweight SBAs and DBAs are consistent with the literature [219]. The total porosity of the SBAs samples S2 and S3 decrease when double-bonded with outer layer (D2, D3) except the S1 sample where the porosity increases of D1. This might be the fact that high thickness of the outer layer forms around the S1 because of higher content of MSWI-FA which has good chemical interaction with the outer layer components.

Table 4.2 Water absorption of SBAs and DBAs.

Sample	Water Absorption (%)	Bulk Density (g/cm^3)
S1	12.87	2.04
S2	13.6	1.95
S3	14.21	1.85
D1	16.62	1.70
D2	16.74	1.68
D3	17.12	1.71

Mercury Intrusion Porosity (MIP)

The characteristic main pore size peak of SBAs, DBAs and outer layer were observed below 1 µm as shown in Figure 4.4. The SBA has shown prominent peaks between 0.1 µm to 1 µm which become more tilted towards 0.1 µm as the MS content increases because it acts as filler materials to reduce pore. The outer layer developed during the double palletization step were manually removed and its MIP analysis was carried out which shows prominent curve in the range of 0.01 – 0.1 µm which indicate meso-pores in it. The pore size of the outer layer decreases due to higher content of OPC (30%) with pozzolanic materials

like GGBFS (50%) and SF (20%) [224]. When the outer layer was applied to the aggregates via double palletization, the intensity of the peaks drops and pore size decreases. In case of D1 sample, the peak slightly drops and shift towards 0.1 µm while for D2 the drop is obvious which clearly indicate that the pore density in that region drops. An additional small curve was observed around 0.01 µm which clearly indicate pores of the outer layer. Different MIP curve was observed for D3 sample with the prominent peak in range of 0.01 – 0.1 µm which is due to the outer layer and higher content of MS.

The total porosity an important property of the aggregate which determines its mechanical strength and permeability [219]. The total porosity of 30.72%, 33.49% and 34.94% for the SBA samples S1, S2 and S3 was observed while for the DBA samples D1, D2, and D3 these values are 34.8%, 31.44% and 32.17% respectively while the value for the only outer layer is 32.20%. The porosity of the samples are on higher side which is due the presences of large pores and small empty space around MS clumps [219]. The porosity of SBAs increases with the decrease in MSWI-FA content and increasing MS content which is due the fact that some of the MS remain in clumps form in the aggregate matrix. The DBAs did not show any increase or decrease trend like for D2 and D3 the porosity drops as compared to the S2 and S3 but in case of D1 sample, its porosity increase as compared to S1 sample. This unusual behavior of the D1 sample is due to the better interaction between the inner core (S1) and outer layer as MSWI-FA content is higher in S1 as compared to other samples which lead to formation of thick outer layer [219]. The MIP observations are consistent with the mechanical performance of the aggregates (Figure 4.3).

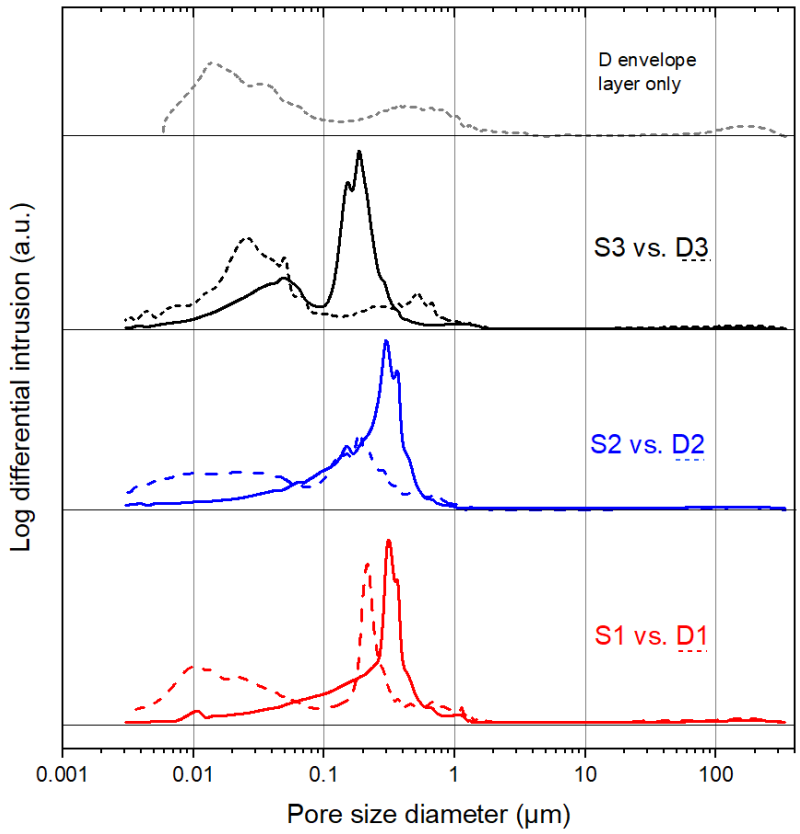

Figure 4.4 Pore size distribution of SBA with corresponding DBA (dashed line). The topmost plot (grayish dashed line) corresponds to the isolated D envelope layer only.

X-ray diffraction (XRD)

The XRD patterns of artificial aggregates with varying compositions of MSWI-FA and MS, as well as an outer layer composed of GGBFS, SF, and OPC, are depicted in Figure 4.5. The XRD reveals that main mineralogical phases of S1, S2 and S3 are hematite, calcite, quartz, hemicarbonate, ettringite, portlandite, calcium silicate hydrate (C-S-H), tricalcium silicate (C_3S) and dicalcium silicate (C_2S). Washed MSWI-FA was used for the preparation of aggregates that have a lower chloride and sulphate content, which benefits durability [225, 226]. In all three SBA samples, dominant peak was found for calcite at 29.4° which is because of MS as it mineralogically composed of calcite (crystalline phase) and mostly remain unreactive and dominate XRD pattern of single bonded aggregates. But in SBA samples, broader diffraction was observed from 2θ equal to 29° and 32° which indicate the presence of poorly crystalline C-S-H which is overlapped by well-ordered calcite main peak because well-polymerized C-S-H is usually not observed in XRD due to amorphous nature

[112, 227, 228]. This diffraction is broader in S1 as compared to S2 and S3 which suggest denser and more cohesive binding matrix which also reflects in their physio-mechanical properties. Another reason for broader peak is the substitution of Al (from MSWI-FA) in poor crystalline C-S-H which might increase structural disorder [229]. With higher MS content, more Ca^{2+} and higher alkalinity favors the precipitation of C-(A)-S-H, which tends to be less dense and less cohesive than pure C-S-H [230]. The intensity of the ettringite ($Ca_6Al_2(SO_4)_3(OH)_{12}\cdot 26H2O$) reflections increased with MS content (S1 < S2 < S3). Because higher Ca availability from MS and limited reactive aluminates from reduced MSWI-FA content, increase the alkalinity and carbonate buffering capacity within aggregate's matrix which promote sulfate-aluminate reaction. Washed MSWI-FA was used for the preparation of aggregates that have a lower chloride and sulphate content (Table No. 1), which benefits durability and not primarily assist in formation of ettringite [225, 226]. Furthermore, the dilution of reactive silicates from MSWI-FA with increasing MS content may have slowed C–S–H formation, leaving more aluminates available for ettringite crystallization.

Hemicarbonate ($Ca_4Al_2(CO_3)_{0.5}(OH)_{13}\cdot 5H_2O$) peaks were observed for SBA samples which typically form through the carbonation of AFm phases produced during OPC hydration [231]. Higher amount of MSWI-FA content in S1 likely provided more reactive aluminates, favoring AFm formation and subsequent conversion to hemicarbonate. Othe minor peaks observed in SBA samples were observed for residue alite ($3CaO\cdot SiO_2$) and belite ($2CaO\cdot SiO_2$) at 32.15° and 32.5° 2θ angle, respectively which were formed due to incomplete hydration because fixed water-solid ratio of 0.26 were used for aggregates preparation irrespective of its composition. It is anticipated that the behavior of the aggregated granules hydration will differ from that of the casted or cement paste samples, as lower w/c is required to achieve optimal liquid agitation of particles through liquid bridge formation and flocculation in initial phase of mechanical cold bonded pelletization [232]. Minor peak was observed for portlandite ($Ca(OH)_2$) attributed to the lower cement percentage in aggregate's matrix and higher percentage of MS (less reactive) and MSWI-FA (SCMs).The MSWI-FA

contains reactive silicates and aluminates, the portlandite undergoes pozzolanic reactions that progressively consumes it and over period of time forms C-S-H or C-(A)-S-H.

The outer layer (composed of GGFS, SF and OPC) have characteristics peaks for calcite, quartz, mullite, cristobalite and hematite. The outer layer in DBA samples, enhanced the mechanical strength of SBA aggregates due to higher content of GGBFS and its Al effectively contribute in the formation of well polymerized C-A-S-H gel [233]. The GGBFS and SF are highly reactive SCMs, they consume portlandite relatively fast [234, 235].

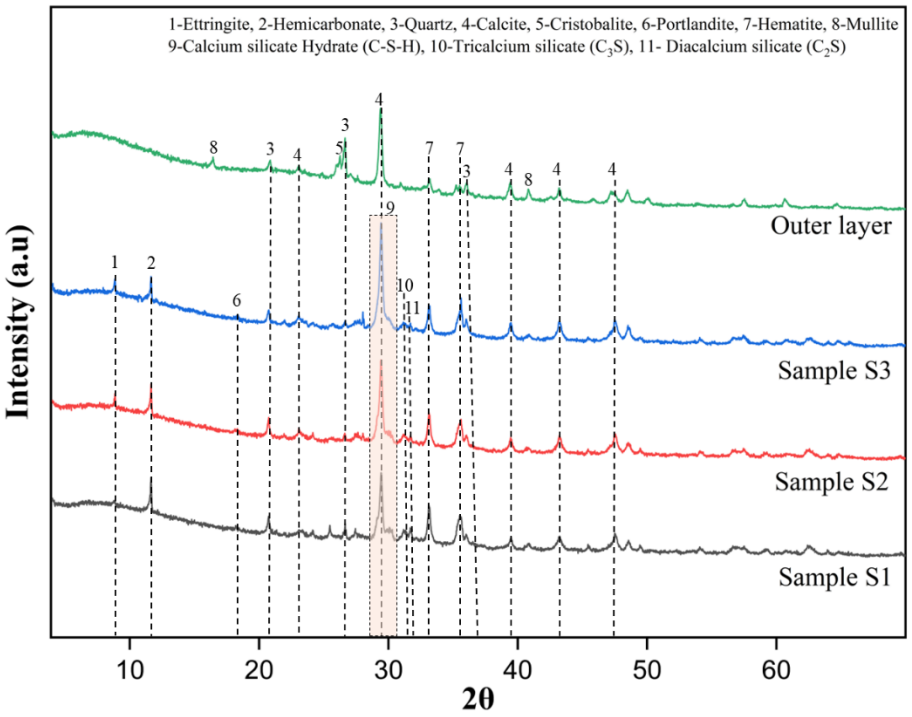

Figure 4.5 XRD patterns for S1, S2, S3 samples and outer layer.

Fourier-transform infrared spectroscopy (FTIR)

Figure 4.6 depicts the Fourier transform-infrared (FTIR) transmission spectra of the prepared artificial aggregates sample (S1, S2, S3) and the outer layer. The FTIR analysis of single bonded aggregates (S1, S2, S3) revealed characteristics stretching for Si-O in hydration products (C-S-H or C-A-S-H), calcite and aluminosilicates (Si-O-Si or Si-O-Al). The narrow peak observed around 3540cm-1 represents complex asymmetric stretching vibration of O-H group

[236, 237], while minor neck at 3410 cm-1 observed in single bonded aggregates corresponds to Al-OH stretching vibration in $[Al(OH)_6]^{3-}$, octahedral structure of ettringite and hydrocalumite [238] for single bonded aggregates. The weak absorption at 1620 cm-1 is associated with the H-O-H bending vibration of the water lattice in C-S-H gel [239]. Asymmetric stretching vibrations in the range of 1410-1430cm^{-1}, out-of-plane bending vibration at 875 cm-1 and in-plan vibration at 712cm^{-1} represent carbonate group CO_3^{2-} (calcite) were observed in single bonded aggregates (S1, S2, S3) due to MS and as well in outer layer which composed 50% of GGBFS [239-241], consistent with XRD analysis. The peak observed at 1120 cm-1 related to stretching vibration of S-O which indicates the presence of sulfates and also prove the existence of gypsum as observed in XRD analysis [236, 242]. The peak appearing at 1004 cm-1 are linked with asymmetric stretching vibration of Si-O-Si group which is formed because of cement hydration and geopolymerization [95, 242] observed in both S1, S2, S3 samples and also in outer layer but slight shifted towards higher wavenumber (1040 cm-1). The peak at 671 cm-1 characterize as T- Si-O (T=Al or Si) band [243] which confirm formation of aluminosilicates and absorption band at 603 cm-1 which is in the range of 648-515 cm-1 corresponds to the Fe-O group [243] which belongs to hematite mineral present in single bonded aggregates as per XRD analysis. The stretching vibration at 436 cm-1correponds to O-T-O (T=Al or Si) which indicates the pozzolanic activity in aggregates matrix [244]. The outer layer have two different peaks at 788 cm-1 and 446 cm-1 which are associated with the Al-O bond [95] and Si-O asymmetrical bending vibration [239] respectively . Al-O bond belongs to the mullite in GGBFS and Si-O indicates the silica which is a precursor in outer layer which is also observed in XRD analysis.

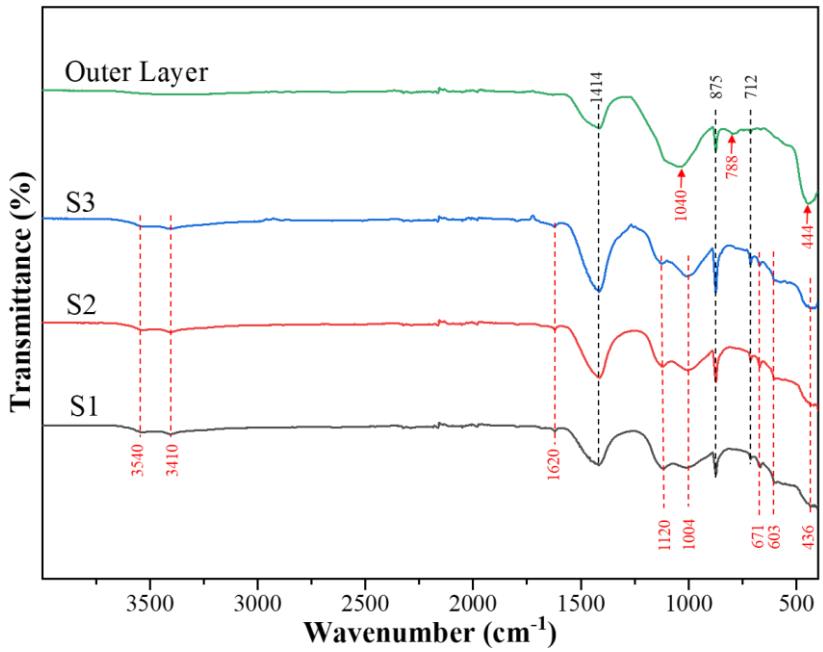

Figure 4.6 FTIR spectra for S1, S2, S3 samples and outer layer.

Thermogravimetric analysis (TGA)

Thermogravimetric analysis describes the formation of hydration products in artificial aggregates sample by analyzing decomposition of reaction products at high temperature. Figure 4.7(a, b) illustrates the weight loss and DTA behavior of SBA samples (S1, S2, S3) and outer layer in the range of 25 – 1000 ℃. The weight loss observed for S1, S2 and S3 are equal to 14.02%, 15.56% and 18.23% respectively, which reflects that the content of MSWI-FA and MS effect weight loss behavior, while 15.45% of weight loss were observed for the outer layer. The weight loss of all samples is divided in three zones according to temperature range: zone 1 (25-300℃), zone 2 (300-700℃) and zone 3 (700-1000℃).

In the zone 1 with the temperature range of 25-300℃, the weight occurs due the loss of physically bonded water and decomposition of C-S-H gel [237, 245], which have clear peak around 100 ℃, and C-A-S-H have slightly lower peak maximum, as Al incorporation increase bound water and lowers thermal stability of gel [246]. The outer layer has more pronounced peak for C-A-S-H gel at lower temperature as compared to SBAs samples as it contains GGBFS [247]. Due to poor crystallinity of these gels, XRD analysis shows that their peaks were overlapped by others, like calcite overlapped C-S-H while FTIR confirm their presences.

The weight loss in zone 2 (300-700°C) represents decomposition of $CaCO_3$ with pronounced major peak at 600-650 °C [105, 237], and dihydroxylation and dehydration of interlayer water from hydration products [248, 249] The $CaCO_3$ decomposition peak is intense for sample S3 as it has 35% of MS while its intensity drops as the MS percentage drops to 15% in sample S1. The outer layer does not have an intense peak for $CaCO_3$ decomposition because it does not contain MS in its composition. The weight loss behavior in zone 2 for SBAs sample is similar but only intensity changes while the behavior for outer layer is different due to its composition. These observations suggest that the washing process has minimal effect on reaction mechanism of the precursor materials in the single bonded aggregates [237]. In SBAs samples weight loss occur in the zone 3 with the temperature range of 700 – 1000 °C which is because of the decarboxylation of carbo-aluminate phase (like hemi-carbonate) [76]. The carbo-aluminate in the form of hemi-carbonate were observed in XRD analysis. The outer layer has shown only small amount of weight loss in zone 3.

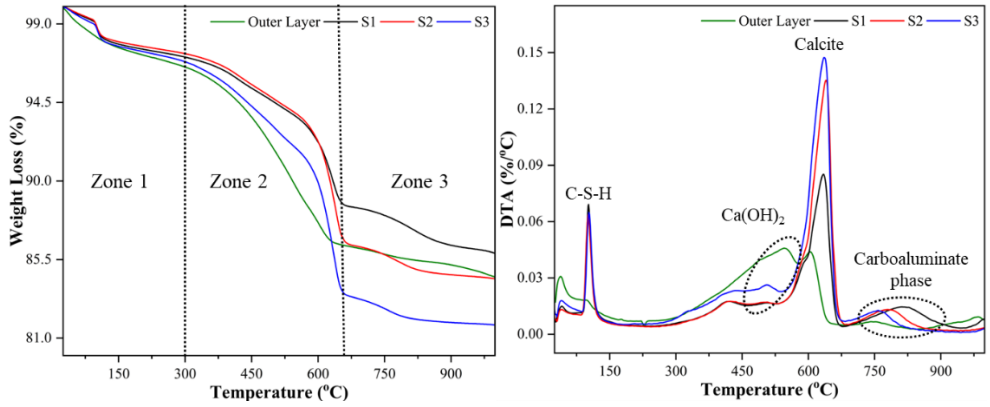

Figure 4.7 Thermogravimetric analysis of S1, S2, S3 samples and outer layer.

Scanning electron microscopy (SEM)

The micro-structure of single bonded aggregates samples (S1, S2, S3) was analyzed using the SEM, as shown in Figure 4.8 at a magnification of x1000. The SEM images show unreacted MSWI-FA in the form of spherical cenospheres, which are mostly visible in S1 sample as compared to S2 and S3 due to its composition. The unreacted MS particles was observed in the SBAs, which have high intensity in S3 as compared to S2 and S1, attributed to its less reactive nature and agglomerate in rounded shape [213]. The $CaCO_3$ grain was

found in the aggregate's morphology. The C-S-H gel were observed in the form of continuous cluster with irregular shape [250] which is distributed throughout the aggregate's surface due to its amorphous nature as confirmed by XRD analysis. In S1 sample, C-S-H gel is more continuous cluster as compared to S2 while S3 has small clusters which is because of the higher MS content in its matrix. As mentioned in Table No. 2 that fixed solid to water ratio (0.26) were used but the aggregate composition changed due to which the formation of hydration products was reduced in order of S3 > S2 > S1. The C-S-H gel embed the unreacted particles of MSWI-FA and MS which positively impact mechanical strength. Also, in later stage pozzolanic reaction between C-S-H gel and MSWI-FA which will enhance the durability of aggregate [251].

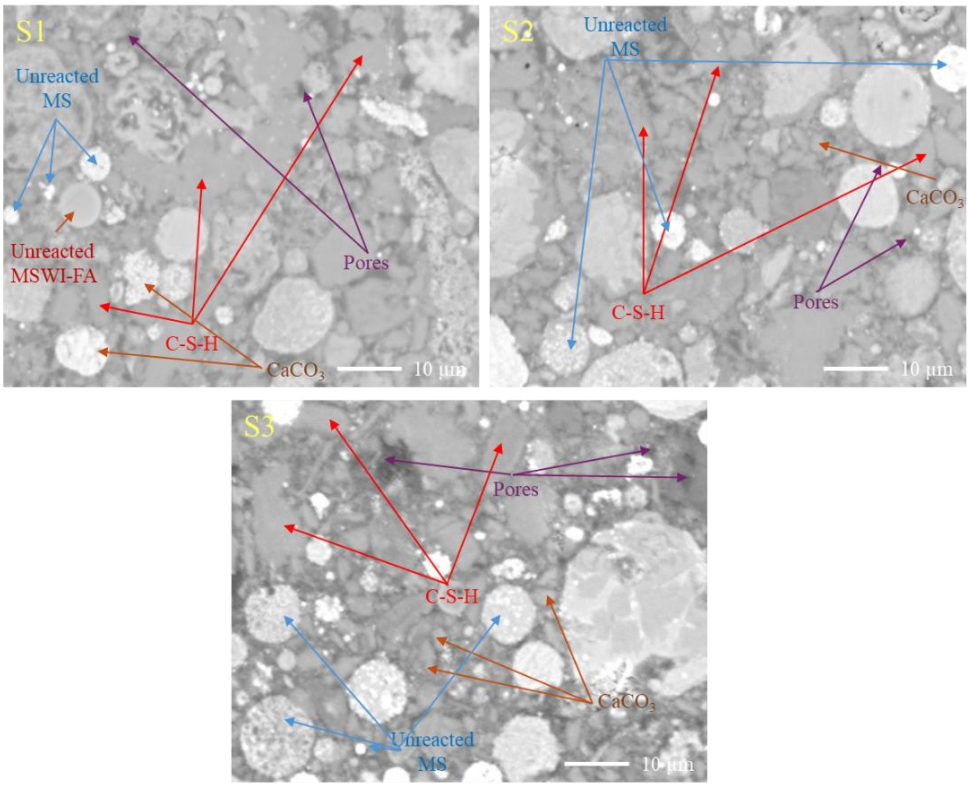

Figure 4.8 SEM micrographs of SBA samples S1, S2 and S3.

Figure 4.9 depicits SEM micrographs of outer layer at a magnifcation of 1000 x and the interface between the inner aggregates (S1, S2, S3) and outer layer at a magnifcation of 100 µm. The outerlayer have dense micro-structure which is developed due to the fromation of more hydration products and better pozzolanic reaction as it composed of 30% OPC, 50% GGBFS and 20% SF which are reactive and have higher tendency towards pozzolanic activity. The

C-S-H gel mostly occupy the microstrucutre of the outerlayer and are in the form of continous clustur. The $CaCO_3$ crystal were found which is due to the presence of GGBFS in outerlayer. The interface of interaction of outerlayer and aggregates surface are shown in Fig. 13 (b,c). In some aggregates it was observed that there is a crack at the interface of the aggregate surface and outerlayer which reduces mechanical performance of aggregates as in mechanical strength analysis higher standard deviation were observed for double bonded aggregates. The cracks at the interface occur because of the different reaction kinetic (hydration and pozzolanic) and dry shrinkage as both the SBAs and outer layer have different materials with different compositions [252]. The quantity of double bonded aggregates with such crack are lower because of the higher content of OPC and better binding ability of GGBFS [253]. The presence of MSWI-FA content in the SBAs samples assure better interaction between the outer and inner layer. Another reason for the crack at the interface is cutting of the aggregates into cross-sections followed by polishing for SEM analysis. The cutting and polishing processes were performed manually and pressure applied during this process which is not uniform and the resistance of outer layer and coated SBA sample also different.

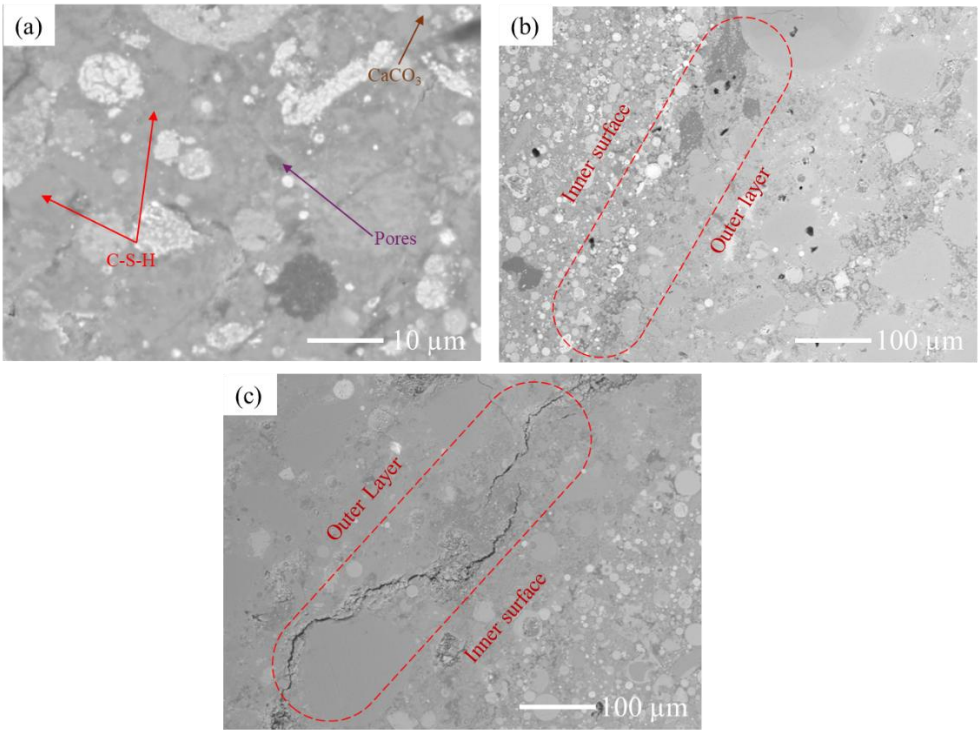

Figure 4.9 SEM micrograph of (a) outer layer, (b) Uncracked and (c) cracked images

of inner and outer layer interface.

Leaching

Table No. 4.3 reports the leaching results of the precursors materials, SBAs and DBAs, which shows that the release of heavy metals is within the limits of values for non-hazardous wastes and according to the legislative limits. But some the heavy elements like Cr, Mo (oxyanion-forming elements), Sb and Hg exceeds the limits in the precursor and as well as in the aggregate's samples. The leaching of these elements exceeds the legislative limits for the release of permissible pollutant content from the industrial waste [232, 254]. The immobilization of Cr in cement-based materials occurs due to its addition or substitution in hydration products, or by forming new compounds [255, 256]. However, in this study, no new Cr-based compounds were observed, and the hydration products formed had poor crystallinity, which led to Cr leaching. Nevertheless, the aggregates still exhibited lower Cr leaching compared to the precursor. The immobilization of Cr in cementitious materials is critical because of the inadequate chemical fixation [257]. Mo is the second element that exceeds the Italian government legislative limits in both precursors and aggregates. MSWI-FA and SBA samples have shown higher leaching values for Mo, but these values decrease when an outer layer is applied to the aggregates, due to its denser microstructure, which

physically prevents leaching. The immobilization of Mo in cement-based materials takes place due to the precipitation of powellite ($CaMoO_4$) [258, 259] and through the substitution of sulfate ions with molybdate ion (MoO_4^{2-}) during the formation of ettringite and AFm [259-262]. But XRD analysis of all samples confirms the absence of Mo-based compounds and AFm formation. A weak peak for ettringite was observed in SBA samples, indicating that Mo is not chemically fixed but physically entrapped.

The leaching value for Sb was found to be above the legislative limits for MSWI-FA and aggregate samples. In aggregate samples, as the MS content increases, Sb leaching also increases due to the unreactive nature of MS, which loosens the microstructure and facilitates the mobility of Sb. Sb does not

effectively stabilize in cement-based materials, as it is not chemically bound in the cement matrix during the hydration process [263]. The Hg leaching value from MSWI-FA and SBA samples exceeds the legislative limit, but in DBA samples, its leaching is significantly reduced because the outer layer resists Hg mobility and physically entraps it in the aggregate matrix. Hg has no chemical interaction with the hydration products and has a strong potential to volatilize from the cementitious material [264, 265]. In general, it was observed that there is a reduction in heavy metal release in aggregates with an outer layer compared to SBAs. This is due to the dense microstructure of the outer layer, which resists the leaching of heavy metals [61].

Table 4.3 Leaching analysis of precursors and artificial aggregates.

Element (mg/kg)	Cr	Ni	Cu	As	Se	Mo	Cd	Sb	Ba	Hg
OPC	2.003	0.029	0.012	0.001	0.017	0.133	0.000	<0.001	2.800	<0.001
GGBFS	2.967	0.001	<0.001	0.011	0.249	2.241	0.002	0.007	1.414	0.001
MSWI-FA	2.717	0.007	0.005	0.050	0.457	38.81	0.031	1.762	0.270	0.007
SF	0.050	0.063	0.149	13.71	4.30	0.242	0.006	0.067	0.000	<0.001
S1 <4mm	2.711	0.005	0.008	0.030	0.348	43.181	0.033	0.848	0.330	0.014
S2 <4mm	2.351	0.007	0.065	0.032	0.333	35.387	0.026	1.514	0.292	0.008
S3 <4mm	2.026	0.009	0.205	0.026	0.209	30.045	0.022	2.202	0.289	0.006
D1 <4mm	2.297	0.006	0.005	0.075	0.227	16.760	0.012	0.839	0.310	0.003
D2 <4mm	2.381	0.004	0.010	0.073	0.211	14.181	0.010	1.135	0.322	0.003
D3 <4mm	2.785	0.007	0063	0.082	0.252	13.272	0.011	1.692	0.389	0.003
S1*	3.571	0.009	0.013	0.034	0.353	49.34	0.053	0.734	0.538	0.017
S2*	2.975	0.008	0.049	0.033	0.341	41.12	0.045	1.049	0.500	0.014
S3*	3.171	0.011	0.429	0.027	0.215	35.27	0.039	1.651	0.508	0.012
D1*	2.922	0.007	0.014	0.087	0.230	16.02	0.017	0.945	0.594	0.007
D2*	3.117	0.007	0.029	0.076	0.211	15.34	0.017	1.142	0.550	0.006
D3*	3.007	0.005	0.034	0.086	0.237	12.21	0.014	1.276	0.624	0.005
DOW	1	1	5	0.2	0.05	1.0	0.01	0.07	10	0.02

Note:

1. *The samples with (*) are those whose size were higher than 4mm.*
2. ***DOW:** Decree on waste (Italian legislation)*

Chapter 5: Future perspective-critical evaluation

The topic of artificial aggregates is currently gaining significant attention worldwide, focusing on goals such as environmental management, resource conservation, and sustainable construction practices. In the future, there are several important issues regarding the enhancement of its performance and the transition from laboratory settings to commercialization, which will be explored in detail in the following sections.

5.1 Applications

CBAAs are produced from agricultural and industrial waste, promoting a circular economy and providing alternative materials for the construction sector to support sustainability. The controllable porosity of CBAAs affects their water absorption capacity, density, mechanical properties, and their ability to chemically and physically immobilize hazardous content, making them suitable for various applications. These include lightweight concrete (LWC), porous eco-concrete, CO_2 sequestration, energy storage, and more.

The CBAAs have higher porosity and lower particle density, making them suitable for preparing light-weight concrete (LWC) for use in structural and non-structural applications. LWC, due to its light weight are considered most suitable for high-rise buildings to reduce the structural dead load [266] and improve thermal and noise insulation [267]. The AAs reduce the autogenous shrinkage of LWC due to their higher water absorption and stable desorption ability which help in effective internal concrete curing [268]. However, concerns remain regarding the durability and strength of LWC, which depend on the mechanical performance of AAs, usually observed on lower side [62]. Literature reports that novel techniques such as compression casting significantly improve the performance of LWC [269]. The AAs show strong potential for CO_2 sequestration, which helps to improve their physical and mechanical characteristics, while also contributing to the reduction of GHG emissions [81, 172, 270, 271]. However, it should be noted that the carbonation parameters, such as CO_2 concentration, temperature, and pressure, affects the performance of the AAs [271], which requires further exploration and study.

The incorporation of phase change materials (PCMs) into construction materials enhances thermal energy storage capacity and improves the thermal comfort of the building envelope, helping to reduce the energy consumption of electrical appliances, particularly heating, ventilation, and air conditioning (HVAC) systems [272]. The microencapsulation of PCMs in the AAs offers significant advantages. The pelletization process used to produce AAs allows precise control of their size and ensures uniform dispersion of the PCMs throughout the aggregate matrix [273]. Furthermore, the surface treatment of such aggregates provides an additional outer layer, which prevents leakage of the PCM [273]. However, it is important to note that incorporating PCMs in AAs compromises their strength, as they do not react with the binder or other precursors, leading to increased porosity of the aggregate [273]. This is a critical aspect and future perspective, as it simultaneously addresses the recycling of waste materials and the use of PCMs to reduce the energy consumption of buildings and maintain thermal comfort.

The emerging and innovative application of AAs is porous eco-concrete (PEC). The porous nature of this concrete offers a sustainable method to prevent slope runoff provides, vegetated slope protection [274], reduces dust, noise and water seepage, and can serve as a water purification filter [275]. Recently, the use of PEC for vegetation concrete has increased significantly for planting on slopes along roadsides, dams, and for the restoration of landfill sites to conserve soil, protect water resources, and enhance environmental aesthetics [276, 277]. The porous nature of AAs aids in retaining moisture and regulating temperature, thereby increasing plant compatibility and highlighting their potential use in PEC [277]. Additionally, as AAs are synthesized aggregates, their preparation allows the incorporation of fertilizers into their rounded pellets, enabling them to act as nutrient carriers for plants and to release these nutrients slowly and in a controlled manner [278]. However, such attractive and innovative applications significantly impact the mechanical performance of concrete, which is the primary requirement. AAs are beneficial in many respects due to their engineered synthesis and properties; some of these were highlighted in the above paragraphs. However, it should be noted that while engineering the properties of AAs, the basic mechanical strength is compromised. Therefore, the field of AAs is of great importance, as it helps the ecological system in various ways, from the utilization of hazardous waste

to plantation and CO_2 sequestration.

5.2 Barries

For a sustainable future and to combat climate change, it is essential to reduce the over-exploitation of natural resources and pollution. To achieve these goals, materials should be recycled (such as recycled aggregate) and waste materials should be transformed into value-added products (such as lightweight artificial aggregate), supporting the implementation of a circular economy. However, cultural, economic, technological, and regulatory barriers hinder the large-scale use of materials like artificial aggregates [279]. As artificial aggregates are newly developed materials, further research is needed because, from a technological perspective, their performance is unpredictable, while the construction industry requires high-quality materials [280, 281]. To enhance their properties, additional processes are required to prepare them, which may burden the economy [279]. Due to technological and economic concerns, the market is also cautious about these materials regarding their durability and effectiveness compared to traditional aggregates [279]. The legal and regulatory framework is also a major concern, as there are either no regulations or insufficient regulations for commercializing and using these materials. Developing a regulatory framework is not straightforward, and regulations vary between countries, adding complexity to the supply chain and making it difficult for the industry to scale up [279, 281]. It is important to create an environment that encourages the use of these materials in the construction industry, which requires coordinated efforts from policymakers, researchers, and industry participants.

5.3 Precursors

The most commonly used precursor materials for producing artificial aggregates are industrial and agricultural wastes such as ashes, sludges, slags, sediments, red mud, and cement kiln dust [41]. Among these wastes, fly ash is frequently used to produce artificial aggregates due to its properties, availability, and cost. However, it should be noted that fly ash is primarily used in the production of cement and concrete, followed by bricks and blocks [282]. Additionally, fly ash has many other applications in various fields, including environmental remediation, water

treatment, pollutant gas absorption, zeolite synthesis, superhydrophobic powder, and others [283, 284]. These divers increase fly ash market demand, which challenges its availability for producing artificial aggregates.

To reduce CO_2 emissions, thermal power plants will gradually be replaced by renewable energy sources in the future, which will also affect the availability of ash. The phased decommissioning of coal-fired power plants is one measure that will reduce ash availability. Geographical location also affects the availability of precursor materials.

5.4 Behavior in cement-matrix

Concrete is the primary matrix in which artificial aggregates are used and affect its fresh properties, mechanical performance, durability, and microstructure. The physio-mechanical performance of artificial aggregates depends on their microstructure, which ultimately affects the mechanical strength and durability of the cement matrix. The use of artificial aggregates in concrete might enhance its workability, thermal insulation behavior, and interface transition zone (ITZ) due to their shape, surface texture, and internal porosity [37]. Artificial aggregates form a continuous and tighter bond with cement, developing an indistinguishable ITZ compared to other aggregates. This may be due to four reasons [37]: (1) the aggregate and cement matrix have similar compositions (both are cementitious materials); (2) water stored in the aggregate provides the necessary internal curing during subsequent hydration of the ITZ; (3) mechanical interlocking forms between the aggregate and matrix due to the penetration of cement paste into the aggregate, resulting in a close bond; (4) a pozzolanic reaction occurs between the fly ash particles (the outer layer of the AA) and calcium hydroxide within the ITZ region. However, despite the development of a strong ITZ, there are additional problems associated with the use of artificial aggregates in the cement matrix. Variability in the characteristics of precursors and the processes used for the preparation of artificial aggregates may result in inconsistent properties, making their use in the cement matrix difficult [37]. Chloride penetration is also a major concern associated with the utilization of artificial aggregates, which limits their application, where sintered aggregates have shown better resistance to chlorination [285]. The durability of concrete with artificial aggregates remains a major concern. Therefore,

further research is required to prepare sustainable, strong, and durable aggregates and to reduce the use of excessive energy (as in sintered aggregates) and cement. The performance of artificial aggregates in concrete mixtures requires further investigation, with particular emphasis on identifying the factors that influence their compatibility and long-term durability.

5.5 Economics

Likewise, in addition to the physio-mechanical and durability performance of artificial aggregates, cost is also an important factor. Cost and properties determine the market and attract consumers to the product. The economics of the product involve several costs, including initial investment capital, production or operational costs, and regulatory costs. Establishing a production facility for artificial aggregates requires high initial investment capital to acquire land, construct facilities, and purchase machinery and technology. Operational costs include raw materials, energy consumption, and skilled labor [58, 286]. Licenses and permits include technology for controlling and monitoring pollution in accordance with government policies and regulations [58, 286]. Environmental regulation for artificial aggregates is necessary because they are produced from potentially hazardous materials. Compared to natural aggregates, the initial cost of artificial aggregates is higher due to energy consumption, technology requirements, and regulatory requirements. However, on the sustainability index, artificial aggregates perform better than natural aggregates, although factors such as binder use, energy consumption, and distance from raw material sources can reduce these benefits [287]. Market or social acceptance of artificial aggregates depends on the type of aggregate, production process, physio-mechanical performance and most importantly market conditions and behaviour [287].

Research and development are important areas that require substantial investment to further explore the potential of artificial aggregates and to establish a pathway for their commercialization from laboratory scale. In the literature, laboratory-scale cost analysis has been examined, but publicly available cost analysis at the commercial scale – from initial investment in facility development to delivery to the end-user – is lacking for artificial aggregates. The initial investment required to establish an artificial aggregates facility is a major concern, as market and social

acceptability are currently insufficient to attract investors. Therefore, the government should develop policies to promote and ensure the use of artificial aggregates in the construction industry, such as through green procurement. Social awareness is also as important as other factors; people should be educated about sustainable approaches. These measures will increase investor interest in establishing larger production facilities for artificial aggregates.

5.6 Legislation

Legislation plays a crucial role in the commercialization of artificial aggregate production from laboratory to industrial scale. Various international, national, and regional guidelines ensure quality, environmental compatibility, and safety in the production of building materials. Waste materials are used to produce artificial aggregates, and the European Union encourages these practices. Green building certification schemes such as LEED (Leadership in Energy and Environmental Design) and BREEAM (Building Research Establishment Environmental Assessment Method) promote the use of sustainable materials, including artificial aggregates. Artificial aggregates must meet several criteria from production to final use. Occupational Safety and Health Administration (OSHA) standards, Construction Products Regulation (EU) No. 305/2011, and the updated Construction Products Regulation (EU) No. 2024/3110 adopted in 2025 must be followed to legally place products on the market. Legislation is essential to ensure that man-made aggregates produced from (hazardous) waste comply with environmental, technical, sustainability, and safety guidelines. It also encourages manufacturers to innovate and improve artificial aggregate production to align with sustainability goals. For innovative building materials, compliance with these legal measures and regulations can be challenging. Therefore, governments and international bodies should provide incentives to manufacturers to attract greater investment.

Chapter 6: Conclusion and Recommendation

6.1 Conclusion

This study focused on remediation procedure of hazardous MSWI-FA and preparation of the alternative materials for construction sector for sustainable future. The following main are the main conclusive remarks derived from above study:

1) The pre-treatment of the MSWI-FA with water in two-steps, considerably reduce the soluble salts like chlorides and sulfates which is confirmed with help of ICP atomic emission spectrophotometry and XRD study. The presences of these salts in MSWI-FA effect its binding ability and hinder stabilization process.

2) In the second step, LWAs were prepared through CBP from MSWI-FA and MS with the help of OPC. These aggregates were named as single-bonded aggregates (SBAs).

3) The SBAs were surface treated with GGBFS, SF and OPC via CBP and the surface treated were named as double bonded aggregates.

4) The physical, mechanical and leaching properties of SBAs and DBAs were compared, and it was observed that surface treatment enhanced the performance. The extra outer layer hindered the leaching of heavy metals from aggregates matrix and reduce it under the legislative limits.

5) The XRD analysis showed the presence of hydration products in the aggregates, but they have weak peaks due to poor crystallinity or amorphous nature but were confirmed by FTIR and TGA analysis.

6) Upgrading the pilot-scale pelletization equipment used in this work is economically viable and does not present any specific technological challenge. The application of this technology will help to decrease landfilling and increase resource efficiency in developing nations.

These considerations provide valuable insights for future research aimed at defining a complete treatment chain, including both pre- and post-treatment phases, to further enhance the properties of aggregates before reuse. Future studies will focus

on durability aspects, with particular attention to the relationship between the long-term evolution of the mineralogical and mechanical properties of stabilizing matrices and their corresponding long-term leaching behavior.

6.2 Recommendation

Artificial aggregates require ongoing investment in research and development to further enhance their performance. To ensure sustainability, low-carbon binders should be identified, and further research should focus on precursor materials to improve both technological and environmental performance. Energy-efficient and renewable energy-integrated plants should be used in aggregate production to reduce indirect greenhouse gas emissions. In addition to technological characteristics, environmental performance should be thoroughly assessed to determine the environmental impact of artificial aggregates and identify areas for improvement. For carbon sequestration, artificial aggregates should be developed to directly absorb greenhouse gases when placed in chimneys or pollution pathways, thereby capturing pollutants and preventing emissions into the environment. Regulatory authorities should establish additional protocols for artificial aggregates to ensure their quality and performance and to promote their use. These protocols should be incorporated into national and international building codes, and governments should provide incentives such as tax relief or subsidies to encourage investment and adoption.

At a commercial scale, integrating artificial aggregate production plants with thermal power plants will reduce transportation needs, and hot flue gases should be used for accelerated curing of cold-bonded aggregates. As flue gases contain CO2, certain types of aggregates will uptake CO_2, reducing the environmental impact of thermal power plants. This technology should be seriously considered, as it offers a sustainable approach in which all waste from the power plant is recycled.

Alternatively, a renewable energy-based production plant for artificial aggregates could be established, using solar panels to generate electricity for plant operations and concentrated solar systems to provide the high temperatures required for aggregate sintering. Both approaches will significantly address the energy and indirect environmental challenges associated with artificial aggregate production,

but some concerns remain. For example, the renewable energy approach requires more land and may necessitate building the plant in a different location, increasing transportation needs, while integrating a thermal power plant with the production facility requires advanced technology.

References

1. Sun, Y.H., et al., *Production of lightweight aggregate ceramsite from red mud and municipal solid waste incineration bottom ash: Mechanism and optimization.* Construction and Building Materials, 2021. **287**: p. 122993.

2. Ul Rehman, M., et al., *Physico-mechanical performance and durability of artificial lightweight aggregates synthesized by cementing and geopolymerization.* Construction and Building Materials, 2020. **232**: p. 117290.
3. (Naturvårdsverket)., S.E.P.A. *Environmental risks from marine aggregate extraction in Swedish waters. Stockholm: Naturvårdsverket.* 2020 [cited 2025; Web Report]. Available from: https://www.naturvardsverket.se/.
4. (UBA), U. *Sustainable construction and resource conservation in Germany.* 2022 [cited 2025; Available from: https://www.umweltbundesamt.de/.
5. Rijkswaterstaat. *Circular economy in infrastructure: The Dutch experience.* 2022 [cited 2025; Available from: https://www.rijkswaterstaat.nl/.
6. Environment, N.M.o.C.a. *Sustainable management of marine resources: National strategy*. 2021 [cited 2025 Web report]; Available from: https://www.regjeringen.no/no/id4/.
7. Chinnu, S.N., et al., *Recycling of industrial and agricultural wastes as alternative coarse aggregates: A step towards cleaner production of concrete.* Construction and Building Materials, 2021. **287**: p. 123056.
8. Shivaprasad, K., B. Das, and S. Krishnadas. *Effect of Curing Methods on the Artificial Production of Fly Ash Aggregates*. in *Recent Trends in Civil Engineering: Select Proceedings of TMSF 2019*. 2021. Springer.
9. Vaverková, M.D., *Landfill Impacts on the Environment—Review.* Geosciences, 2019. **9**(10): p. 431.
10. Tang, P. and H.J.H. Brouwers, *Integral recycling of municipal solid waste incineration (MSWI) bottom ash fines (0-2mm) and industrial powder wastes by cold-bonding pelletization.* Waste Manag, 2017. **62**: p. 125-138.
11. Kou, S.C., C.S. Poon, and F. Agrela, *Comparisons of natural and recycled aggregate concretes prepared with the addition of different mineral admixtures.* Cement & Concrete Composites, 2011. **33**(8): p. 788-795.
12. Poon, C.S., et al., *Properties of concrete blocks prepared with low grade recycled aggregates.* Waste Manag, 2009. **29**(8): p. 2369-77.
13. Moon, G.D., S. Oh, and Y.C. Choi, *Effects of the physicochemical properties of fly ash on the compressive strength of high-volume fly ash mortar.* Construction and Building Materials, 2016. **124**: p. 1072-1080.
14. Aubert, J.E., B. Husson, and A. Vaquier, *Metallic aluminum in MSWI fly ash: quantification and influence on the properties of cement-based products.* Waste Manag, 2004. **24**(6): p. 589-96.
15. Song, Y.M., et al., *Feasibility study on utilization of municipal solid waste incineration bottom ash as aerating agent for the production of autoclaved aerated concrete.* Cement & Concrete Composites, 2015. **56**: p. 51-58.
16. Tang, P. and H.J.H. Brouwers, *The durability and environmental properties of self-compacting concrete incorporating cold bonded lightweight aggregates produced from combined industrial solid wastes.* Construction and Building Materials, 2018. **167**: p. 271-285.
17. Kaza, S., et al., *What a waste 2.0: a global snapshot of solid waste management to 2050*. 2018: World Bank Publications.
18. Vaitkus, A., et al., *An algorithm for the use of MSWI bottom ash as a building material in road pavement structural layers.* Construction and Building Materials, 2019. **212**: p. 456-466.
19. Lin, K.L., W.C. Chang, and D.F. Lin, *Pozzolanic characteristics of pulverized incinerator bottom ash slag.* Construction and Building Materials, 2008. **22**(3): p.

324-329.
20. Ferraro, A., et al., *Pre-treatments of MSWI fly-ashes: A comprehensive review to determine optimal conditions for their reuse and/or environmentally sustainable disposal.* Reviews in Environmental Science and Bio/Technology, 2019. **18**: p. 453-471.
21. Ren, J., et al., *Effect of silica fume on the mechanical property and hydration characteristic of alkali-activated municipal solid waste incinerator (MSWI) fly ash.* Journal of Cleaner Production, 2021. **295**: p. 126317.
22. Li, Z.L., et al., *Research on the durability and Sustainability of an artificial lightweight aggregate concrete made from municipal solid waste incinerator bottom ash (MSWIBA).* Construction and Building Materials, 2023. **365**: p. 129993.
23. Zhang, Y., et al., *Treatment of municipal solid waste incineration fly ash: State-of-the-art technologies and future perspectives.* J Hazard Mater, 2021. **411**: p. 125132.
24. Chen, L., et al., *Sustainable stabilization/solidification of municipal solid waste incinerator fly ash by incorporation of green materials.* Journal of Cleaner Production, 2019. **222**: p. 335-343.
25. Wang, P., Y.A. Hu, and H.F. Cheng, *Municipal solid waste (MSW) incineration fly ash as an important source of heavy metal pollution in China.* Environmental Pollution, 2019. **252**: p. 461-475.
26. Race, M., *Applicability of alkaline precipitation for the recovery of EDDS spent solution.* J Environ Manage, 2017. **203**(Pt 1): p. 358-363.
27. Yang, Z., et al., *Effect of water-washing on the co-removal of chlorine and heavy metals in air pollution control residue from MSW incineration.* Waste Manag, 2017. **68**: p. 221-231.
28. Huber, F. and J. Fellner, *Integration of life cycle assessment with monetary valuation for resource classification: The case of municipal solid waste incineration fly ash.* Resources Conservation and Recycling, 2018. **139**: p. 17-26.
29. Mathews IV, G., R. Sinnan, and M. Young, *Evaluation of reclaimed municipal solid waste incinerator sands in concrete.* Journal of Cleaner Production, 2019. **229**: p. 838-849.
30. Quina, M.J., et al., *Technologies for the management of MSW incineration ashes from gas cleaning: New perspectives on recovery of secondary raw materials and circular economy.* Sci Total Environ, 2018. **635**: p. 526-542.
31. by Deloitte, B., *Study to assess the impacts of different classification approaches for hazard property "HP 14" on selected waste streams–Final report.* Prepared for the European Commission (DG ENV), in collaboration with INERIS, 2015.
32. Quina, M.J., J.C. Bordado, and R.M. Quinta-Ferreira, *Treatment and use of air pollution control residues from MSW incineration: an overview.* Waste Manag, 2008. **28**(11): p. 2097-121.
33. Hennebert, P., et al., *Hazard property classification of waste according to the recent propositions of the EC using different methods.* Waste Manag, 2014. **34**(10): p. 1739-51.
34. Ferraro, A., et al., *Cold-bonding process for treatment and reuse of waste materials: Technical designs and applications of pelletized products.* Critical Reviews in Environmental Science and Technology, 2021. **51**(19): p. 2197-2231.
35. Bates, E. and C. Hills, *Stabilization and solidification of contaminated soil and waste: A manual of practice.* Édit Media H, 2015.
36. Tang, P., M. Florea, and H. Brouwers, *Employing cold bonded pelletization to produce lightweight aggregates from incineration fine bottom ash.* Journal of

Cleaner Production, 2017. **165**: p. 1371-1384.
37. Ren, P.F., T.C. Ling, and K.H. Mo, *Recent advances in artificial aggregate production.* Journal of Cleaner Production, 2021. **291**: p. 125215.
38. Behera, M., et al., *Recycled aggregate from C&D waste & its use in concrete–A breakthrough towards sustainability in construction sector: A review.* Construction and building materials, 2014. **68**: p. 501-516.
39. Xiao, J., et al., *An overview of study on recycled aggregate concrete in China (1996–2011).* Construction and building materials, 2012. **31**: p. 364-383.
40. EPA, U., *Sustainable management of construction and demolition materials*. 2017.
41. Bekkeri, G.B., K.K. Shetty, and G. Nayak, *Synthesis of artificial aggregates and their impact on performance of concrete: a review.* Journal of Material Cycles and Waste Management, 2023. **25**(4): p. 1988-2011.
42. Thomas, J. and B. Harilal, *Properties of cold bonded quarry dust coarse aggregates and its use in concrete.* Cement & Concrete Composites, 2015. **62**: p. 67-75.
43. Ramamurthy, K. and K.I. Harikrishnan, *Influence of binders on properties of sintered fly ash aggregate.* Cement & Concrete Composites, 2006. **28**(1): p. 33-38.
44. Abouhussien, A.A., A.A.A. Hassan, and M.K. Ismail, *Properties of semi-lightweight self-consolidating concrete containing lightweight slag aggregate.* Construction and Building Materials, 2015. **75**: p. 63-73.
45. Rashad, A.M., *Lightweight expanded clay aggregate as a building material–An overview.* Construction and Building Materials, 2018. **170**: p. 757-775.
46. Yliniemi, J., et al., *Lightweight aggregates produced by granulation of peat-wood fly ash with alkali activator.* International Journal of Mineral Processing, 2016. **149**: p. 42-49.
47. Ducman, V. and B. Mirtic, *Water vapour permeability of lightweight concrete prepared with different types of lightweight aggregates.* Construction and Building Materials, 2014. **68**: p. 314-319.
48. Dacić, A., et al., *The Obstacles to a Broader Application of Alkali-Activated Binders as a Sustainable Alternative—A Review.* Materials, 2023. **16**(8): p. 3121.
49. Shivaprasad, K.N. and B.B. Das, *Study on the Production Factors in the Process of Production and Properties of Fly Ash-Based Coarse Aggregates.* Advances in Civil Engineering, 2021. **2021**(1): p. 4309569.
50. Almadani, M., et al., *Geopolymer-Based Artificial Aggregates: A Review on Methods of Producing, Properties, and Improving Techniques.* Materials (Basel), 2022. **15**(16): p. 5516.
51. Nadesan, M.S. and P. Dinakar, *Structural concrete using sintered flyash lightweight aggregate: A review.* Construction and Building Materials, 2017. **154**: p. 928-944.
52. Li, B., et al., *Effects of a two-step heating process on the properties of lightweight aggregate prepared with sewage sludge and saline clay.* Construction and Building Materials, 2016. **114**: p. 119-126.
53. Charitha, V., et al., *Use of different agro-waste ashes in concrete for effective upcycling of locally available resources.* Construction and Building Materials, 2021. **285**: p. 122851.
54. de Brito, J. and R. Kurda, *The past and future of sustainable concrete: A critical review and new strategies on cement-based materials.* Journal of Cleaner Production, 2021. **281**: p. 123558.
55. Sun, J.W. and P. Zhang, *Effects of different composite mineral admixtures on the early hydration and long-term properties of cement-based materials: A comparative study.* Construction and Building Materials, 2021. **294**: p. 123547.

56. Gesoğlu, M., T. Özturan, and E. Güneyisi, *Effects of fly ash properties on characteristics of cold-bonded fly ash lightweight aggregates.* Construction and Building Materials, 2007. **21**(9): p. 1869-1878.
57. Liu, J., et al., *Valorization of municipal solid waste incineration bottom ash (MSWIBA) into cold-bonded aggregates (CBAs): Feasibility and influence of curing methods.* Sci Total Environ, 2022. **843**: p. 157004.
58. Petrillo, A., et al., *Multi-criteria analysis for Life Cycle Assessment and Life Cycle Costing of lightweight artificial aggregates from industrial waste by double-step cold bonding palletization.* Journal of Cleaner Production, 2022. **351**: p. 131395.
59. Tajra, F., et al., *Properties of lightweight concrete made with core-shell structured lightweight aggregate.* Construction and Building Materials, 2019. **205**: p. 39-51.
60. Shahane, H.A. and S. Patel, *Influence of curing method on characteristics of environment-friendly angular shaped cold bonded fly ash aggregates.* Journal of Building Engineering, 2021. **35**: p. 101997.
61. Ferraro, A., et al., *Production and characterization of lightweight aggregates from municipal solid waste incineration fly-ash through single-and double-step pelletization process.* Journal of Cleaner Production, 2023. **383**: p. 135275.
62. Tajra, F., M. Abd Elrahman, and D. Stephan, *The production and properties of cold-bonded aggregate and its applications in concrete: A review.* Construction and Building Materials, 2019. **225**: p. 29-43.
63. Duxson, P., et al., *Geopolymer technology:: the current state of the art.* Journal of Materials Science, 2007. **42**(9): p. 2917-2933.
64. Gesoğlu, M., T. Özturan, and E. Güneyisi, *Effects of cold-bonded fly ash aggregate properties on the shrinkage cracking of lightweight concretes.* Cement and Concrete Composites, 2006. **28**(7): p. 598-605.
65. Gesoğlu, M., E. Güneyisi, and H.Ö. Öz, *Properties of lightweight aggregates produced with cold-bonding pelletization of fly ash and ground granulated blast furnace slag.* Materials and structures, 2012. **45**: p. 1535-1546.
66. Terzić, A., L. Andrić, and V. Mitić, *Mechanically activated coal ash as refractory bauxite shotcrete microfiller: Thermal interactions mechanism investigation.* Ceramics International, 2014. **40**(8): p. 12055-12065.
67. Terzić, A., et al., *Artificial fly ash based aggregates properties influence on lightweight concrete performances.* Ceramics International, 2015. **41**(2): p. 2714-2726.
68. Terzic, A., et al., *Artificial fly ash based aggregates properties influence on lightweight concrete performances.* Ceramics International, 2015. **41**(2): p. 2714-2726.
69. Colangelo, F., F. Messina, and R. Cioffi, *Recycling of MSWI fly ash by means of cementitious double step cold bonding pelletization: Technological assessment for the production of lightweight artificial aggregates.* J Hazard Mater, 2015. **299**: p. 181-91.
70. Raza, J., et al., *5 - Properties of concrete containing polyethylene terephthalate and artificial lightweight aggregates: a case study*, in *Reuse of Plastic Waste in Eco-Efficient Concrete*, F. Pacheco-Torgal, et al., Editors. 2024, Woodhead Publishing. p. 85-112.
71. Gao, W., et al., *A low-carbon approach to recycling engineering muck to produce non-sintering lightweight aggregates: Physical properties, microstructure, reaction mechanism, and life cycle assessment.* Journal of Cleaner Production, 2023. **385**: p. 135650.

72. Dzaye, E.D., G. De Schutter, and D.G. Aggelis, *Monitoring early-age acoustic emission of cement paste and fly ash paste.* Cement and Concrete Research, 2020. **129**: p. 105964.
73. Jia, R.Q., Q. Wang, and T. Luo, *Understanding the workability of alkali-activated phosphorus slag pastes: Effects of alkali dose and silicate modulus on early-age hydration reactions.* Cement & Concrete Composites, 2022. **133**: p. 104649.
74. Colangelo, F. and R. Cioffi, *Use of Cement Kiln Dust, Blast Furnace Slag and Marble Sludge in the Manufacture of Sustainable Artificial Aggregates by Means of Cold Bonding Pelletization.* Materials (Basel), 2013. **6**(8): p. 3139-3159.
75. Manikandan, R. and K. Ramamurthy, *Effect of curing method on characteristics of cold bonded fly ash aggregates.* Cement & Concrete Composites, 2008. **30**(9): p. 848-853.
76. Narattha, C. and A. Chaipanich, *Effect of curing time on the hydration and material properties of cold-bonded high-calcium fly ash–Portland cement lightweight aggregate.* Journal of Thermal Analysis and Calorimetry, 2020. **145**(5): p. 2277-2286.
77. Ouyang, G.S., et al., *Valorization of alkali-activated fly ash-slag claddings to enhance the mechanical and leaching properties of phosphogypsum-based cold-bonded aggregates.* Developments in the Built Environment, 2024. **18**: p. 100464.
78. Xu, L.-Y., et al., *Recent advances in molecular dynamics simulation of the NASH geopolymer system: modeling, structural analysis, and dynamics.* Construction and Building Materials, 2021. **276**: p. 122196.
79. Mahmad Nor, A., et al., *A Review on the Manufacturing of Lightweight Aggregates Using Industrial By-Product.* MATEC Web Conf., 2016. **78**: p. 01067.
80. Qian, L.-P., et al., *Artificial alkali-activated aggregates developed from wastes and by-products: A state-of-the-art review.* Resources, Conservation and Recycling, 2022. **177**: p. 105971.
81. Zhao, Q.X., et al., *Investigation of various curing methods on the properties of red mud-calcium carbide slag-based artificial lightweight aggregate ceramsite fabricated through alkali-activated cold-bonded pelletization technology.* Construction and Building Materials, 2023. **401**: p. 132956.
82. Lin, J.Y., et al., *Municipal woody biomass waste ash-based cold-bonded artificial lightweight aggregate produced by one-part alkali-activation method.* Construction and Building Materials, 2023. **394**: p. 131619.
83. Pacheco-Torgal, F., J. Castro-Gomes, and S. Jalali, *Alkali-activated binders: A review. Part 2. About materials and binders manufacture.* Construction and Building Materials, 2008. **22**(7): p. 1315-1322.
84. Yip, C.K., et al., *Carbonate mineral addition to metakaolin-based geopolymers.* Cement & Concrete Composites, 2008. **30**(10): p. 979-985.
85. Shi, Y.X., et al., *Preparation and curing method of red mud-calcium carbide slag synergistically activated fly ash-ground granulated blast furnace slag based eco-friendly geopolymer.* Cement & Concrete Composites, 2023. **139**: p. 104999.
86. Nasir, M., et al., *Influence of heat curing period and temperature on the strength of silico-manganese fume-blast furnace slag-based alkali-activated mortar.* Construction and Building Materials, 2020. **251**: p. 118961.
87. Nguyen, H.T. *Synthesis and Characteristics of Inorganic Polymer Materials Geopolymerized from Ash of Brickyard*. in *Materials Science Forum*. 2019. Trans Tech Publ.
88. Hoang, M.D., Q.M. Do, and V.Q. Le, *Effect of curing regime on properties of red*

mud based alkali activated materials. Construction and Building Materials, 2020. **259**: p. 119779.
89. Yliniemi, J., et al., *Alkali Activation–Granulation of Hazardous Fluidized Bed Combustion Fly Ashes.* Waste and Biomass Valorization, 2016. **8**(2): p. 339-348.
90. Rudić, O., et al., *Aggregates Obtained by Alkali Activation of Fly Ash: The Effect of Granulation, Pelletization Methods and Curing Regimes.* Materials, 2019. **12**(5): p. 776.
91. Keyte, L., *Fly ash glass chemistry and inorganic polymer cements*, in *Geopolymers*. 2009, Elsevier. p. 15-36.
92. Criado, M., A. Fernández-Jiménez, and A. Palomo, *Alkali activation of fly ash. Part III: Effect of curing conditions on reaction and its graphical description.* Fuel, 2010. **89**(11): p. 3185-3192.
93. Bui, L.A.T., et al., *Manufacture and performance of cold bonded lightweight aggregate using alkaline activators for high performance concrete.* Construction and Building Materials, 2012. **35**: p. 1056-1062.
94. Lin, J.Y., et al., *Optimization of the manufacturing process and properties of alkali-activated palm oil fuel ash-based cold-bonded aggregates.* Journal of Cleaner Production, 2024. **437**: p. 140714.
95. Zhou, X.L., et al., *Preparation of artificial lightweight aggregate using alkali-activated incinerator bottom ash from urban sewage sludge.* Construction and Building Materials, 2022. **341**: p. 127844.
96. Kumar, S., R. Kumar, and S.P. Mehrotra, *Influence of granulated blast furnace slag on the reaction, structure and properties of fly ash based geopolymer.* Journal of Materials Science, 2010. **45**(3): p. 607-615.
97. Li, Z.J. and S.F. Liu, *Influence of slag as additive on compressive strength of fly ash-based geopolymer.* Journal of Materials in Civil Engineering, 2007. **19**(6): p. 470-474.
98. Zhang, Y., et al., *Effect of alkali activator and granulated blast furnace slag on the properties of lithium slag-based high-strength lightweight aggregates.* Sci Rep, 2025. **15**(1): p. 30115.
99. Asadizadeh, M., et al., *The impact of slag on the process of geopolymerization and the mechanical performance of mine-tailings-based alkali-activated lightweight aggregates.* Construction and Building Materials, 2024. **411**: p. 134347.
100. Asadizadeh, M., et al., *The effect of class F fly ash on the geopolymerization and compressive strength of lightweight aggregates made from alkali-activated mine tailings.* Construction and Building Materials, 2023. **395**: p. 132275.
101. Han, R.B., et al., *Turning waste into treasure: Preparation, physical properties and microstructure of alkali-activated phosphorus tailings-based fully solid waste non-sintered lightweight aggregates.* Journal of Cleaner Production, 2025. **527**: p. 146693.
102. Zhang, N., H. Li, and X. Liu, *Hydration mechanism and leaching behavior of bauxite-calcination-method red mud-coal gangue based cementitious materials.* J Hazard Mater, 2016. **314**: p. 172-180.
103. Balapour, M., et al., *Potential use of lightweight aggregate (LWA) produced from bottom coal ash for internal curing of concrete systems.* Cement & Concrete Composites, 2020. **105**: p. 103428.
104. Gomathi, P., et al., *Crushing strength properties of furnace slag-fly ash blended lightweight aggregates.* ARPN Journal Engineering and Applied Sciences, 2013. **8**(4): p. 246-251.

105. Liu, J., et al., *The performance and microstructure of alkali-activated artificial aggregates prepared from municipal solid waste incineration bottom ash.* Construction and Building Materials, 2023. **403**: p. 133012.
106. Li, J.Q., et al., *The chemistry and structure of calcium (alumino) silicate hydrate: A study by XANES, ptychographic imaging, and wide- and small-angle scattering.* Cement and Concrete Research, 2019. **115**: p. 367-378.
107. Garcia-Lodeiro, I., et al., *Compatibility studies between N-A-S-H and C-A-S-H gels. Study in the ternary diagram Na2O–CaO–Al2O3–SiO2–H2O.* Cement and Concrete Research, 2011. **41**(9): p. 923-931.
108. Huo, W.W., et al., *Effect of synthesis parameters on the development of unconfined compressive strength of recycled waste concrete powder-based geopolymers.* Construction and Building Materials, 2021. **292**: p. 123264.
109. Walkley, B., et al., *Structural evolution of synthetic alkali-activated CaO-MgO-Na 2 O-Al 2 O 3 -SiO 2 materials is influenced by Mg content.* Cement and Concrete Research, 2017. **99**: p. 155-171.
110. Rashad, A.M. and S.R. Zeedan, *The effect of activator concentration on the residual strength of alkali-activated fly ash pastes subjected to thermal load.* Construction and Building Materials, 2011. **25**(7): p. 3098-3107.
111. Atiş, C.D., et al., *Influence of activator on the strength and drying shrinkage of alkali-activated slag mortar.* Construction and building materials, 2009. **23**(1): p. 548-555.
112. Dong, B.Q., et al., *Fly ash-based artificial aggregates synthesized through alkali-activated cold-bonded pelletization technology.* Construction and Building Materials, 2022. **344**: p. 128268.
113. Vali, K.S. and B. Murugan, *Impact of Nano SiO2on the Properties of Cold-bonded Artificial Aggregates with Various Binders.* International Journal of Technology, 2019. **10**(5): p. 897.
114. Vali, K.S. and S.B. Murugan, *Effect of different binders on cold-bonded artificial lightweight aggregate properties.* Advances in Concrete Construction, 2020. **9**(2): p. 183-193.
115. Gomathi, P. and A. Sivakumar, *Research Article Cold Bonded Fly Ash Lightweight Aggregate Containing Different Binders.* Research Journal of Applied Sciences, Engineering and Technology, 2014. **7**(6): p. 1101-1106.
116. Vali, K.S. and S.B. Murugan, *Properties of Glass Fiber Reinforced Cold-Bonded Artificial Lightweight Aggregates with Different Binders.* Revista Romana De Materiale-Romanian Journal of Materials, 2020. **50**(1): p. 40-50.
117. Narattha, C. and A. Chaipanich, *Phase characterizations, physical properties and strength of environment-friendly cold-bonded fly ash lightweight aggregates.* Journal of Cleaner Production, 2018. **171**: p. 1094-1100.
118. Cioffi, R., et al., *Manufacture of artificial aggregate using MSWI bottom ash.* Waste Manag, 2011. **31**(2): p. 281-8.
119. Zhang, C., et al., *Investigation of hierarchical porous cold bonded lightweight aggregates produced from red mud and solid-waste-based cementitious material.* Construction and Building Materials, 2021. **308**: p. 124990.
120. Kim, D., et al., *New cold-bonded artificial aggregate using a Ba(OH)2-activated cementless binder for cement-free concrete production.* Construction and Building Materials, 2024. **428**: p. 136333.
121. Chen, Y.X., et al., *Development of cement-free bio-based cold-bonded lightweight aggregates (BCBLWAs) using steel slag and miscanthus powder via CO2 curing.*

Journal of Cleaner Production, 2021. **322**: p. 129105.
122. Zhang, C., et al., *Collaborative recycling of red mud and FGD-gypsum into multi-shell cold bonded lightweight aggregates: Synergistic effect, structure design and application in sustainable concrete.* Construction and Building Materials, 2023. **379**: p. 131134.
123. Sun, Q., et al., *Efficient Synchronous Extraction of Nickel, Copper, and Cobalt from Low-Nickel Matte by Sulfation Roasting–Water Leaching Process.* Sci Rep, 2020. **10**(1): p. 9916.
124. Chen, Q.Y., et al., *Immobilisation of heavy metal in cement-based solidification/stabilisation: a review.* Waste Manag, 2009. **29**(1): p. 390-403.
125. Honorio, T., *Permeability of C-S-H.* Cement and Concrete Research, 2024. **176**: p. 107408.
126. Yuan, X. *Leaching behavior of heavy metals from cement pastes containing solid wastes*. in *IOP Conference Series: Earth and Environmental Science*. 2018. IOP Publishing.
127. Liu, J., et al., *The impact of cold-bonded artificial lightweight aggregates produced by municipal solid waste incineration bottom ash (MSWIBA) replace natural aggregates on the mechanical, microscopic and environmental properties, durability of sustainable concrete.* Journal of Cleaner Production, 2022. **337**: p. 130479.
128. Zhang, M., et al., *Immobilization of Cr (VI) by hydrated Portland cement pastes with and without calcium sulfate.* Journal of hazardous materials, 2018. **342**: p. 242-251.
129. Wang, X.J., et al., *Heavy metals migration during the preparation and hydration of an eco-friendly steel slag-based cementitious material.* Journal of Cleaner Production, 2021. **329**: p. 129715.
130. Ding, C., et al., *Physical properties, strength, and impurities stability of phosphogypsum-based cold-bonded aggregates.* Construction and Building Materials, 2022. **331**: p. 127307.
131. Wang, G., et al., *Comparison of Curing Conditions on Physical Properties, Mechanical Strength Development, and Pore Structures of Phosphogypsum-Based Cold-Bonded Aggregates.* Materials (Basel), 2024. **17**(20).
132. Peys, A., et al., *Transformation of mine tailings into cement-bound aggregates for use in concrete by granulation in a high intensity mixer.* Journal of Cleaner Production, 2022. **366**: p. 132989.
133. Villagran-Zaccardi, Y., L. Horckmans, and A. Peys, *Performance of mortar and concrete containing artificial aggregate from cold-bonded sulphidic mine tailings.* Construction and Building Materials, 2023. **409**: p. 134049.
134. Long, W.J., et al., *Recycled use of municipal solid waste incinerator fly ash and ferronickel slag for eco-friendly mortar through geopolymer technology.* Journal of Cleaner Production, 2021. **307**: p. 127281.
135. Zhang, C., et al., *c.* Construction and Building Materials, 2021. **308**: p. 124990.
136. Liu, J., et al., *Sustainable utilization of concrete slurry waste in eco-friendly artificial lightweight cold-bonded aggregates: An alternative pathway for efficiently sequestrating CO2.* Construction and Building Materials, 2024. **421**: p. 135759.
137. Pandey, B., S.D. Kinrade, and L.J. Catalan, *Effects of carbonation on the leachability and compressive strength of cement-solidified and geopolymer-solidified synthetic metal wastes.* J Environ Manage, 2012. **101**: p. 59-67.
138. Keulen, A., et al., *High performance of treated and washed MSWI bottom ash granulates as natural aggregate replacement within earth-moist concrete.* Waste Management, 2016. **49**: p. 83-95.

139. Colangelo, F., et al., *Recycling of non-metallic automotive shredder residues and coal fly-ash in cold-bonded aggregates for sustainable concrete.* Composites Part B-Engineering, 2017. **116**: p. 46-52.
140. Ouyang, G.S., et al., *Investigation on macroscopic properties, leachability and microstructures of surface reinforced phosphogypsum-based cold-bonded aggregates.* Journal of Building Engineering, 2023. **69**: p. 106305.
141. Shi, C. and A. Fernandez-Jimenez, *Stabilization/solidification of hazardous and radioactive wastes with alkali-activated cements.* J Hazard Mater, 2006. **137**(3): p. 1656-63.
142. Alvarez-Ayuso, E., et al., *Environmental, physical and structural characterisation of geopolymer matrixes synthesised from coal (co-)combustion fly ashes.* J Hazard Mater, 2008. **154**(1-3): p. 175-83.
143. Fernández-Pereira, C., et al., *Immobilization of heavy metals (Cd, Ni or Pb) using aluminate geopolymers.* Materials Letters, 2018. **227**: p. 184-186.
144. El-Eswed, B.I., O.M. Aldagag, and F.I. Khalili, *Efficiency and mechanism of stabilization/solidification of Pb (II), Cd (II), Cu (II), Th (IV) and U (VI) in metakaolin based geopolymers.* Applied Clay Science, 2017. **140**: p. 148-156.
145. Jin, M.T., et al., *Resistance of metakaolin-MSWI fly ash based geopolymer to acid and alkaline environments.* Journal of Non-Crystalline Solids, 2016. **450**: p. 116-122.
146. Ji, Z.H. and Y.S. Pei, *Immobilization efficiency and mechanism of metal cations (Cd , Pb and Zn) and anions (AsO and Cr O) in wastes-based geopolymer.* Journal of Hazardous Materials, 2020. **384**: p. 121290.
147. Sun, J., et al., *Green synthesis of ceramsite from industrial wastes and its application in selective adsorption: Performance and mechanism.* Environ Res, 2022. **214**(Pt 1): p. 113786.
148. Kinnunen, P., et al., *Efficiency of Chemical and Biological Leaching of Copper Slag for the Recovery of Metals and Valorisation of the Leach Residue as Raw Material in Cement Production.* Minerals, 2020. **10**(8): p. 654.
149. Ardit, M., et al., *Ceramisation of hazardous elements: Benefits and pitfalls of the inertisation through silicate ceramics.* Journal of Hazardous Materials, 2022. **423**: p. 126851.
150. Song, B., et al., *Mechanistic insights into the leaching and environmental safety of arsenic in ceramsite prepared from fly ash.* Chemosphere, 2023. **344**: p. 140292.
151. Izquierdo, M., et al., *The role of open and closed curing conditions on the leaching properties of fly ash-slag-based geopolymers.* J Hazard Mater, 2010. **176**(1-3): p. 623-8.
152. Chen, Y., et al., *Leaching Mechanism of Harmful Substances in Alkali-Activated Blast Furnace Slag-Secondary Aluminum Ash Sintered Fine Powder Cementitious Materials.* Acs Sustainable Chemistry & Engineering, 2025. **13**(33): p. 13318-13330.
153. Righi, C., et al., *Benefits of pre-treating MSWI fly ash before alkali-activation.* Sustainable Chemistry and Pharmacy, 2022. **27**: p. 100671.

154. Lancellotti, I., et al., *Alkali Activation of Metallurgical Slags: Reactivity, Chemical Behavior, and Environmental Assessment.* Materials, 2021. **14**(3): p. 639.
155. Chen, Z.X., et al., *CO mineralization into waste-valorized lightweight artificial aggregate.* Construction and Building Materials, 2023. **409**: p. 133861.
156. Chen, Y.X., et al., *Development of cement-free bio-based cold-bonded lightweight aggregates (BCBLWAs) using steel slag and miscanthus powder via CO curing.* Journal of Cleaner Production, 2021. **322**: p. 129105.
157. Tang, P., et al., *Investigation of cold bonded lightweight aggregates produced with incineration sewage sludge ash (ISSA) and cementitious waste.* Journal of Cleaner Production, 2020. **251**: p. 119709.
158. Tang, P., et al., *Valorization of concrete slurry waste (CSW) and fine incineration bottom ash (IBA) into cold bonded lightweight aggregates (CBLAs): Feasibility and influence of binder types.* J Hazard Mater, 2019. **368**: p. 689-697.
159. Jiang, Y. and T.-C. Ling, *Production of artificial aggregates from steel-making slag: Influences of accelerated carbonation during granulation and/or post-curing.* Journal of CO2 Utilization, 2020. **36**: p. 135-144.
160. Li, L. and M. Wu, *An overview of utilizing CO for accelerated carbonation treatment in the concrete industry.* Journal of Co2 Utilization, 2022. **60**: p. 102000.
161. Kelly, K.E., et al., *An evaluation of ex situ, industrial-scale, aqueous CO mineralization.* International Journal of Greenhouse Gas Control, 2011. **5**(6): p. 1587-1595.
162. Mo, L.W., et al., *Accelerated carbonation and performance of concrete made with steel slag as binding materials and aggregates.* Cement & Concrete Composites, 2017. **83**: p. 138-145.
163. Gunning, P.J., C.D. Hills, and P.J. Carey, *Production of lightweight aggregate from industrial waste and carbon dioxide.* Waste Manag, 2009. **29**(10): p. 2722-8.
164. Bouzar, B. and Y. Mamindy-Pajany, *Manufacture and characterization of carbonated lightweight aggregates from waste paper fly ash.* Powder Technology, 2022. **406**: p. 117583.
165. Shi, M.J., et al., *Turning concrete waste powder into carbonated artificial aggregates.* Construction and Building Materials, 2019. **199**: p. 178-184.
166. Zhang, T.L., et al., *A wet carbonation enhancement approach to synergistic preparation of alkali-activated artificial aggregates from waste concrete powder and ground granulated blastfurnace slag.* Construction and Building Materials, 2025. **486**: p. 142012.
167. Shang, X., et al., *Lightweight concrete with low-carbon artificial aggregates recycled from biomass ash and slurry waste.* Construction and Building Materials, 2024. **429**: p. 136368.
168. Li, Z., et al., *Preparation of municipal waste incineration fly ash artificial aggregate using CO_2 curing and its properties.* Journal of CO2 Utilization, 2025. **93**: p. 103042.
169. Chen, Y., Q. Yu, and H. Brouwers, *Acoustic performance and microstructural analysis of bio-based lightweight concrete containing miscanthus.* Construction and Building Materials, 2017. **157**: p. 839-851.
170. Liu, J., et al., *The role of different ratios of biochar in the artificial lightweight cold-bonded aggregates (ALCBAs) containing high volume of red mud (RM).* Construction and Building Materials, 2024. **422**: p. 135815.
171. Badar, M.S., et al., *Corrosion of steel bars induced by accelerated carbonation in low and high calcium fly ash geopolymer concretes.* Construction and Building

Materials, 2014. **61**: p. 79-89.
172. Chen, Z.X., et al., *CO2 mineralization into waste-valorized lightweight artificial aggregate.* Construction and Building Materials, 2023. **409**: p. 133861.
173. Bernal, S.A., et al., *Gel nanostructure in alkali-activated binders based on slag and fly ash, and effects of accelerated carbonation.* Cement and Concrete Research, 2013. **53**: p. 127-144.
174. Ma, J., et al., *Performance Analysis of Industrial-Waste-Based Artificial Aggregates: CO_2 Uptake and Applications in Bituminous Pavement.* Buildings, 2023. **13**(11): p. 2823.
175. Tang, P., et al., *Use of CO_2 curing to enhance the properties of cold bonded lightweight aggregates (CBLAs) produced with concrete slurry waste (CSW) and fine incineration bottom ash (IBA).* J Hazard Mater, 2020. **381**: p. 120951.
176. Nielsen, P., et al., *Accelerated carbonation of steel slag monoliths at low CO_2 pressure–microstructure and strength development.* Journal of CO2 Utilization, 2020. **36**: p. 124-134.
177. Pan, S.Y., et al., *Systematic approach to determination of maximum achievable capture capacity via leaching and carbonation processes for alkaline steelmaking wastes in a rotating packed bed.* Environ Sci Technol, 2013. **47**(23): p. 13677-85.
178. Yadav, S. and A. Mehra, *Dissolution of steel slags in aqueous media.* Environ Sci Pollut Res Int, 2017. **24**(19): p. 16305-16315.
179. Chen, Z.Y., W.K. O'Connor, and S.J. Gerdemann, *Chemistry of aqueous mineral carbonation for carbon sequestration and explanation of experimental results.* Environmental Progress, 2006. **25**(2): p. 161-166.
180. Wang, A., et al., *Performance investigation and optimization of the granulation-CO concentration for the production of high-strength BOFS aggregates.* Journal of Co2 Utilization, 2022. **64**: p. 102160.
181. Ren, P., T.-C. Ling, and K.H. Mo, *CO_2 pretreatment of municipal solid waste incineration fly ash and its feasible use as supplementary cementitious material.* Journal of hazardous materials, 2022. **424**: p. 127457.
182. Ghouleh, Z., R.I.L. Guthrie, and Y.X. Shao, *High-strength KOBM steel slag binder activated by carbonation.* Construction and Building Materials, 2015. **99**: p. 175-183.
183. Liang, C.F., et al., *Utilization of CO curing to enhance the properties of recycled aggregate and prepared concrete: A review.* Cement & Concrete Composites, 2020. **105**: p. 103446.
184. Rostami, V., et al., *Microstructure of cement paste subject to early carbonation curing.* Cement and Concrete Research, 2012. **42**(1): p. 186-193.
185. Mo, L., F. Zhang, and M. Deng, *Mechanical performance and microstructure of the calcium carbonate binders produced by carbonating steel slag paste under CO_2 curing.* Cement and Concrete Research, 2016. **88**: p. 217-226.
186. Directive, W.F., *Available online: https://eur-lex. europa. eu/legal-content/EN*. 2000, TXT.
187. Chen, Z., et al., *Physicochemical and pozzolanic properties of municipal solid waste incineration fly ash with different pretreatments.* Waste Manag, 2023. **160**: p. 146-155.
188. Sarmiento, L.M., et al., *Critical examination of recycled municipal solid waste incineration ash as a mineral source for portland cement manufacture–A case study.* Resources, Conservation and Recycling, 2019. **148**: p. 1-10.
189. Guo, X.L., et al., *Performance and risk assessment of alinite cement-based materials from municipal solid waste incineration fly ash (MSWIFA).* Materials and Structures,

2016. **49**(6): p. 2383-2391.
190. Colangelo, F., et al., *Innovative Materials in Italy for Eco-Friendly and Sustainable Buildings.* Materials (Basel), 2021. **14**(8): p. 2048.
191. Wang, L., et al., *Introducing Reactive Magnesia to Activate Chloride/Sulfate in Waste Incinerator Fly Ash for Immobilization of Potentially Toxic Elements.* Acs Sustainable Chemistry & Engineering, 2024. **12**(26): p. 9602-9611.
192. Mao, Y., et al., *Pretreatment of municipal solid waste incineration fly ash and preparation of solid waste source sulphoaluminate cementitious material.* J Hazard Mater, 2020. **385**: p. 121580.
193. Colangelo, F., et al., *Life cycle assessment of recycled concretes: A case study in southern Italy.* Sci Total Environ, 2018. **615**: p. 1506-1517.
194. Molino, B., et al., *Recycling of Clay Sediments for Geopolymer Binder Production. A New Perspective for Reservoir Management in the Framework of Italian Legislation: The Occhito Reservoir Case Study.* Materials (Basel), 2014. **7**(8): p. 5603-5616.
195. Diamond, S., S. Sahu, and N. Thaulow, *Reaction products of densified silica fume agglomerates in concrete.* Cement and Concrete Research, 2004. **34**(9): p. 1625-1632.
196. Kuo, W.T. and T.C. Hou, *Engineering properties of alkali-activated binders by use of desulfurization slag and GGBFS.* Construction and Building Materials, 2014. **66**: p. 229-234.
197. Fang, G., H. Bahrami, and M. Zhang, *Mechanisms of autogenous shrinkage of alkali-activated fly ash-slag pastes cured at ambient temperature within 24 h.* Construction and Building Materials, 2018. **171**: p. 377-387.
198. Das, S.K., S.K. Singh, and S. Mustakim, *Incorporation of ultrafine rice husk ash (URHA) in Geopolymer concrete.* ASTM International, 2019.
199. Santos, T., J.P. Gonçalves, and H.M.C. Andrade, *Partial replacement of cement with granular marble residue: effects on the properties of cement pastes and reduction of CO2 emission.* SN Applied Sciences, 2020. **2**(9): p. 1605.
200. Bie, R.S., et al., *Characteristics of municipal solid waste incineration fly ash with cement solidification treatment.* Journal of the Energy Institute, 2016. **89**(4): p. 704-712.
201. Guo, Y.Y., et al., *Development of magnesium oxychloride cement with enhanced water resistance by adding silica fume and hybrid fly ash-silica fume.* Journal of Cleaner Production, 2021. **313**: p. 127682.
202. Cong, P.L. and L.N. Mei, *Using silica fume for improvement of fly ash/slag based geopolymer activated with calcium carbide residue and gypsum.* Construction and Building Materials, 2021. **275**: p. 122171.
203. Abdila, S.R., et al., *Evaluation on the Mechanical Properties of Ground Granulated Blast Slag (GGBS) and Fly Ash Stabilized Soil via Geopolymer Process.* Materials (Basel), 2021. **14**(11): p. 2833.
204. Wang, L., H. Chen, and Y. Zhang, *Study on Mechanical Properties and Hydration Characteristics of Bauxite-GGBFS Alkali-Activated Materials, Based on Composite Alkali Activator and Response Surface Method.* Materials (Basel), 2025. **18**(7): p. 1466.
205. Pappu, A., R. Chaturvedi, and P. Tyagi, *Sustainable approach towards utilizing Makrana marble waste for making water resistant green composite materials.* Sn Applied Sciences, 2020. **2**(3): p. 347.
206. Bakshi, P., et al., *Sustainable Development of Particulate Reinforced Composites by Recycling Marble Waste for Advanced Construction Applications: Ultra-low Water*

Absorption, Remarkable Thermal and Mechanical Behaviour. Waste and Biomass Valorization, 2021. **12**(12): p. 6449-6464.
207. Jeong, S.G., et al., *Preparation and evaluation of thermal enhanced silica fume by incorporating organic PCM, for application to concrete.* Energy and Buildings, 2013. **62**: p. 190-195.
208. Ahmed, K., et al., *Characterization of Mechanical Properties of Marble Sludge/Natural Rubber Composites.* Journal of the Chemical Society of Pakistan, 2012. **34**(6): p. 1468-1476.
209. Tome, S., et al., *Characterization and Leachability Behaviour of Geopolymer Cement Synthesised from Municipal Solid Waste Incinerator Fly Ash and Volcanic Ash Blends.* Recycling, 2018. **3**(4): p. 50.
210. Kumar, V. and P. Kumar, *Self-compacted geopolymer concrete incorporating waste ceramic powder.* Multiscale and Multidisciplinary Modeling Experiments and Design, 2024. **7**(6): p. 5187-5202.
211. Liu, D.G., et al., *Cotreatment of MSWI Fly Ash and Granulated Lead Smelting Slag Using a Geopolymer System.* Int J Environ Res Public Health, 2019. **16**(1): p. 156.
212. Astm, C., *618.* Standard specification for coal fly ash and raw or calcined natural pozzolan for use in concrete, 2003. **1**.
213. Ergün, A., *Effects of the usage of diatomite and waste marble powder as partial replacement of cement on the mechanical properties of concrete.* Construction and building materials, 2011. **25**(2): p. 806-812.
214. Ahmed, A., et al., *Potential of Waste Marble Sludge for Repressing Alkali-Silica Reaction in Concrete with Reactive Aggregates.* Materials, 2022. **15**(11): p. 3962.
215. Prošek, Z., V. Nežerka, and P. Tesárek, *Enhancing cementitious pastes with waste marble sludge.* Construction and Building Materials, 2020. **255**: p. 119372.
216. Liu, S.L., et al., *Effects of SCMs particles on the compressive strength of micro-structurally designed cement paste: Inherent characteristic effect, particle size refinement effect, and hydration effect.* Powder Technology, 2018. **330**: p. 1-11.
217. Rashwan, M.A., et al., *Behaviour of fresh and hardened concrete incorporating marble and granite sludge as cement replacement.* Journal of Building Engineering, 2020. **32**: p. 101697.
218. Gencel, O., et al., *Properties of concrete paving blocks made with waste marble.* Journal of Cleaner Production, 2012. **21**(1): p. 62-70.
219. Ferraro, A., et al., *Production and characterization of lightweight aggregates from municipal solid waste incineration fly-ash through single- and double-step pelletization process.* Journal of Cleaner Production, 2023. **383**: p. 135275.
220. Tajra, F., et al., *Performance assessment of core-shell structured lightweight aggregate produced by cold bonding pelletization process.* Construction and Building Materials, 2018. **179**: p. 220-231.
221. Bentz, D.P. and K.A. Snyder, *Protected paste volume in concrete - Extension to internal curing using saturated lightweight fine aggregate.* Cement and Concrete Research, 1999. **29**(11): p. 1863-1867.
222. Cusson, D. and T. Hoogeveen, *Internal curing of high-performance concrete with pre-soaked fine lightweight aggregate for prevention of autogenous shrinkage cracking.* Cement and Concrete Research, 2008. **38**(6): p. 757-765.
223. Alexander, M. and S. Mindess, *Aggregates in concrete*. 2005: CRC Press.
224. Panesar, D.K. and J. Francis, *Influence of limestone and slag on the pore structure of cement paste based on mercury intrusion porosimetry and water vapour sorption measurements.* Construction and Building Materials, 2014. **52**: p. 52-58.

225. Wi, K., et al., *Characterization and evaluation of cement-based systems containing solution-treated municipal solid-waste incineration fly ash.* Construction and Building Materials, 2024. **416**: p. 135230.
226. Abdi, E., et al., *Using Municipal Solid-Waste Incinerator Fly Ash, Wash Water, and Propylene Fibers in Self-Compacting Repair Mortar, Greenhouse Gas Emissions Potential.* International Journal of Concrete Structures and Materials, 2024. **18**(1): p. 57.
227. Adediran, A., T. Van Truong, and P. Perumal, *Novel non-conventional raw materials as supplementary cementitious materials for low-carbon composite cement: Chemical reactivity, fresh and hardened state characterization.* Environ Res, 2025. **271**: p. 121146.
228. Xiao, B., et al., *Hydration and Hardening Properties of High Fly-Ash Content Gel Material for Cemented Paste Backfill Utilization.* Gels, 2024. **10**(10): p. 623.
229. Kapeluszna, E., et al., *Incorporation of Al in CASH gels with various Ca/Si and Al/Si ratio: Microstructural and structural characteristics with DTA/TG, XRD, FTIR and TEM analysis.* Construction and Building Materials, 2017. **155**: p. 643-653.
230. Ruiz-Agudo, C. and H. Colfen, *Exploring the Potential of Nonclassical Crystallization Pathways to Advance Cementitious Materials.* Chem Rev, 2024. **124**(12): p. 7538-7618.
231. Georget, F., et al., *Stability of hemicarbonate under cement paste-like conditions.* Cement and Concrete Research, 2022. **153**: p. 106692.
232. Tesovnik, A., L.M. Ottosen, and V. Ducman, *Carbonation of lightweight alkali-activated aggregates based on biomass fly ash: Effect on microstructure and leaching behavior.* Case Studies in Construction Materials, 2025. **23**: p. e05014.
233. Zuaiter, M., et al., *Effect of blending GGBS and silica fume on the mechanical properties of geopolymer concrete.* Sci Rep, 2025. **15**(1): p. 9091.
234. Alzaza, A., K. Ohenoja, and M. Illikainen, *Improved strength development and frost resistance of Portland cement ground-granulated blast furnace slag binary binder cured at 0 °C with the addition of calcium silicate hydrate seeds.* Journal of Building Engineering, 2022. **48**: p. 103904.
235. Phung, Q.T., et al., *Understanding hydration heat of mortars containing supplementary cementitious materials with potential to immobilize heavy metal containing waste.* Cement & Concrete Composites, 2021. **115**: p. 103859.
236. Fan, C., et al., *A comparative study on characteristics and leaching toxicity of fluidized bed and grate furnace MSWI fly ash.* J Environ Manage, 2022. **305**: p. 114345.
237. Ren, Z.C., et al., *Study on hydration and heavy metal leaching of washed MSWI FA as a green cementitious material.* Journal of Building Engineering, 2024. **97**: p. 110636.
238. Liu, X., et al., *Intermediate-calcium based cementitious materials prepared by MSWI fly ash and other solid wastes: hydration characteristics and heavy metals solidification behavior.* J Hazard Mater, 2018. **349**: p. 262-271.
239. Gado, R.A., *The feasibility of recycling marble & granite sludge in the polymer-modified cementitious mortars Part A: In polymer-modified cementitious adhesive mortar.* Process Safety and Environmental Protection, 2022. **159**: p. 978-991.
240. Shi, T., et al., *FTIR study on early-age hydration of carbon nanotubes-modified cement-based materials.* Advances in Cement Research, 2019. **31**(8): p. 353-361.
241. Singh, A., et al., *Valorization of Mustard and Groundnut Oil Quintessence Ashes as Sustainable Alternatives to Limestone and Scms in Cementitious Systems.* Available

at SSRN 5264964.
242. Yang, J., et al., *Preparation and properties of alkali-activated red mud-based artificial lightweight aggregates.* Construction and Building Materials, 2024. **449**: p. 138304.
243. Chen, Z., et al., *Compressive strength and microstructural properties of dry-mixed geopolymer pastes synthesized from GGBS and sewage sludge ash.* Construction and Building Materials, 2018. **182**: p. 597-607.
244. Al Sekhaneh, W., et al., *Use of FTIR and thermogravimetric analysis of ancient mortar from The Church of the Cross in Gerasa (Jordan) for conservation purposes.* Mediterranean Archaeology and Archaeometry, 2020. **20**(3): p. 159-159.
245. Long, L., et al., *Improving stabilization/solidification of MSWI fly ash with coal gangue based geopolymer via increasing active calcium content.* Sci Total Environ, 2023. **854**: p. 158594.
246. Kapeluszna, E., et al., *Incorporation of Al in C-A-S-H gels with various Ca/Si and Al/Si ratio: Microstructural and structural characteristics with DTA/TG, XRD, FTIR and TEM analysis.* Construction and Building Materials, 2017. **155**: p. 643-653.
247. Sun, J., et al., *Effect of ground granulated blast furnace slag on cement hydration and autogenous healing of concrete.* Construction and Building Materials, 2022. **315**: p. 125365.
248. Gholizadeh-Vayghan, A., et al., *Thermal Reactivation of Hydrated Cement Paste: Properties and Impact on Cement Hydration.* Materials (Basel), 2024. **17**(11): p. 2659.
249. Wang, G.M., et al., *Study on the high-temperature behavior and rehydration characteristics of hardened cement paste.* Fire and Materials, 2015. **39**(8): p. 741-750.
250. Yan, Y. and G.Q. Geng, *Evolution of C-S-H morphology at early age: New insights from direct TEM observation.* Journal of Building Engineering, 2023. **73**: p. 106764.
251. Yang, H., Y. Che, and F. Leng, *High volume fly ash mortar containing nano-calcium carbonate as a sustainable cementitious material: microstructure and strength development.* Sci Rep, 2018. **8**(1): p. 16439.
252. Nemati, K.M., *Fracture analysis of concrete using scanning electron microscopy.* Scanning, 1997. **19**(6): p. 426-430.
253. Oh, S., et al., *Effects of fineness and substitution rate of GGBFS on material characteristics of GGBFS-blended cement mortars: Hydration, non-evaporable water, pore structure, mechanical properties, self-desiccation, and autogenous shrinkage.* Journal of Building Engineering, 2024. **92**: p. 109741.
254. Kriskova, L., et al., *Alkali-Activated Mineral Residues in Construction: Case Studies on Bauxite Residue and Steel Slag Pavement Tiles.* Materials (Basel), 2025. **18**(2): p. 257.
255. Ben Maaouia, O., et al., *Chromium stabilization and trapping in the cement matrix of recycled concrete aggregates.* Construction and Building Materials, 2018. **191**: p. 667-678.
256. Halim, C.E., et al., *Implications of the structure of cementitious wastes containing Pb(II), Cd(II), As(V), and Cr(VI) on the leaching of metals.* Cement and Concrete Research, 2004. **34**(7): p. 1093-1102.
257. Zhang, M., et al., *Immobilization potential of Cr(VI) in sodium hydroxide activated slag pastes.* J Hazard Mater, 2017. **321**: p. 281-289.
258. Minocha, A. and M. Goyal, *Immobilization of molybdenum in ordinary Portland cement.* J. Chem. Eng. Process Technol, 2013. **4**: p. 162.

259. Diaz Caselles, L., et al., *Immobilization of molybdenum by alternative cementitious binders and synthetic C-S-H: An experimental and numerical study.* Sci Total Environ, 2021. **789**: p. 148069.
260. Grambow, B., et al., *Retention and diffusion of radioactive and toxic species on cementitious systems: Main outcome of the CEBAMA project.* Applied Geochemistry, 2020. **112**: p. 104480.
261. Lange, S., et al., *Uptake and retention of molybdenum in cementitious systems.* Applied Geochemistry, 2020. **119**: p. 104630.
262. Vollpracht, A. and W. Brameshuber, *Binding and leaching of trace elements in Portland cement pastes.* Cement and Concrete Research, 2016. **79**: p. 76-92.
263. Álvarez-Ayuso, E., *Stabilization and encapsulation of arsenic-/antimony-bearing mine waste: Overview and outlook of existing techniques.* Critical Reviews in Environmental Science and Technology, 2021. **52**(20): p. 3720-3752.
264. Hamilton, W.P. and A.R. Bowers, *Determination of acute Hg emissions from solidified/stabilized cement waste forms.* Waste Management, 1997. **17**(1): p. 25-32.
265. Piao, H. and P.L. Bishop, *Stabilization of mercury-containing wastes using sulfide.* Environ Pollut, 2006. **139**(3): p. 498-506.
266. Behera, D., et al., *Innovations and Applications in Lightweight Concrete: Review of Current Practices and Future Directions.* Buildings, 2025. **15**(12): p. 2113.
267. Pokorný, J., et al., *Bio-based aggregate in the production of advanced thermal-insulating concrete with improved acoustic performance.* Construction and Building Materials, 2022. **358**: p. 129436.
268. Chen, Y.H., et al., *Effect of artificial aggregate (AACSBMS) hydrothermal solidified with carbide slag, boron mud and sludge on shrinkage and hydration characteristics of concrete.* Construction and Building Materials, 2025. **470**: p. 140558.
269. Zheng, W.T., et al., *Improving the mechanical properties of cold-bonded coarse aggregate concrete from municipal solid waste incineration bottom ash through compression casting technology.* Case Studies in Construction Materials, 2025. **23**: p. e05218.
270. Xu, Z., et al., *Preparation, properties, ecological evaluation and structural analysis of magnesium slag aggregate by wet carbonation.* Ceramics International, 2025. **51**(24): p. 40905-40916.
271. Liu, J., et al., *Research on carbon capture and storage of cold bonded lightweight aggregate from incineration bottom ash.* Construction and Building Materials, 2025. **496**: p. 143777.
272. Pomianowski, M., P. Heiselberg, and Y. Zhang, *Review of thermal energy storage technologies based on PCM application in buildings.* Energy and Buildings, 2013. **67**: p. 56-69.
273. Zhang, W., et al., *Design and performance of artificial aggregates from concrete slurry waste with embedded phase change materials.* Construction and Building Materials, 2025. **494**: p. 143466.
274. Faiz, H., S. Ng, and M. Rahman, *A state-of-the-art review on the advancement of sustainable vegetation concrete in slope stability.* Construction and Building Materials, 2022. **326**: p. 126502.
275. Lv, G.Y. and Y.L. Shi, *Effect of ecological concrete applied to water pollution control of urban river.* Desalination and Water Treatment, 2018. **121**: p. 6-13.
276. Chen, F., et al., *Effects of concrete content on seed germination and seedling establishment in vegetation concrete matrix in slope restoration.* Ecological Engineering, 2013. **58**: p. 99-104.

277. Niu, R., et al., *An innovative disc shell-making method for preparing porous eco-concrete with cold-bonded lightweight aggregates.* Environ Res, 2025. **266**: p. 120499.
278. Niu, R.J., et al., *Controlled release fertilizer eco-concrete: Utilization of solid waste for the sustainable cleaner products conducive to ecological construction.* Construction and Building Materials, 2025. **463**: p. 140017.
279. Kirchherr, J., et al., *Barriers to the Circular Economy: Evidence From the European Union (EU).* Ecological Economics, 2018. **150**: p. 264-272.
280. Hart, J., et al., *Barriers and drivers in a circular economy: the case of the built environment.* 26th Cirp Conference on Life Cycle Engineering (Lce), 2019. **80**: p. 619-624.
281. Los Santos-Ortega, J., E. Fraile-García, and J. Ferreiro-Cabello, *Environmental and Economic Viability of Using Concrete Block Wastes from a Concrete Production Plant as Recycled Coarse Aggregates.* Materials, 2024. **17**(7): p. 1560.
282. Xu, G. and X.M. Shi, *Characteristics and applications of fly ash as a sustainable construction material: A state-of-the-art review.* Resources Conservation and Recycling, 2018. **136**: p. 95-109.
283. Alterary, S.S. and N.H. Marei, *Fly ash properties, characterization, and applications: A review.* Journal of King Saud University - Science, 2021. **33**(6): p. 101536.
284. Belviso, C., *State-of-the-art applications of fly ash from coal and biomass: A focus on zeolite synthesis processes and issues.* Progress in Energy and Combustion Science, 2018. **65**: p. 109-135.
285. Stempkowska, A. and T. Gawenda, *Artificial lightweight aggregate made from alternative and waste raw materials, hardened using the hybrid method.* Sci Rep, 2024. **14**(1): p. 16880.
286. Shang, X., et al., *Production, properties and life cycle assessment of artificial lightweight aggregates produced with corn straw ash (CSA) and concrete slurry waste (CSW).* Construction and Building Materials, 2024. **411**: p. 134274.
287. Shang, X.Y., et al., *Life cycle sustainable assessment of natural vs artificial lightweight aggregates.* Journal of Cleaner Production, 2022. **367**: p. 133064.